Title
CLASSICAL THEORY AND CALCULATIONS OF CIRCULAR DICHROISM IN INFINITE HELICAL POLYMERS

Author
Levin, Alan Isadore.

Publication Date
1976-09-01

LBL-5376
c. 1

CLASSICAL THEORY AND CALCULATIONS OF CIRCULAR DICHROISM IN INFINITE HELICAL POLYMERS

Alan Isadore Levin
(Ph. D. thesis)

September 1976

Prepared for the U. S. Energy Research and
Development Administration under Contract W-7405-ENG-48

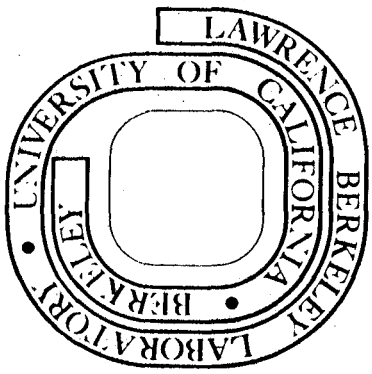

LBL-5376
c. 1

DISCLAIMER

CLASSICAL THEORY AND CALCULATIONS OF CIRCULAR DICHROISM IN INFINITE HELICAL POLYMERS

ALAN ISADORE LEVIN

Lawrence Berkeley Laboratory
University of California
Berkeley, California

This work was done with support from the U.S. Energy and Research Development Administration

CLASSICAL THEORY AND CALCULATIONS OF CIRCULAR DICHROISM IN HELICAL POLYMERS

by

Alan Isadore Levin

ABSTRACT

In this thesis we derive a new theory of optical activity in helical polymers. Helical symmetry and periodic boundary conditions are applied to classical polarizability theory. This allows us to express the infinite polymer result in closed form. Our result is all order in inter-monomer interactions, and gives the polymer circular dichroism bandshape in terms of monomer transition bandshapes. While the theory is essentially equivalent to time-dependent Hartree theory, the use of empirical monomer bandshapes, rather than ab initio wavefunctions, makes calculations much more practical. We also explicitly treat a complex unit of symmetry containing many optical transitions.

This theory is applied to calculate the following polynucleotide sequences: poly(A), poly(T), poly(G), poly(C), poly(A·T), poly(G·C) poly[(A-T)·(A-T)], poly[(G-C)·(G-C)], poly(A-T), poly(G-C), poly[(A-G)·(C-T)], poly[(A-C)·(G-T)], poly(A-C), poly(G-T), poly(A-G), poly(C-T) in RNA, and B and C form DNA geometries. In addition, calculations are carried out for poly[(A-A-T)·(A-T-T)] and poly[(A-G-C)·(G-C-T)] in RNA and B-DNA geometries. Calculations are presented for

polyadenylic acid and polyionsinic acid in non-standard geometries. Chainlength studies indicate that previous assumptions in the oligomer calculations were justified; an oligomer containing 10 base pairs gives a reasonable approximation to the polymer CD (± 20% at the first long wavelength maximum). Comparison of the calculations with experiment suggests that certain monomer properties, particularly those of guanine, are in error.

Polarizability theory is also applied to study the melting behavior of adenine and thymine containing polynucleotides. CD spectra of polyd(A), polyd(T), poly[d(A)·d(T)] and poly [d(A-T)·d(A-T)] have been measured as a function of temperature. From these data difference spectra have been calculated by subtracting the spectrum measured at low temperature from the spectra measured at higher temperatures. The CD difference spectra obtained upon melting of the two double stranded polymers are very similar. From a comparison of these difference spectra with calculated ones we suggest that optical transitions near 272 nm (on A) and 288 nm (most probably on T) are present. The premelting changes of the CD spectrum of poly[d(A-T)·d(A-T)] are due to a change in conformation in which the secondary structure goes from C- to B-type spectrum by increasing the A-type nature of the polymer. Such a change is not observed for poly[d(A)·d(T)]. Instead a transition between two different B-type geometries occurs.

To Judy, Aaron, and all my family whose love and support not only made my goals reachable, but made them worth reaching.

ACKNOWLEDGMENTS

It is a pleasure to thank my research director Nacho Tinoco. His help and guidance have been invaluable. He has also set the tenor for a group in which the expression: "Friends and colleagues", is a reality rather than a tired euphemism. I am particularly indebted to Werner Hug for helping me get started, and Dexter Moore for valuable discussions and for kindly allowing me to use figures from his thesis. Marc Maestre has been very helpful; he and Jan Greve are responsible for the experimental data in Chapter VI. Special credit is due Marshall Tuttle for a superb job of preparing a monstrous manuscript, and Margaret Knight for her patient help.

The special character of the Tinoco group is largely due to the efforts of Barbara Dengler, our "den-person", and David Koh our ambassador to the Bay Area. All the members of the group, past and present, have made their unique contributions. In particular, my "classmates" Soo Freier and Kyong Yoon and I have shared a lot (in the past few months they have taken a lot) over the past four years. It is most difficult to acknowledge the contributions of my close friend, Mark Watts and my close though very recent comrade, Carlos Bustamente.

Finally, I would like to thank Charles Levin for giving me that final boost. In his "Judelian" way, he prepared 18 diagrams in two days.

INTRODUCTION

One of the central tenets of modern molecular biology is the belief that structure determines function. This is a strong motivation for the physical chemical approach to biology. Of course, the concept of structure must be extended to include more than the organization of covalent bonds in a macromolecule. These higher levels of structural organization are generally referred to as the conformation of the polymer.

Watson and Crick's classic work [Nature 171, 737 (1953)] is a monument to this structure-function principle. Their model for the structure of DNA not only accounted for the X-ray diffraction data, but suggested how genetic information is passed from one generation to the next. As more structural data was amassed, the general importance of helical structures in both biological and synthetic macromolecules was recognized.

A helical molecule does not have a superimposable mirror image, and thus exhibits optical activity. Optically active molecules show characteristic differences in the refraction and absorption of right and left circularly polarized light. It is not surprising, therefore, that optical rotary dispersion (ORD) and circular dichroism (CD) are particularly sensitive probes of helical conformation in solution. In fact, optical solution studies corroborate the X-ray crystal evidence for many helical polymers.

However, the X-ray data cannot always be applied directly to solution studies. Tunis-Schneider and Maestre [J. Mol. Biol. 52, 521 (1970)] and Ivanov et. al., [Biopolymers 12, 89 (1973)] have demonstrated that both native and synthetic polynucleotides in solution have a wide and relatively continuous range of analogues to the predicted crystal structures.

While optical properties, especially CD, have been used to monitor conformational changes in solution, they have not yielded more detailed structural information. We need a practical and reliable means of calculating polymer optical properties from a given model geometry. With such a tool we could translate the observed optical changes into changes in structure.

While there has been considerable refinement in the quantum mechanical theories of polymer optical activity, calculations based on these approaches are extremely difficult. As usual for large systems (several atoms), it is hard to obtain useful wave functions. We will, therefore, focus our attention on classical and semi-classical theories of polymer optical activity. (Of course we cannot expect to calculate monomer optical properties classically, and must use quantum mechanics or empirical monomer data instead.)

In the first three chapters we examine theories of optical activity for polymers or aggregates of arbitrary structure. We lay the groundwork of the classical theory in Chapter I. Beginning with an analysis of Maxwell's

equations in matter, we develop the classical formalism and finish with an example which demonstrates the progression from a simple molecular polarizability to the absorption and refraction of a solution. This preliminary material is important, not only to see where the more general theory comes from (Chapter III), but to understand the nature of the approximations involved in deriving classical polarizability theory.

We discuss the physical basis of optical activity, the quantum theory of optical activity, and two semi-classical attempts to calculate the optical activity of polymers in Chapter II. In Chapter III we present DeVoe's all order polarizability theory [J. Chem. Phys. 43, 3199 (1965)], and compare it to the earlier theories.

In the second half of this thesis we develop and apply a new theory of optical activity in helical polymers. This is the first classical theory to incorporate helical symmetry and periodic boundary conditions. This is also the first explicit treatment of a complex unit of symmetry containing many optical transitions. Like the DeVoe result, our theory is a consistent treatment of the polymer CD bandshape in terms of the monomer absorption spectra. For these reasons we think that our approach is the most practical and reliable method currently available for calculating the optical properties of helical polymers.

Chapter IV contains the derivation as well as a discussion of helical symmetry, and a comparison of our result and

recent quantum theories for helical polymers. In Chapter V, polynucleotide CD calculations based on the results of Chapter IV are compared with earlier oligomer calculations and previously measured CD spectra. Finally, in Chapter VI, we measure the spectra of adenine and thymine containing deoxy-polymers and use polarizability theory to interpret these spectra. The changes in the CD of these polymers with temperature are related to conformational change which precede melting. Our analysis of these data also suggests the presence of new transitions in the near UV spectra of adenine and thymine.

TABLE OF CONTENTS

Chapter I

Classical Electrostatics and Theory of Dispersion

I. Maxwell's Equations in Matter

We will consider the microscopic electric response of matter in detail and give the magnetic response by analogy. Our starting point is the following:

$$\nabla \cdot \mathbf{E} = 4\pi\rho$$

$\mathbf{E}$ is the electric field vector and ρ is the charge density. The formal solution of this equation is:

$$\mathbf{E}(\mathbf{r}) = -\nabla \int \frac{\rho(\mathbf{r}')}{|\mathbf{r}-\mathbf{r}'|}\, d\mathbf{r}'. \qquad (1)$$

For simple systems all we need do is specify the location and magnitude of each charge in the system. For a description of matter, however, this equation is inapplicable. The charge density will fluctuate wildly over the dimensions of a single molecule, and the number of charges in any macroscopic quantity of matter is very large. For these reasons we will settle for a less detailed solution which gives the average field over some volume containing many molecules, but that is still small compared with macroscopic dimensions. Our basic measure of macroscopic dimensions will be the wavelength of light that interacts with the system. This wavelength is an indication of the variation of the external electric field which interacts with the system.

For a point **R** in the microvolume v equation (1) becomes:

$$\mathbf{E}(\mathbf{R}) = -\nabla \int \frac{\rho(\mathbf{r}')}{|\mathbf{R}-\mathbf{r}'-\mathbf{r}|}\, d\mathbf{r}' \qquad (2)$$

where **r** is some origin in the molecule and the integration is carried out over molecular coordinates **r'**. We will assume that $|\mathbf{R}-\mathbf{r}| >> |\mathbf{r}'|$ and expand equation (2) in a Taylor's series in **r'** about $|\mathbf{R}-\mathbf{r}|$. This is just a multipole expansion (see section VI A). Retaining only the monopole and dipole terms:

$$\mathbf{E}(\mathbf{R}) = -\nabla\left[\frac{q}{|\mathbf{R}-\mathbf{r}|} + \nabla_r\left(\frac{1}{|\mathbf{R}-\mathbf{r}|}\right)\cdot\boldsymbol{\mu}\right] \qquad (3)$$

$$q = \int \rho(\mathbf{r}')d\mathbf{r}' \qquad \boldsymbol{\mu} = \int \mathbf{r}'\rho(\mathbf{r}')d\mathbf{r}'$$

q is the monopole and $\boldsymbol{\mu}$ is the dipole of the molecule. This approximation will be good as long as the macroscopic fields vary over dimensions large compared to the molecular dimensions. If necessary, the quadrupole and higher terms could be retained in equation (3);[2] however we will drop them in the rest of our work. Equation (3) gives the electric field at **R** due to the molecule at **r**. The average contribution to the electric field at **R** from all the molecules in the microvolume is given by:

$$\mathbf{E}(\mathbf{R}) = -\nabla \int_v d\mathbf{r}\, N(\mathbf{r})\left[\frac{\langle q\rangle}{|\mathbf{R}-\mathbf{r}|} + \langle\boldsymbol{\mu}\rangle\cdot\nabla\left(\frac{1}{|\mathbf{R}-\mathbf{r}|}\right)\right] \qquad (4)$$

where $N(\mathbf{r})$ is the number density and $\langle q\rangle$ and $\langle\boldsymbol{\mu}\rangle$ are the average monopole and dipole of the molecules in v. In substituting

these average quantities, we have assumed that averaging and differentiation are interchangeable:[1]

$$\frac{\partial \overline{G}}{\partial x} = \overline{\left(\frac{\partial G}{\partial x}\right)} .$$

Taking the divergence of both sides of equation (4) gives:

$$\nabla \cdot \mathbf{E} = 4\pi N\langle q\rangle - 4\pi N \nabla\langle \mu\rangle .$$

In deriving this result we have used the identity:

$$\nabla^2\left(\frac{1}{|\mathbf{R}-\mathbf{r}|}\right) = -4\pi\delta(\mathbf{R}-\mathbf{r})$$

(see section VI B). We see that in matter, to our degree of approximation there is an added term: $-\nabla(4\pi N\langle\mu\rangle)$, this is called the polarization charge. Another way of expressing these relations is by defining the new field:

$$\mathbf{D} = \mathbf{E} + 4\pi\mathbf{P} \qquad \mathbf{P} = N\langle\mu\rangle$$

$$\rho' = N\langle q\rangle \qquad \nabla\cdot\mathbf{D} = 4\pi\rho' .$$

Again $N\langle q\rangle$ and $N\langle\mu\rangle$ are the average charge and average induced dipole of the molecules in the volume v with N molecules per unit volume. ρ' is recognized as the free charge density and **P** is the polarization. To a first approximation

$$\mathbf{P} = \chi_e(t)\mathbf{E}$$

where χ_e is the electric susceptibility tensor. This approximation is generally valid for the electric fields of light in the one photon processes we will consider.

Taking the Fourier transforms we find:

$$\alpha(\omega) = \int_{-\infty}^{\infty} \chi_e(t)\, e^{i\omega t}\, dt$$

and $\alpha(\omega)$ is called the electric polarizability. By a completely analogous analysis for the magnetostatics:[2]

$$\mathbf{B} = \mathbf{H} + 4\pi\mathbf{M} \qquad \mathbf{M} = N\langle\mathbf{m}\rangle$$

$$\nabla\cdot\mathbf{B} = 0 \qquad \mathbf{M} = \beta(\omega)\mathbf{H}$$

where $\mathbf{M}$ is the magnetization, $\beta(\omega)$ is the magnetic polarizability and $\mathbf{m}$ is the magnetic dipole. Finally we add the other two important equations:

$$\nabla \times \mathbf{E} = -\frac{1}{c}\frac{\partial \mathbf{B}}{\partial t} \qquad \nabla \times \mathbf{H} = \frac{4\pi}{c}\mathbf{J} + \frac{1}{c}\frac{\partial \mathbf{D}}{\partial t}\,.$$

We now have a complete description of the response of our molecular system to light. In the absence of free charges and conductance:

$$\nabla\cdot\mathbf{D} = 0 \qquad \nabla\cdot\mathbf{B} = 0$$

$$\nabla \times \mathbf{E} = -\frac{1}{c}\frac{\partial \mathbf{B}}{\partial t} \qquad \nabla \times \mathbf{H} = \frac{1}{c}\frac{\partial \mathbf{D}}{\partial t}\,.$$

For plane monochromatic wave solutions the last two equations are:

$$\mathbf{k} \times \mathbf{E} = \frac{\omega}{c}\mathbf{B} \qquad \mathbf{k} \times \mathbf{H} = -\frac{\omega}{c}\mathbf{D}$$

where $|\mathbf{k}| = n\omega/c$ is called the dispersion relation. c is the

speed of light in vacuo and n is the refractive index, ω is the circular frequency. **k** is the direction of propagation of the wave train and **E**, **D**, **B** and **H** are perpendicular to **k**. All these solutions for **E**, **D**, **B** and **H** look alike:

$$\mathbf{E}(\mathbf{r},\omega) = \mathbf{E}_o e^{\mp i\mathbf{k}\cdot\mathbf{r} \mp i\omega t} .$$

Using the dispersion relation and the two curl equations

$$n^2 - 1 = 4\pi \mathbf{E}^* \cdot [\mathbf{P} - \frac{c}{\omega} \mathbf{k} \times \mathbf{M}] / |\mathbf{E}|^2 \qquad (6)$$

* denotes complex conjugate. This is a very important relation since the complex refractive index is expressed in terms of the induced electric and magnetic moments. The refractive index contains all the information about the system's optical response. The major difficulty will be calculating the **P** and **M** for an individual molecule. In practice one usually tries to express α and β in terms of molecular parameters.

II. Internal and External Fields

We will now discuss the influence of an external field on a molecule in solution. Again we will take a microvolume large compared to molecular dimensions containing one solute molecule. Now we ask; "What is the influence of the solute molecules outside this microvolume on the field of the molecules inside the microvolume?". According to equation (4) in the absence of free charge, the exterior field is:

$$\mathbf{E}(\mathbf{R}) = -\nabla \int_{v'} \mathbf{P}(\mathbf{R}) \; \nabla \frac{1}{|\mathbf{R}-\mathbf{r}|} \, d\mathbf{r} \; .$$

This integration is over the total volume of the solution excluding the microvolume. Using the identity: $\nabla(\mathbf{AB}) = (\nabla\mathbf{A})\mathbf{B} + \mathbf{A}(\nabla\mathbf{B})$

$$\mathbf{E}(\mathbf{R}) = -\nabla \int_{v'} \nabla\left(\frac{\mathbf{P}(\mathbf{r})}{|\mathbf{R}-\mathbf{r}|}\right) d\mathbf{r} + \nabla \int_{v'} \frac{\mathbf{P}(\mathbf{r})}{|\mathbf{R}-\mathbf{r}|} \, d\mathbf{r}$$

Applying Gauss's theorem to the first integral gives:

$$\mathbf{E}(\mathbf{R}) = -\nabla\left[\int_{\Sigma'} \frac{\mathbf{P}(\mathbf{r})\cdot\mathbf{n}}{|\mathbf{R}-\mathbf{r}|} \, dS + \int_{v'} \frac{(-\nabla\cdot\mathbf{P}(\mathbf{r}))}{|\mathbf{R}-\mathbf{r}|} \, d\mathbf{r}\right].$$

So, for any volume v' bounded by the surface Σ' the field external to that volume is

$$\mathbf{E}(\mathbf{R}) = \int_{\Sigma'} \frac{\mathbf{P}(\mathbf{r})\cdot\mathbf{n}(\mathbf{R}-\mathbf{r})}{|\mathbf{R}-\mathbf{r}|^3} \, dS + \int_{v'} \frac{(-\nabla\cdot\mathbf{P}(\mathbf{r}))}{|\mathbf{R}-\mathbf{r}|^3} (\mathbf{R}-\mathbf{r}) \, d\mathbf{r}$$

$\mathbf{P}(\mathbf{r})\cdot\mathbf{n}$ is the surface polarization charge density and $-\nabla\cdot\mathbf{P}(\mathbf{r})$ is the polarization charge density. If we now return to our microvolume v bounded by surface Σ inside the macroscopic volume v' bounded by surface Σ'.

$$\mathbf{E}(\mathbf{R}) = \int_{v'-v} \frac{(-\nabla\cdot\mathbf{P}(\mathbf{r}))(\mathbf{R}-\mathbf{r})}{|\mathbf{R}-\mathbf{r}|^3} \, d\mathbf{r} + \int_{\Sigma'} \frac{\mathbf{P}(\mathbf{r})\cdot\mathbf{n}(\mathbf{R}-\mathbf{r})}{|\mathbf{R}-\mathbf{r}|^3} \, dS$$

$$+ \int_{\Sigma} \frac{\mathbf{P}(\mathbf{r})\cdot\mathbf{n}(\mathbf{R}-\mathbf{r})}{|\mathbf{R}-\mathbf{r}|^3} \, dS \qquad (7)$$

where "v", the microvolume is excluded from the first integral. Since the polarization is constant over the microscopic surface Σ, we can set $\mathbf{P}(\mathbf{r}) = \mathbf{P}(R)$. Making the following substitutions:

$$(R-r) = |r|\ \hat{r} \qquad dS = |r|^2 \sin\theta\ d\theta\ d\phi$$

$$n\cdot P = |P|\cos\theta$$

the last integral in equation (7) becomes:

$$|P|\int_0^{2\pi}\int_0^{\pi} \hat{r}\cos\theta\sin\theta\ d\theta\ d\phi. \qquad (8)$$

So that we have defined a polar spherical coordinate system with P along the polar axis. If we now express $\hat{r}$ in terms of the right handed orthogonal cartesian system $\varepsilon_1 \times \varepsilon_2 = \varepsilon_3$ with ε_3 along the polar axis parallel to P:

$$\hat{r} = \sin\theta\cos\phi\ \varepsilon_1 + \sin\theta\sin\phi\ \varepsilon_2 + \cos\theta\ \varepsilon_3\ .$$

Substituting this into the integral equation 8 we find that the integrals with coefficients ε_1 and ε_2 vanish since they contain an odd power of $\cos\phi$ or $\sin\phi$. The result is thus just $\frac{4\pi}{3}|P|\ \varepsilon_3$. But our coordinates were chosen so that P is along ε_3. Therefore the integral over the surface Σ in equation (7) is just $\frac{4\pi P}{3}$. This process is just a special case of space averaging of all the polarization contributions from solute molecules outside the microvolume (see section IV).

Since the polarization is constant over the microscopic surface, $\nabla\cdot\mathbf{P}(\mathbf{r})$, (the microvolume) makes no contribution to the first integral, i.e. it is not necessary to exclude v from the volume integral since it makes no contribution.

Thus the field in the microvolume is:

$$E(R) = \int_{v'} \frac{(-\nabla\cdot P(r))(R-r)}{|R-r|^3}\, dr + \int_{\Sigma'} \frac{P(r)\cdot n(R-r)}{|R-r|^3}\, dS + \frac{4\pi P}{3}$$

but this is just the external field for the entire solution plus $\frac{4\pi P}{3}$. So $E_{int} = E_{ext} + \frac{4\pi P}{3}$. In later chapters we will be concerned with polymers in dilute solution. Within each microvolume containing one polymer we will have to consider the interactions and fields within this polymer, but not interpolymer interactions specifically. In the above expression the influence of other polymers in solution is essentially a continuum effect.

III. Intrapolymer Interactions and Monopoles

Inside the microvolume of a single polymer molecule we will generally ignore static fields and couple the optical transitions of the monomers dynamically. This will involve calculating the energy of interaction of transition charge densities of the monomers. If we follow the method of the first section and expand the total charge densities in multipoles we find that the first nonzero term is the familiar dipole-dipole interaction:[1]

$$V_{ij} = \mu_i \cdot T_{ij} \cdot \mu_j$$

$$T_{ij} = \frac{e_i e_j}{R_{ij}^3} - \frac{3\, e_i\cdot R_{ij}\; e_j\cdot R_{ij}}{R_{ij}^5}$$

where e_i is the unit direction vector of dipole μ_i and R_{ij}

is the vector between the centers of transitions i and j. There are no monopole terms since the monopole of a transition charge density is zero. The approximation will only be good if the distance between the transitions is large compared with the distances over which the transitions are delocalized. This is equivalent to the assumption that $|\mathbf{R}-\mathbf{r}| >> \mathbf{r}'$ which was necessary in deriving equation (3). For many polymers this is not the case, and another approach must be found for calculating V_{ij}. We will follow the method of London[3] as elucidated by Hirschfelder and Haugh.[4] The form of the potential is:

$$\int \frac{\rho_i(\mathbf{r}_i)\ \rho_j(\mathbf{r}_j)\ d\mathbf{r}_i\ d\mathbf{r}_j}{|\mathbf{r}_i-\mathbf{r}_j+\mathbf{R}_{ij}|}$$

where ρ_i and ρ_j are the transition charge densities. This expression is also the starting point for the dipole-dipole interaction given above. However if $\mathbf{r}_i$ and $\mathbf{r}_j$ are similar in magnitude to $\mathbf{R}_{ij}$ the multipole expansion may not even be convergent. Instead we divide each transition charge density into regions of like charge. The charge is integrated over each region (this is the monopole of the region), and placed according to the first moment:

$$q_i^S = \int_S \rho_i(\mathbf{r}_S)\ d\mathbf{r}_S \qquad \mathbf{R}_S^i = \int_S \mathbf{r}_S \rho_i(\mathbf{r}_S)\ d\mathbf{r}_S.$$

We then calculate V_{ij} according to Coulomb's law:

$$V_{ij} = \sum_{S,T} q_i^S\ q_j^T / |\mathbf{R}_S^i - \mathbf{R}_T^j + \mathbf{R}_{ij}|$$

Hirschfelder and Haugh have derived this expression by expanding the interactions between the regions in multipoles. The dipole terms in their expansion are zero due to the choice of origin in each region. The approximation is good as long as the distance between the monopoles is large compared with the size of the regions defining the monopoles. If this is not the case, the dipole terms are still zero, but higher moments become important.

In deriving the classical theory we will always have the electric field of light interact with the electric dipole moments in our system. However, we will find it necessary to express intramolecular interactions with different approximations for the reasons outlined above. Because the future discussions are couched in polarizabilities and local fields, we must be able to express the intramolecular interactions involving the dipole of i interacting with the field due to transition j. Since the energy of interaction of the dipole μ_i with the field E_j is $\mu_i \cdot E_j$, we ask, "What is the field at r_i due to the transition j that will give rise to a given interaction V_{ij}?" Clearly:

$$e_i \cdot E_j(r_i) = \frac{V_{ij}}{|\mu_i|} \tag{8a}$$

V_{ij} is perfectly general. The only assumption is that only the dipole of transition i interacts with the field of transition j. This is how the monopole-monopole interaction (or any other interaction) is introduced into the local

field theory. Another approach used by Johnson and Tinoco[7] is to simply calculate the monopole field and set:

$$V_{ij} = \mu_i \cdot E_j^{mon}(r_i)$$

where

$$E_j^{mon}(r_i) = \sum_S \frac{q_i^S}{|R_{ij}-r_S|^3} (R_{ij}-r_S) .$$

The next step in this progression is to write the interaction:

$$V_{ij} = \mu_i \cdot E_j^{dip}(r_i) = \mu_i \cdot (T_{ij} \cdot \mu_j) = \mu_i \cdot T_{ij} \cdot \mu_j$$

where the dipole field of the monopoles is used. This brings us full circle back to the dipole-dipole interaction.

IV. Space Averaging

To calculate some vector quantity of a molecule such as the polarization, we generally choose some convenient coordinate system fixed in the molecule. This will be called the internal or molecular coordinate system. Since we are interested in properties in solutions with random orientations, we will have to average our calculated quantities over all these orientations. In the absence of any preferred direction in space, the average of any vector quantity over random orientations is zero. For example, a solution of molecules with permanent dipoles will not have a net dipole moment unless there is an external field present. In the case of induced moments there is always a

lab fixed preferred direction, for example in the case of electric polarization it is the direction of the external field. In our optical studies the lab fixed axes will be determined by the polarization and propagation directions of the incident light. If **A**, **B** and **C** are vectors in the internal coordinate system, and ε_1, ε_2, ε_3 are lab fixed axes, we will have to space average the terms:

$$\langle \mathbf{A}\cdot\varepsilon_1 \; \mathbf{B}\cdot\varepsilon_2 e^{\pm i\mathbf{k}\cdot\mathbf{r}} \rangle \tag{9a}$$

$$\langle \mathbf{A}\cdot\varepsilon_1 \; \mathbf{B}\cdot\varepsilon_1 e^{\pm i\mathbf{k}\cdot\mathbf{r}} \rangle \tag{9b}$$

$$\mathbf{k} = |\mathbf{k}| \; \varepsilon_3 .$$

Of course in taking the space average **A**, **B**, and **r** are always fixed relative to each other. In typical discussions of space averaging[5] it is demonstrated that:

$$\langle \mathbf{A}\cdot\varepsilon_i \; \mathbf{B}\cdot\varepsilon_j \rangle = \frac{1}{3} \mathbf{A}\cdot\mathbf{B} \; \delta_{ij}$$

$$\langle \mathbf{A}\cdot\varepsilon_i \, \mathbf{B}\cdot\varepsilon_j \; \mathbf{C}\cdot\varepsilon_k \rangle = \frac{1}{6}\delta_{ijk} \; \mathbf{A}\times\mathbf{B}\cdot\mathbf{C}$$

where δ_{ij} is the Kroeneker delta and δ_{ijk} is zero if any of the i,j,k are the same and ± 1 according to whether ijk is an odd or even permutation of 123, i.e. $\delta_{123} = 1$, $\delta_{213} = -1$. There are several ways to deduce these relations. They may be derived from the general properties of orthogonal transformations between vector spaces, or by expressing the transformation in terms of Euler angles and integrating. Expanding the exponentials in equations (9a) and (9b) gives:

$$\langle \mathbf{A}\cdot\varepsilon_1\ \mathbf{B}\cdot\varepsilon_2(1\pm i\mathbf{k}\cdot\mathbf{r})\rangle = \pm\frac{i|\mathbf{k}|}{6}\ \mathbf{A}\times\mathbf{B}\cdot\mathbf{r} \qquad (10a)$$

$$\langle \mathbf{A}\cdot\varepsilon_1\ \mathbf{B}\cdot\varepsilon_1(1\pm i\mathbf{k}\cdot\mathbf{r})\rangle = \frac{1}{3}\ \mathbf{A}\cdot\mathbf{B} \qquad (10b)$$

We will now derive the expressions for equations (9a) and (9b) keeping the full exponential. In doing so we will follow a course intermediate between the brute force integrations and the vector analysis mentioned earlier. The necessary integrals can be found in section VI. To average (9a) we first take **r** along **k**:

$$\mathbf{A} = |\mathbf{A}|(\sin\theta_A\cos\phi_A\,\varepsilon_1 + \sin\theta_A\sin\phi_A\,\varepsilon_2 + \cos\theta_A\,\varepsilon_3)$$

$$\mathbf{B} = |\mathbf{B}|(\sin\theta_B\cos\phi_B\,\varepsilon_1 + \sin\theta_B\sin\phi_B\,\varepsilon_2 + \cos\theta_B\,\varepsilon_3)$$

$$\mathbf{A}\cdot\varepsilon_1\ \mathbf{B}\cdot\varepsilon_2 = |\mathbf{A}|\ |\mathbf{B}|\ \sin\theta_A\sin\theta_B\cos\phi_A\sin\phi_B.$$

Letting $\phi_A = \phi_A + \phi$, and $\phi_B = \phi_B + \phi$ we integrate over ϕ:

$$\frac{\int_0^{2\pi}\cos(\phi_A+\phi)\,\sin(\phi_B+\phi)\,d\phi}{\int_0^{2\pi}d\phi} =$$

$$\frac{\int_0^{2\pi}(\cos\phi_A\cos\phi - \sin\phi_A\sin\phi)(\sin\phi_B\cos\phi + \sin\phi\cos\phi_B)d\phi}{\int_0^{2\pi}d\phi}$$

$$\langle \mathbf{A}\cdot\varepsilon_1\ \mathbf{B}\cdot\varepsilon_2\rangle_{\varepsilon_3} = \frac{1}{2}\ |\mathbf{A}|\ |\mathbf{B}|\ \sin\theta_A\sin\theta_B\sin(\phi_B-\phi_A)$$

but $|\mathbf{A}|\sin\theta_A$ and $|\mathbf{B}|\sin\theta_B$ are the projections of **A** and **B**

into the plane perpendicular to $\mathbf{k}$, and $\sin(\phi_B-\phi_A)$ is their cross product so:

$$e^{\pm i\mathbf{k}\cdot\mathbf{r}}\langle \mathbf{A}\cdot\boldsymbol{\varepsilon}_1\ \mathbf{B}\cdot\boldsymbol{\varepsilon}_2\rangle = \frac{\frac{1}{2}\,\mathbf{A}\times\mathbf{B}\cdot\mathbf{k}}{|\mathbf{k}|}\, e^{\pm i\mathbf{k}\cdot\mathbf{r}} .$$

Now it remains to average over all possible orientations of $\mathbf{k}$ relative to $\mathbf{r}$ with $\mathbf{A}$ and $\mathbf{B}$ fixed relative to $\mathbf{r}$. We choose:

$$\mathbf{D} = \frac{\mathbf{A}\times\mathbf{B}}{2|\mathbf{k}|} = D_x\boldsymbol{\varepsilon}_1 + D_y\boldsymbol{\varepsilon}_2 + D_z\boldsymbol{\varepsilon}_3$$

$$\mathbf{r} = |\mathbf{r}|\ \boldsymbol{\varepsilon}_3$$

$$\mathbf{k}\cdot\mathbf{r} = |\mathbf{k}|\ |\mathbf{r}|\ \cos\theta$$

$$\mathbf{k}\cdot\mathbf{D} = (\sin\theta\ \cos\phi\, D_x + \sin\theta\ \sin\phi\ D_y + \cos\theta\ D_z)|\mathbf{k}|$$

$$\mathbf{r}\cdot\mathbf{D} = |\mathbf{r}|\ D_z$$

We will integrate over θ and ϕ:

$$\int_0^{2\pi}\int_0^{\pi} \sin\theta\ d\theta\ d\phi = 4\pi$$

$$\langle\cos\phi\rangle = \langle\sin\phi\rangle = 0$$

so:

$$\left\langle \frac{\mathbf{k}\cdot\mathbf{D}}{2|\mathbf{k}|}\, e^{\pm i\mathbf{k}\cdot\mathbf{r}} \right\rangle =$$

$$\frac{D_z}{2}\int_0^{\pi} \cos\theta\ e^{\pm|\mathbf{k}|\ |\mathbf{r}|\ \cos\theta}\ \sin\theta\ d\theta \Big/ \int_0^{\pi} \sin\theta\ d\theta$$

$$= \frac{\pm i|k|}{2} A\times B\cdot r\left[\frac{\sin(|k|\ |r|)}{(|k|\ |r|)^3} - \frac{\cos(|k|\ |r|)}{(|k|\ |r|)^2}\right]. \qquad (11)$$

To evaluate equation (9b) we again begin by averaging around k.

$$\varepsilon_1\cdot A\ \varepsilon_1\cdot B = \sin\theta_A \sin\theta_B\ |A|\ |B|\ \cos\phi_A \cos\phi_B$$

$$\langle A\cdot\varepsilon_1\ B\cdot\varepsilon_1\rangle_{\varepsilon_3} = \sin\theta_A \sin\theta_B\ |A|\ |B| \int_0^{2\pi} \cos(\phi_A+\phi)\cos(\phi_B+\phi)d\phi/2\pi$$

$$= \sin\theta_A \sin\theta_B\ |A||B| \int_0^{2\pi} (\cos\phi_A \cos\phi - \sin\phi_A \sin\phi)$$

$$\times (\cos\phi_B \cos\phi - \sin\phi_B \sin\phi)\ d\phi/2\pi$$

$$= \frac{|A|\ |B|}{2} \sin\theta_A \sin\theta_B \cos(\phi_A-\phi_B)$$

but

$$|A|\ \sin\theta_A = |k\times A|$$

and

$$|B|\ \sin\theta_B = |k\times B|$$

and $\cos(\phi_A-\phi_B)$ is just the angle between the vectors:

$$\langle\varepsilon_1\cdot A\ \varepsilon_1\cdot B\rangle_{e_3} = \frac{(k\times A)\cdot(k\times B)}{2|k|^2} = \frac{1}{2|k|^2} \begin{vmatrix} k\cdot k & k\cdot B \\ A\cdot k & A\cdot B \end{vmatrix}$$

$$= \frac{1}{2}\left[A\cdot B - \frac{(A\cdot k)(k\cdot B)}{|k|^2}\right]$$

Now once again we average over all the orientations of $\mathbf{k}$ relative to $\mathbf{r}$ with $\mathbf{A}$ and $\mathbf{B}$ fixed relative to $\mathbf{r}$:

$$\mathbf{r} = |\mathbf{r}|\,\varepsilon_3$$

$$\mathbf{k} = |\mathbf{k}|(\sin\theta\cos\phi\,\varepsilon_1 + \sin\theta\sin\phi\,\varepsilon_2 + \cos\theta\,\varepsilon_3)$$

$$\mathbf{k}\cdot\mathbf{r} = |\mathbf{k}|\,|\mathbf{r}|\cos\theta$$

$$\frac{(\mathbf{k}\cdot\mathbf{A})(\mathbf{k}\cdot\mathbf{B})}{|\mathbf{k}|^2} = \sin^2\theta(\cos^2\phi\,A_xB_x + \sin^2\phi\,A_yB_y) + \cos^2\theta\,A_zB_z$$

where we have dropped any terms containing odd powers of $\sin\phi$ or $\cos\phi$. $\langle\cos^2\phi\rangle = \langle\sin^2\phi\rangle = \frac{1}{2}$.

$$\frac{\mathbf{A}\cdot\mathbf{B}\int_0^\pi e^{\pm i\cos\theta\,|\mathbf{k}|\,|\mathbf{r}|}\sin\theta d\theta}{\int_0^\pi \sin\theta\,d\theta} = \frac{\mathbf{A}\cdot\mathbf{B}\,\sin(|\mathbf{k}|\,|\mathbf{r}|)}{|\mathbf{k}|\,|\mathbf{r}|}$$

$$\frac{A_zB_z\int_0^\pi \cos^2\theta\,e^{\pm i\cos\theta\,|\mathbf{k}||\mathbf{r}|}\sin\theta\,d\theta}{\int_0^\pi \sin\theta\,d\theta} =$$

$$A_zB_z\left[\frac{\sin(|\mathbf{k}|\,|\mathbf{r}|)}{|\mathbf{k}|\,|\mathbf{r}|} - 2\left(\frac{\sin(|\mathbf{k}|\,|\mathbf{r}|)}{(|\mathbf{k}|\,|\mathbf{r}|)^3} - \frac{\cos(|\mathbf{k}|\,|\mathbf{r}|)}{(|\mathbf{k}|\,|\mathbf{r}|)^2}\right)\right]$$

$$\frac{(A_xB_x + A_yB_y)\int_0^\pi \sin^2\theta\,e^{\pm i\cos\theta\,|\mathbf{k}|\,|\mathbf{r}|}\sin\theta\,d\theta}{\int_0^\pi \sin\theta\,d\theta} =$$

$$(A_x B_x + A_y B_y)(2)\left[\frac{\sin(|k|\ |r|)}{(|k|\ |r|)^3} - \frac{\cos(|k|\ |r|)}{(|k|\ |r|)^2}\right]$$

$$\langle \mathbf{A}\cdot\boldsymbol{\varepsilon}_1\ \mathbf{B}\cdot\boldsymbol{\varepsilon}_1\ e^{\pm i\mathbf{k}\cdot\mathbf{r}}\rangle =$$

$$\frac{\mathbf{A}^{\perp}\cdot\mathbf{B}^{\perp}}{2}\left[\frac{\sin(|k|\ |r|)}{|k|\ |r|} - \left(\frac{\sin(|k|\ |r|)}{(|k|\ |r|)^3} - \frac{\cos(|k|\ |r|)}{(|k|\ |r|)^2}\right)\right]$$

$$+ \mathbf{A}^{\parallel}\cdot\mathbf{B}^{\parallel}\left[\frac{\sin(|k|\ |r|)}{(|k|\ |r|)^3} - \frac{\cos(|k|\ |r|)}{(|r|\ |r|)^2}\right] \qquad (12)$$

where $\mathbf{A}^{\perp}$ is projected in the plane perpendicular to $\mathbf{r}$ and $\mathbf{A}^{\parallel}$ is projected along $\mathbf{r}$.

If we take the limit of $|k|\ |r| \to 0$:

$$\frac{\sin(|k|\ |r|)}{|k|\ |r|} = 1 - \frac{(|k|\ |r|)^2}{3!} + \cdots;$$

$$\lim_{|k||r|\to 0} = 1$$

$$\frac{1}{|k|\ |r|^3}\left[\sin(|k|\ |r|) - |k|\ |r|\ \cos(|k|\ |r|\ )\right] =$$

$$\left[\frac{1}{2!} - \frac{1}{3!} + \cdots\right];$$

$$\lim_{|k||r|\to 0} = \frac{1}{3}$$

and to first order in $|k|$

$$\lim_{|k||r|\to 0} \langle \varepsilon_1 \cdot A \; \varepsilon_2 \cdot B e^{\pm i k \cdot r} \rangle = \frac{i|k|}{6} A \times B \cdot r$$

$$\lim_{|k||r|\to 0} \langle \varepsilon_1 \cdot A \; \varepsilon_1 \cdot B e^{\pm i k \cdot r} \rangle = \frac{A^{\perp} \cdot B^{\perp}}{2} \left(1 - \frac{1}{3}\right) + \frac{1}{3} A^{\parallel} \cdot B^{\parallel}$$

$$= \frac{1}{3} A \cdot B$$

which is identical with the results in equations (10a) and (10b). The result equation (11) has been published recently.[6] Both (11) and (12) are necessary to calculate the optical properties of a system in which the exponential cannot be expanded.

The previous workers were interested only in the optical activity, but the simple absorption and refraction of a very large system will also stray from the dipole limit (expanding the exponentials). These equations are important if transitions within a system interact over distances comparable to the wavelength of light or if transitions are delocalized over large distances. Figure 1 shows the functions:

$$f = \frac{\sin x}{x}$$

$$g = 3 \times \left[\frac{\sin x}{x^3} - \frac{\cos x}{x^2} \right] .$$

The use of equations (10a) and (10b) rather than equations

Figure 1: $\frac{\sin x}{x}$ ———————, $3[\frac{\sin x}{x^3} - \frac{\cos x}{x^2}] \cdots$.

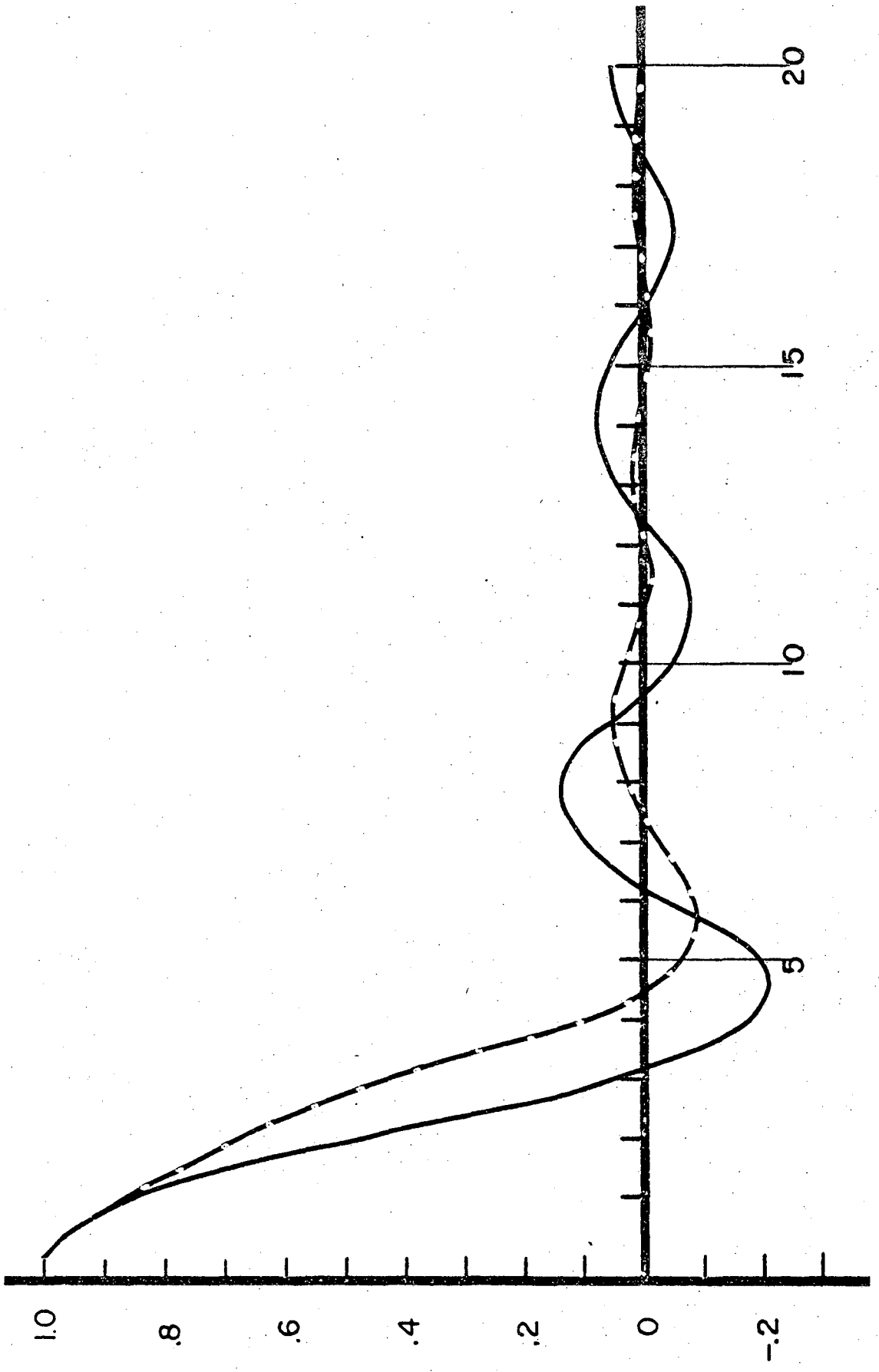
1.0
.8
.6
.4
.2
0
-.2
5
10
15
20

(11) and (12) will grossly overestimate the optical activity and absorption (or refraction) of an extended conjugated system.

V. A Simple Example

We will now apply the principles discussed in the previous sections of this chapter to a simple solution. A model is necessary to derive the polarizability of a single solute molecule in a random solution. We take as our model a harmonically bound electron constrained to move in one direction and having viscous (proportional to velocity) damping forces:

$$m\ddot{x} = -m\omega_o^2 x - m\gamma\dot{x} + e\varepsilon_1 \cdot E_o e^{i\omega t}. \qquad (13)$$

x is the displacement from equilibrium, the dots are time derivatives, $m\omega_o^2$ is the restoring force constant, and $m\gamma$ is a dissipative constant which includes radiation damping as well as any other viscous damping. We have assumed that the oscillations are small in amplitude compared with the variation of the electric field so that:

$$E_o e^{-ikr} \simeq E_o$$

Our molecular reference frame is chosen so that the electron moves along the ε_1 axis, m and e are the electron mass and charge. The steady state solutions to equation (13) are:[1]

$$x = \frac{e}{m} \frac{(\omega_o^2 - \omega^2) - i\gamma\omega}{(\omega_o^2 - \omega^2)^2 + \gamma^2\omega^2} \varepsilon_1 \cdot E_o .$$

Multiplying both sides by $e\varepsilon_1$ we recognize the polarizability:

$$\alpha(\omega) = \frac{e^2}{m} \frac{(\omega_o^2-\omega^2) - i\gamma\omega}{(\omega_0^2-\omega^2)^2 + \gamma^2\omega^2} \varepsilon_1\varepsilon_1 = |\alpha|\varepsilon_1\varepsilon_1. \quad (14)$$

Since we have not considered any coupling between oscillators, this is a model for a nomoner polarizability. This simple complex polarizability is said to have a Lorentzian line-shape. Its real and imaginary parts are related to each other by the Kronig-Kramers transforms:

$$\alpha = \alpha' + i\alpha''$$

$$\alpha'(\omega) = \frac{2}{\pi} \fint_0^{\infty\pi} \frac{\omega'\alpha''(\omega')\, d\omega'}{(\omega')^2 - \omega^2} \quad (15a)$$

$$\alpha''(\omega) = -\frac{2\pi}{\omega} \fint_0^{\infty} \frac{\alpha'(\omega')\, d\omega'}{(\omega')^2 - \omega^2} \quad (15b)$$

$\fint$ indicates the principal part of the integral is taken. These relations hold for the real and imaginary part of any function which is the Fourier transform of a causal response function. A mathematically precise derivation of these relations involves complex analysis which is described elsewhere,[5] however the need for such relations may be argued as follows: A system that has a causal response function will depend on past but not future times. By Fourier transforming we are mapping this response from half a line (the real time line) onto the complex plane:

$$\alpha(\omega) = \int_{-\infty}^{0} e^{i\omega t} \chi(t)\, dt$$

we immediately see that $\alpha(-\omega) = \alpha^*(\omega)$, so that we are mapping from half a line onto half a plane. Since we do not create information by the Fourier transform, the real and imaginary parts of α cannot be independent. The Kronig-Kramers relations are a consequence of the causality of the original response function. In this sense the Kronig-Kramers transforms are a Fourier transform of causality. We will find these transforms useful repeatedly for determining one part of a complex function from its companion. For example, absorption and refraction are related by the Kronig-Kramers transforms. Now back to our model system.

The polarization is given by:

$$P = N\langle \alpha \cdot E_{int} \rangle .$$

According to equation (9b) the average indicated by the angle brackets is just:

$$\frac{1}{3} |\alpha| E_{int} = \frac{1}{3} |\alpha| (E_o + \frac{4\pi}{3} P)$$

solving for P:

$$P = \frac{1}{3} |\alpha| E_o / (1 - \frac{4\pi}{9} |\alpha|).$$

We can now determine the refractive index according to equation (6) with $M = 0$ since there are no magnetic moments:

$$n^2 - 1 = \frac{\frac{4\pi}{3} |\alpha|}{1 - \frac{4\pi}{9} |\alpha|}$$

or:

$$\frac{n^2 - 1}{n^2 + 2} = \frac{4\pi}{9}\alpha. \qquad (16)$$

We will assume that n" is negligible compared to n' and that $n' \approx n_s$, the refractive index of the solvent. Taking the real part of both sides of equation (16) gives an expression for the refraction, [R]. The extinction coefficient is derived as follows. Beer's law is: $\log(I_o/I) = \varepsilon c \ell$ where ε is the extinction coefficient, ℓ is the path length and c is the concentration. In passing through a sample, the electric field of the light looks like:

$$E = E_o e^{+i|k|\ell} e^{i\omega t}$$

if n is complex, $n = n' + in''$

$$E = E_o e^{+in'\omega\ell/c} e^{-n''\omega\ell/c} e^{i\omega t} .$$

The real part of the refractive index determines the difference in phase velocity compared to vacuum. As we indicated above it determines dispersive properties of the medium such as refraction. The imaginary part of the refractive index causes an exponential decrease in the field as it transverses the medium. It is responsible for absorptive properties of the medium. Since the intensity is proportional to $|E|^2$:

$$\log \frac{I_o}{I} = \frac{-2n''\omega\ell}{2303\ c}$$

and

$$\varepsilon = \frac{-2n'' N_o}{2303\ N} \frac{\omega}{c} . \qquad (17)$$

N_o is Avogadro's number and N is the number of molecules per unit volume.

Taking the imaginary part of both sides of equation (16) and substituting into equation (17) gives:

$$\varepsilon = - \left[\frac{(n_s^2+2)^2}{9n_s} \right] \frac{4\pi\ N_o}{6909\ N} \frac{\omega}{c} \alpha'' . \qquad (18)$$

While we have used a simple model to derive the polarizability of this system, the rest of our calculation of the refraction and absorption is more general and will be used in subsequent chapters. The bracketed term in equation (18) involving the refractive index of the solvent is due to our inclusion of internal fields in solution. To simplify the rest of the derivations in this work, the internal fields will be ignored, i.e. $E_{int} = E_{ext}$, however the internal field and the solvent effects can always be added to any of our results if the result (for extinction) is multiplied by the term in brackets in equation (18).

VI. Multipoles and Miscellaneous Mathematics

A Taylor expansion is just:

$$f(x+h) = \sum_{n=1}^{\infty} \frac{1}{n!} f^n(x)(h-x)^n \qquad (19)$$

where:

$$f^n(x) = \frac{d^n f(x')}{dx'} \Big|_{x'=x} .$$

This is an expansion of f in h about x. We will use the first several terms of this expansion to approximate various functions through this work. We have used it implicitly in expressing the exponentials:

$$e^{i\mathbf{k}\cdot\mathbf{r}} = 1 + i\mathbf{k}\cdot\mathbf{r} + \cdots.$$

Another important and useful example is the expansion of $1/|\mathbf{R}-\mathbf{r}|$ in $\mathbf{r}$ about $\mathbf{R}$:

$$\frac{1}{|\mathbf{R}-\mathbf{r}|} = \frac{1}{[(\mathbf{R}-\mathbf{r})^2]^{1/2}} = \frac{1}{[R^2-2\mathbf{R}\cdot\mathbf{r}+r^2]^{1/2}} \tag{20}$$

dividing by R^2:

$$\frac{1}{|\mathbf{R}-\mathbf{r}|} = \frac{1}{\left[R^2\left(1-\frac{2\mathbf{r}\cdot\hat{\mathbf{R}}}{|\mathbf{R}|}+\frac{r^2}{R^2}\right)\right]^{1/2}} =$$

$$\frac{1}{|\mathbf{R}|}\ \frac{1}{\left(1-\frac{2\mathbf{r}\cdot\hat{\mathbf{R}}}{|\mathbf{R}|}+\frac{r^2}{R^2}\right)^{1/2}} \tag{21}$$

where $\hat{\mathbf{R}}$ is a unit direction vector and $|\mathbf{R}|$ denotes length. Using the Taylor expansion of $(1+x)^{-1/2}$

$$(1+x)^{-1/2} = 1 - \frac{1}{2}x + \frac{3}{8}x^2$$

this will converge as long as $-1 \leq x \leq 1$ and will converge rapidly if $|x| << 1$. Now we let $x = -\frac{2\mathbf{r}\cdot\hat{\mathbf{R}}}{|\mathbf{R}|}+\frac{r^2}{R^2}$ and

$$(1+x)^{-1/2} = 1 + \frac{\mathbf{r}\cdot\hat{\mathbf{R}}}{|\mathbf{R}|} - \frac{|\mathbf{r}|}{2|\mathbf{R}|^2} + \frac{3(\mathbf{r}\cdot\mathbf{R})^2}{2|\mathbf{R}|^2}$$

we have included all terms through $\left(\frac{|\mathbf{r}|}{|\mathbf{R}|}\right)^2$. Substituting this result into equation (21) gives:

$$\frac{1}{|\mathbf{R}-\mathbf{r}|} = \frac{1}{|\mathbf{R}|} + \frac{\mathbf{r}\cdot\mathbf{R}}{|\mathbf{R}|^3} + \frac{3(\mathbf{r}\cdot\mathbf{R})^2 - r^2}{2|\mathbf{R}|^5} .$$

We can now use this result to express the electrostatic potential at R due to the density $\rho(\mathbf{r})$:

$$V(\mathbf{R}) = \frac{\int\rho(\mathbf{r})\,d\mathbf{r}}{|\mathbf{R}|} + \frac{\mathbf{R}\cdot\int\mathbf{r}\rho(\mathbf{r})\,d\mathbf{r}}{|\mathbf{R}|^3} + \frac{\int\rho(\mathbf{r})(3(\mathbf{r}\cdot\mathbf{R})^2 - r^2)\,d\mathbf{r}}{2|\mathbf{R}|^5} \quad (22)$$

The three numerators in equation (22) are called the monopole, dipole and quadrupole moments of the charge distribution $\rho(\mathbf{r})$. Thus at sufficiently large distances we can express the potential due to a charge distribution as a sum of moments or averages of the distribution (integrations over r) which are independent of the observation point R. Note the R dependence of each term. At very large distances the distribution acts as if it were concentrated at a single point through its monopole. The form of the quadropole given in equation (22) is not the most convenient form, but we will take it no further since we drop it in all of what follows.

B. To evaluate $\nabla^2 \frac{1}{|\mathbf{r}-\mathbf{r}'|}$ we will examine it in polar coordinates with r'=0:

$$\nabla^2 \frac{1}{r} = \frac{1}{r} \frac{d^2}{dr^2} (r \cdot \frac{1}{r}) = 0, \quad \text{for all } r \neq 0$$

However for $r=0$ this is not well defined so we must consider a volume integral around the origin:

$$\int_v \nabla^2 \frac{1}{r} \, dv = \int_S n\nabla \cdot \frac{1}{r} \, da$$

where we have used Gauss's theorem and :

$$\nabla \frac{1}{r} = \frac{\partial}{\partial r} \frac{1}{r} = -\frac{1}{r^2} \qquad da = r^2 \sin\theta \, d\theta \, d\phi$$

so:

$$\int_v \nabla^2 \frac{1}{r} \, dv = \int_0^{2\pi} \int_0^{\pi} -(\frac{1}{r^2}) \, r^2 \sin\theta \, d\theta \, d\phi = -4\pi \, .$$

This is true for any volume integral which includes the origin. Another way of writing this is:

$$\nabla^2 \frac{1}{r} = -4\pi\delta(r)$$

or finally with a shift of origin:

$$\nabla^2 \frac{1}{|r-r'|} = -4\pi\delta(r-r')$$

C. Integrals involved in space averaging

$$\int_0^{2\pi} \cos^2\phi \, d\phi = \pi$$

$$\int_0^{2\pi} \sin^2\phi \, d\phi = \pi$$

1.

$$\int_0^{\pi} e^{\pm i a\cos\theta} \sin\theta \, d\theta$$

let $\alpha = \pm ia$ and $x = \cos$:

$$-\int_1^{-1} e^{\alpha x} \, dx = \frac{-e^{\alpha x}}{\alpha}\Bigg|_1^{-1} = \frac{e^{\alpha}-e^{-\alpha}}{\alpha} = \frac{e^{\pm ia}-e^{\mp ia}}{\pm ia}$$

$$= \frac{2\sin a}{a} .$$

2.

$$\int_0^{\pi} \cos\theta \, e^{\pm i a\cos\theta} \sin\theta \, d\theta = -\int_1^{-1} x \, e^{\alpha x} \, dx$$

integrating by parts:

$$\frac{-xe^{\alpha x}}{\alpha}\Bigg|_1^{-1} + \frac{e^{\alpha x}}{\alpha^2}\Bigg|_1^{-1} = e^{\alpha x}\left(\frac{1}{\alpha^2} - \frac{x}{\alpha}\right)\Bigg|_1^{-1}$$

$$= \frac{e^{\alpha}+e^{-\alpha}}{\alpha} - \frac{e^{\alpha}-e^{-\alpha}}{\alpha^2} = \pm 2i\left[\frac{\sin a}{a^2} - \frac{\cos a}{a}\right]$$

3.

$$\int_0^{\pi} \cos^2\theta \, e^{\pm i a\cos\theta} \sin\theta \, d\theta = -\int_1^{-1} x^2 e^{\alpha x} \, dx$$

integrating by parts twice:

$$= -e^{\alpha x}\left[\frac{x^2}{\alpha} - \frac{2x}{\alpha^2} + \frac{2}{\alpha^3}\right]\Bigg|_1^{-1}$$

$$= (e^{\alpha}-e^{-\alpha})(\frac{1}{\alpha} + \frac{2}{\alpha^3}) - (e^{\alpha}+e^{-\alpha})\frac{2}{\alpha^2}$$

$$= 2\sin a(\frac{1}{a} - \frac{2}{a^3}) + \frac{4\cos a}{a^2}$$

4.

$$\int_0^{\pi} \sin^2\theta\, e^{\pm i a\cos\theta} \sin\theta\, d\theta =$$

$$\int_0^{\pi} (1-\cos^2\theta)e^{\pm i a\cos\theta} \sin\theta\, d\theta$$

using results 1. and 3.:

$$= \frac{4\sin a}{a^3} - \frac{4\cos a}{a^2} .$$

Chapter I Bibliography

1. L. Rosenfeld, Theory of Electrons Dover, Inc., New York, N.Y. (1965).

2. J.D. Jackson, Classical Electrodynamics, John Wiley and Sons, Inc., New York, N.Y. (1962).

3. F. London, J. Physical Chem. 46, 305 (1942).

4. E.R. Haugh and J.D. Hirschfelder, J. Chem. Phys. 23, 1778 (1955).

5. D.J. Caldwell and H. Eyring, The Theory of Optical Activity, Wiley-Interscience, New York, N.Y. (1971).

6. I. Tobias, T.R. Brocki, and N.L. Balazs, J. Chem. Phys. 62, 4181 (1975).

7. W.C. Johnson, Jr., and I. Tinoco, Jr., Biopolymers 7, 727 (1969).

Chapter II

Optical Activity

I. The Physical Basis of Optical Activity

This is not intended as a review, but merely as a sketch of previous work on optical activity. Optical rotation (or optical rotatory dispersion ORD) is the dispersive form of optical activity. Due to a difference in phase velocity for right and left circularly polarized light in a medium, the plane of polarization will be rotated as the light passes through the medium. Right and left circular polarization are described by the + and - respectively:

$$E_{\pm} = \varepsilon_{\pm} E_o e^{ik\cdot r}$$
$$\varepsilon_{\pm} = (1/\sqrt{2})(\varepsilon_1 \pm i\varepsilon_2)$$

An equal mixture of right and left circularly polarized rays gives a linearly polarized ray. The polarization direction depends on the phase difference between the rays:

$$\varepsilon_+ e^{i\delta} + \varepsilon_- e^{-i\delta} = \frac{2}{\sqrt{2}} (\cos\delta\ \varepsilon_1 - \sin\delta\ \varepsilon_2).$$

For a phase difference of 2δ, the plane is rotated clockwise through δ as seen looking into the light ray. (This is right handed for chemists and left handed for physicists.) To see how this phase difference comes about we will consider light propagating along the ε_3 axis in the molecular frame:

$$k\cdot r = \frac{n\omega}{c} z \qquad\qquad k = \frac{n\omega}{c} \varepsilon_3 .$$

Let us start with plane polarization along ε_1 ($\delta=0$). If the right and left handed components have slightly different phase velocities (real part of the refractive index), then after travelling the distance Δz:

$$E_+ = \varepsilon_+ E_o \exp[in_+\omega\Delta z/c]$$

$$E_- = \varepsilon_- E_o \exp[in_-\omega\Delta z/c] .$$

We are for the moment ignoring any absorptive phenomena (the imaginary part of the refractive index). The phase difference is:

$$\frac{\omega}{c}(n_+ - n_-)\Delta z$$

or

$$\delta = \frac{\pi}{\lambda}(n_+ - n_-)\Delta z = \frac{\omega}{c}\frac{(n_+ - n_-)}{2}\Delta z .$$

So that rotation comes about because of the difference in refractive indices for right and left circularly polarized light. We can extend this to include absorptive phenomena by letting the refractive indices be complex, and considering a complex rotary parameter:

$$[\delta] = \frac{\omega}{c}(n_+ - n_-) \qquad n_\pm = n'_\pm + n''_\pm .$$

Taking the real and imaginary parts:

$$[\phi] = \frac{9N_o}{\pi N}\frac{\omega}{c}(n'_- - n'_+)$$

$$[\theta] = \frac{9N_o}{\pi N}\frac{\omega}{c}(n''_+ - n''_-) \qquad (1)$$

$$\varepsilon_L - \varepsilon_R = \frac{-\omega^2}{2303c}(n''_- - n''_+).$$

$[\phi]$ and $[\theta]$ are the molar rotation and ellipticity in units of degrees-mole^{-1}-liter-meter^{-1}. CD = $\varepsilon_L - \varepsilon_R$, is the difference in extinction coefficient for right and left circularly polarized light (see equation I.17) or the circular dichroism (CD). Obviously in equation (1) $[\theta]$ and $\varepsilon_L - \varepsilon_R$ are just different units for the same phenomenon. The combined absorptive and dispersive effects give rise to elliptically polarized light, which is an unequal mixture of right and left handed rays. The rotation is the angle between the initial plane and the major axis of the ellipse. The ellipticity (and thus the CD) can be related to the ratio of the major and minor axes of the ellipse.

II. Quantum Theory of Optical Rotation

In the past, most efforts have been to calculate $[\phi]$ at wavelengths far from any absorption bands. An expression due to Stephens,[2] derived from quantum field theory of scattering is a more general form of the expressions used by Rosenfeld,[3] Condon,[1] and Kirkwood.[4] All of these expressions involve a time dependent first order perturbation expansion of the interaction between the system and the light in the eigenfunctions of the unperturbed system. This is not to be confused with the time independent perturbation methods used in later sections to express a polymer Hamiltonian as a sum of monomer Hamiltonians plus inter-monomer interaction. Here the unperturbed Hamiltonian is the total polymer Hamiltonian. For rotation about the ε_3 axis, Stephens

expression is:

$$[\delta]_{33} = \frac{-e^2N}{hm^2\nu c} \sum_A \frac{\langle 0|p_2 e^{i\frac{\omega}{c}r_3}|A\rangle\langle A|p_1 e^{i\frac{\omega}{c}r_3}|0\rangle}{\nu_A + \nu}$$

$$+ \frac{\langle 0|p_1 e^{i\frac{\omega}{c}r_3}|A\rangle\langle A|p_2 e^{i\frac{\omega}{c}r_3}|0\rangle}{\nu_A - \nu} \qquad (2)$$

h is Planck's constant, $\nu = \omega/2\pi$, p_1 is the ε_1 component of the linear momentum, $p_1 = \mathbf{p}\cdot\varepsilon_1$, and r_3 is the ε_3 component of the position. If we expand equation (2) to first order in $\mathbf{r}$ and take the average:

$$[\delta] = \frac{1}{3}([\delta]_{11} + [\delta]_{22} + [\delta]_{33})$$

we find:

$$[\delta] = \frac{8\pi N}{3hc} \sum_A \langle 0|\boldsymbol{\mu}|A\rangle\langle A|\mathbf{m}|0\rangle \frac{\nu^2}{\nu_A^2 - \nu^2}$$

where:

$$\langle 0|\boldsymbol{\mu}|A\rangle = \frac{ie}{2\pi m\nu_A}\langle 0|\mathbf{p}|A\rangle$$

and

$$\mathbf{m} = \frac{e}{2mc}(\mathbf{r}\times\mathbf{p}).$$

This is just the Rosenfeld result, and the expansion of the exponential is just the Rosenfeld approximation. We assumed that $\omega/c \ll \mathbf{r}$ or $\lambda \gg 2\pi r$. $\mathrm{Im}(\langle 0|\boldsymbol{\mu}|A\rangle\langle A|\mathbf{m}|0\rangle)$ is called the rotational strength of transition A. If we sum over all transitions:

$$\sum_A R_A = \sum_A \mathrm{Im}\,\langle 0|\boldsymbol{\mu}|A\rangle\langle A|\mathbf{m}|0\rangle = \mathrm{Im}\,\langle 0|\boldsymbol{\mu}\cdot\mathbf{m}|0\rangle = 0 \qquad (3)$$

We have used the identity $\sum_A |A><A| = 1$ to contract, and the expectation value of $\mu \cdot m$ in the ground state is real. Equation (3) is called the rotational strength sum rule. The difficult quantum mechanical problem is now to find the quantities such as μ, m, and ν in equations (2) or (3). This brings us to the not yet age old problem of finding useful wavefunctions. Also, equation (2) is derived based on scattering theory. This means that it is only applicable far from any absorption, and it treats only electronic line spectra.

III. Kirkwood's Polarizability Theory

For real polymer systems in solution, we will need to treat lineshapes, i.e. how to let the monomers interact over a range of frequencies rather than just one. We will examine two semi-classical attempts to deal with these difficulties. These examples are instructive because of the semi-classical approach to the problems of deriving rotational strengths and bandshapes.

The basic assumptions of semi-classical theory is no electron exchange and no electron overlap. This allows the electrons to be assigned to definite monomers in a polymer or definite groups in a molecule. The Hamiltonian for the polymer is written as the sum of monomer Hamiltonians plus inter-monomer interactions, the wave function is written as a product of monomer wavefunctions, and all the integrations become localized.

According to Kirkwood:[4]

$$\langle 0|\mu|A\rangle\langle A|\mathbf{m}|0\rangle = \sum_i \{\langle 0|\mu_i|A\rangle\langle A|\mathbf{m}_i|0\rangle\}$$

$$+ \frac{i\pi}{c} \sum_{j\neq i} \nu_A \langle 0|\mu_i|A\rangle \cdot \mathbf{R}_j \times \langle A|\mu_j|0\rangle$$

$$+ \sum_{j\neq i} \langle 0|\mu_i|A\rangle\langle A|\mathbf{m}_j|0\rangle$$

or

$$R_A = \sum_i \{R_A^i - \frac{-\pi}{c} \nu_A \sum_{j\neq i} \mathrm{Re}[\langle 0|\mu_i|A\rangle \times \langle A|\mu_j|0\rangle \cdot \mathbf{R}_{ij}]$$

$$+ \sum_{j\neq i} \mathrm{Im}[\langle 0|\mu_i|A\rangle\langle A|\mathbf{m}_j|0\rangle]\} \qquad (4)$$

where $\mathbf{R}_{ij}$ is the vector between the centers of monomers i and j. The subscript i in the electric magnetic dipoles refers to electrons localized to monomer i. Writing the polymer Hamiltonian as:

$$H = \sum_i H_i + \sum_i \sum_{j>i} V_{ij}$$

where V_{ij} is the interaction between monomers i and j (we will consider only dynamic coupling; for static field, see reference 5). The wave functions may be written as products of the eigenfunctions of the H_i:

$$|0\rangle = \prod_i |0\rangle_i \qquad H_i |0\rangle_i = E_o |0\rangle_i$$

Kirkwood dropped the first and third terms in equation (4) and expressed the second term using time independent perturbation theory:

$$R_A = -\frac{2\pi}{c} \sum_i \sum_{j\neq i} \sum_{a\neq b} \frac{V_{ioa\ job}\nu_a\nu_b R_{ij}\cdot\mu_{job}\times\mu_{ioa}}{h(\nu_b^2-\nu_a^2)} \qquad (5)$$

$$\mu_{job} = {}_j\langle 0|\mu|b\rangle_j \qquad \nu_b \quad \frac{1}{h}\langle b|H|b\rangle .$$

Kirkwood went on to approximate $V_{ioa\ job}$ by a dipole-dipole interaction:

$$V_{ioa\ job} = \mu_{ioa}\cdot\mathbf{T}_{ij}\cdot\mu_{job} .$$

We now have an expression for R_A, the polymer rotational strength, in terms of the μ_{ioa} and ν_a, the monomer transition dipole and transition frequency. These can be measured empirically. The transition direction may be studied by crystal reflectance,[6] stretched film studies,[7] or fluorescence depolarization.[8] The square of the transition dipole is proportional to the integrated absorption band, and the band center may be taken as ν_a. Of course, the polymer rotational strength also depends on the geometry of the polymer through the R_{ij} and $V_{ioa\ job}$.

Kirkwood's polarizability approximation deals with contributions of bands in the far ultraviolet (UV). (This was Kirkwood's primary interest in fact.) The far UV transitions (the μ_{job} in this case) are all placed at one frequency, ν_o. Then equation (5) becomes:

$$R_A = -\frac{2\pi}{hc}\frac{\nu_o\nu_a}{\nu_o^2-\nu_a^2} \sum_{i\neq j} \sum_{a\neq b} G_{ij}\,|\mu_{ioa}|^2|\mu_{job}|^2\,\mathbf{e}_{job}\times\mathbf{e}_{ioa}\cdot R_{ij}$$

where $\mathbf{e}_{job}$ is the unit direction vector of μ_{job}, and

$$G_{ij} = \frac{V_{ij}}{|\mu_{ioa}|\,|\mu_{job}|}$$

but the far UV polarizability is just:[9]

$$\alpha(\nu) = \sum_j \alpha_j = \sum_j \sum_b \frac{2\nu_o \mu_{job} \mu_{job}}{h(\nu_o^2 - \nu^2)} .$$

The summation over b includes only the far UV transitions. If monomer j has the three principal polarization axes: $(\alpha_j)_{rr}$ r=1,2,3; then for the far UV

$$R_A = \frac{\pi}{c} \sum_i \sum_{j \neq i} \sum_{r=1}^{3} \nu_a |\mu_{ioa}|^2 G_{ij}(\alpha_j(\nu_a))_{rr} \times e_i \cdot R_{ij} \quad (6)$$

If we had really good polarizability data we could substitute each polarizability into equation (5) without placing all the far UV transitions at ν_o. In fact, the polarizability data used by Kirkwood was Na D line electronic polarizability and equation (6) is appropriate. Kirkwood went on to substitute the polarizability of μ_{ioa} into equation (6) as well. He was interested in the contribution of the far UV only.

Let us examine the results in equations (5) and (6). We developed only the second term in equation (4). Although the first term in equation (4) is just the monomer optical activity, it is important to realize that it will be modified by interactions with other groups; i.e., the perturbed wave functions must be used to calculate R_i. We have chosen to ignore the first and third terms in equation (4) because we are primarily interested in electrically allowed magnetically forbidden transitions. (Tinoco later developed the theory to include magnetic transitions as well as static field effects.[5]) We will include magnetic transitions in our development in chapters III and IV.

Equations (5) and (6) are first order in the potential $V_{ioa,job}$. Although a dipole-dipole interaction was used by Kirkwood, more general potential functions may be used (see Chapter I, section III). The transitions only couple at a single frequency, i.e., the theory is time independent. We can calculate rotational strengths but no dispersion information. The Kirkwood theory does, however, allow us to calculate far and near UV contributions to the polymer rotational strength based on the empirical line spectra and polarizabilities of the monomers and the geometry of the polymer.

IV. Johnson-Tinoco Theory

In an effort to calculate the CD of a polymer, Johnson and Tinoco[10] first extended the theory to include degenerate near UV transitions. Degenerate perturbation theory (exciton theory) is used to calculate the near UV contribution to the rotational strength. There are now excited states:

$$|A_k\rangle = \sum_i C_{aik}|A_i\rangle \qquad |A_i\rangle = \frac{|a\rangle_i}{|0\rangle_i} \prod_j |0\rangle_j .$$

There will be a rotational strength contribution, R_k from each state $|A_k\rangle$:

$$R_k = \frac{-\pi}{2c} \nu_k \sum_{i,j} \langle 0|\mu_i|A_k\rangle\times\langle A_k|\mu_j|0\rangle \cdot R_{ij}$$

$$- \frac{\pi}{c} \nu_k \sum_{i,j} \langle 0|\mu_i|\dot{A}_k\rangle\times\langle B_k|\mu_j|0\rangle \cdot R_{ij} . \qquad (7)$$

The first term is the rotational strength due to the interaction of the degenerate near UV transitions, and the second term is the rotational strength due to the interaction of the near UV transitions with the far UV transitions B. In the polarizability approximation

$$\langle B_k|\mu_j|0\rangle = \alpha_j \cdot E_{bk}(r_j)$$

where E_{bk} is the field due to all the monomers in the k transition:

$$E_{bk}(r_j) = \sum_{\ell} \Sigma\ C_{\ell bk}\ E_{b\ell}(r_j)$$

$E_{b\ell}$ is the field at r_j due to the transition b on monomer ℓ. Using the exciton coefficients:

$$R_k = R_{A_k} + R_{B_k}$$

$$R_{A_k} = \frac{-\pi}{2c} \sum_{i,j} \sum_{a,b} C_{iak}\ C_{jbk}\ \nu_{ioa}\ R_{ij} \cdot \mu_{ioa} \times \mu_{job} \tag{8}$$

$$R_{B_k} = \frac{\pi}{c} \sum_{i,j} \sum_{\ell} \sum_{a,b} C_{iak}\ C_{\ell bk}\ \nu_{ioa}\ E_{b\ell}(r_j) \cdot \alpha_j \times \mu_{ioa} \cdot R_{ij}$$

$$\mu_{ioa} = {}_i\langle 0|\mu_i|a\rangle_i \ .$$

α includes the far UV polarizability only. The circular dichroism (CD) is given by

$$\frac{\varepsilon_L - \varepsilon_R}{\nu} = \sum_k R_k\ f(\nu - \nu_k)$$

we have assumed all exciton bands have the same shape.

Expanding $f(\nu-\nu_k)$ in ν about $\bar{\nu}$:

$$\frac{\varepsilon_L-\varepsilon_R}{\nu} = \sum_k R_k\, f(\nu-\bar{\nu}) - \sum_k R_k \frac{\partial f(\nu-\bar{\nu})}{\partial \nu}\,(\nu_k-\nu).$$

Because of the sum rule: $\Sigma\, R_{A_k} = 0$

$$\sum_k R_k\, f(\nu-\bar{\nu}) = f(\nu-\bar{\nu}) \sum_k R_{B_k}$$

using the orthogonality of the exciton coefficients:

$$f(\nu-\bar{\nu}) \sum_k R_{B_k} = \frac{\pi}{c} f(\nu-\bar{\nu}) \sum_{i,j} \sum_a \nu_{ioa}\, E_{ia}(r_j)\cdot\alpha_j \times \mu_{ioa}\cdot R_{ij}.$$

The exciton coefficients are solutions to the eigenvalue problem:

$$\nu_k = \nu_{ioa} + \sum_{i,\ell} C_{iak}\, C_{\ell bk}\, \frac{V_{ia\ell b}}{h}\,. \qquad (9)$$

Thus $(\bar{\nu}-\nu_k)$ is first order in V, and since R_{B_k} is already first order in $V_{ij} = E_{ia}(r_j)\cdot\alpha_j/|\mu_j|$

$$\sum_k (\bar{\nu}-\nu_k) \frac{\partial f(\nu-\bar{\nu})}{\partial \nu} R_k = \frac{\partial f(\nu-\bar{\nu})}{\partial \nu} \sum_k (\bar{\nu}-\nu_k)\, R_{A_k} \qquad (10)$$

again using the orthogonality of the C_{iak} equation (10) becomes:

$$\frac{\partial f(\nu-\bar{\nu})}{\nu} \frac{\pi}{2hc} \sum_{i,j} \sum_{a,b} \nu_{ioa}\, R_{ij}\cdot\mu_{ioa}\times\mu_{job}\, V_{iajb}$$

and the CD is:

$$\varepsilon_L-\varepsilon_R = \frac{\pi\nu}{2hc} \sum_{i,j} \sum_{a,b} \nu_{ioa}\, V_{iojb}\, \mu_{ioa}\times\mu_{job}\cdot R_{ij} \frac{\partial f(\nu-\bar{\nu})}{\partial \nu}$$

$$+ \frac{\pi\nu}{c} \sum_{i,j} \sum_a \nu_{ioa}\, E_{ia}(r_j)\cdot\alpha_j\times\mu_{ioa}\cdot R_{ij}\, f(\nu-\bar{\nu}). \qquad (11)$$

Let us reexamine this derivation and follow closely the approximations concerning V_{iajb}. We separated the rotational strength into two parts in equation (7). The first part due to the exciton coupling of the near UV was solved to zero order in V. The second part expressed rotational strength in the near UV due to coupling with the far UV using Kirkwood's theory which is first order in V.

Likewise the bandshape $f(\nu-\nu_k)$ was expanded to first order in ν_k (which is first order in V). $f(\nu-\bar{\nu})$ is zero order and $\frac{\partial f(\nu-\bar{\nu})}{\partial \nu}(\bar{\nu}-\nu_k)$ is first order in V. Taking the product of the band shape and the rotational strength, and keeping only first order terms gives equation (10). Note that R_{B_k} is just the Kirkwood result with the interaction written explicitly in terms of the field and the polarizability. $f(\nu-\bar{\nu})$ is taken to be the absorption spectrum of the monomer in the near UV. As before α is a static, frequency independent polarizability. The major advantage of the Johnson-Tinoco theory is that the polymer CD bandshape can be calculated from the monomer absorption spectrum and its first derivative. Also, the theory is essentially classical since the exciton coefficients do not appear in the final result. In other words we need not solve the eigenvalue equation (9).

As we mentioned earlier, this theory is first order in V. However, the question of time dependence is not as clear. The far UV bands are centered at a single frequency and

interact with the near UV only at that frequency. The near UV bands interact and their degeneracy is split. This splitting is accounted for by the Taylor's expansion of the near UV bandshape, but the bandsdo not really interact at more than one frequency (the original ν_{ioa}). (In this sense the bandshape is added in a rather ad hoc fashion.) We will have more to say about this when comparing Johnson-Tinoco theory with our classical result.

Chapter II Bibliography

1. E.A. Condon, Rev. Mod. Phys. 9, 432 (1937).
   A. Moscowitz, Adv. Chem. Phys. 4, 67 (1962) and ref. 5.
2. M.J. Stephen, Proc. Cambridge Phil. Soc. 54, 81 (1958).
3. L. Rosenfeld, Z. Physik 52, 161 (1928).
4. J.G. Kirkwood, J. Chem. Phys. 5, 479 (1937).
5. I. Tinoco, Jr., Adv. Chem. Phys. 4, 113 (1962).
6. H.H. Chen and L.B. Clark, J. Chem. Phys. 51, 1862 (1969).
7. J. Brahms, J. Pilet, H. Damany and J. Chrandrasekharan, PNAS 60, 1130 (1968).
8. P.R. Callis and W.T. Simpson, J. Amer. Chem. Soc. 92, 3593 (1970).
9. W. Kauzman, Quantum Chemistry.
10. W.C. Johnson and I. Tinoco, Jr., Biopolymers 7, 727 (1969).

Chapter III

De Voe's Classical Polarizability Theory

I. Derivation

In this section we will reproduce the local field theory of De Voe.[1,2] It is an extension of the classical procedures outlined in Chapter I.

According to equation I.6 we must find P and M to calculate the optical properties of our polymer solution via the refractive index. The electric vector of the light is

$$E(r) = E_o\, e^{-ik\cdot r} \tag{1}$$

and

$$\begin{aligned} P &= v^{-1} \sum_i \langle \mu_i\, e^{ik\cdot r_i} \rangle \\ M &= v^{-1} \sum_i \langle m_i\, e^{ik\cdot r_i} \rangle \end{aligned} \tag{2}$$

where the sums are over all transitions in the microvolume v. r_i is the center of the i transition, and the angle brackets denote space averaging (see Chapter I section IV). Since our microvolume contains only one polymer molecule, the sum is over all the transitions in the molecule. The heart of the classical (De Voe[1,2]) theory is

$$\mu_i = \alpha_i [E_i'(r_i)\cdot e_i - \frac{\beta_i}{c} \dot{H}(r_i)\cdot e_i']e_i \tag{3a}$$

$$m_i = \frac{\beta}{c} [\dot{E}'\cdot e_i]e_i' \tag{3b}$$

$$\beta_i = b_i \alpha_i \qquad b_i = \frac{c}{i} \operatorname{Im} \frac{|m_{io}|}{|\mu_{io}|} \tag{3c}$$

$|m_{io}|$ and $|\mu_{io}|$ are the electronic electric and magnetic dipole magnitudes, and e_i and e_i' are their respective unit direction vectors. $\mathbf{E}_i'$ and $\mathbf{H}_i$ are the local electric and magnetic fields. α_i is a scalar (we assign single oscillators to the electronic transitions) complex frequency dependent polarizability. It includes the absorptive as well as the dispersive behavior of transition i. In fact:

$$\alpha_i(\omega) = \alpha_i'(\omega) + i\alpha_i''(\omega)$$
$$\alpha_i''(\omega) = -\frac{6909N}{4\pi N_o}\frac{c}{\omega}\varepsilon_i(\omega) \qquad (4)$$

N_o is Avogadro's number and $\varepsilon(\omega)$ is the molar extinction of a solution of monomer transitions with N transitions per unit volume. We calculate $\alpha_i'(\omega)$ from $\alpha_i''(\omega)$ using the Kronig-Kramers transforms (equations I.15a and I.15b). Actually equation (4) is the same relationship we derived in Chapter I section V, equation I.18. However, now we are generalizing $\alpha_i''(\omega)$ to be an empirical function, that is the monomer absorption bandshape. In our simple model $\alpha_i''(\omega)$ was a Lorentzian line derived from an harmonically bound damped electron. We will give up such a detailed mechanical model of the electron motion in favor of the generalized empirical definition of the monomer polarizability (equation (4)). $\mathbf{H}'$ and $\mathbf{E}'$ in equations (2a) and (2b) are the local fields. $\mathbf{E}'$ has contributions from the external fields, the internal fields of the solution outside the microvolume, and the fields due to the other transitions in the microvolume:

$$E'(r_i) = E(r_i) + \frac{4\pi}{3}P - [G_{ij}\ \mu_j \cdot e_j]e_i \qquad (5)$$

We have assumed that the field at r_i is linear in the dipoles of the other transitions. Comparison with equation I.8a shows that:

$$e_i \cdot E_j(r_i) = G_{ij}|\mu_j|$$

or:

$$G_{ij} = \frac{V_{ij}}{|\mu_i|\ |\mu_j|} ;$$

If we assume plane monochromatic solutions and approximate H' by B then equations (2a) and (2b) are: (see section I of Chapter I)

$$\mu_i = \alpha_i[E'(r_i)\cdot e_i - ib_i\ k\times E\cdot e_i']e_i \qquad (6a)$$

$$m_i = \frac{i\omega b_i \alpha_i}{c} E'(r_i)\cdot e_i\ e_i' \ . \qquad (6b)$$

In order to simplify the following equations we will drop the $\frac{4\pi}{3}$ P term from the local field. As was shown in Chapter I section V, this term involves only environmental solvent effects. Substituting equation (5) into equation (6a)

$$\mu_i = \alpha_i[E(r_i)\cdot e_i - \sum_j G_{ij}\ \mu_j \cdot e_j - ib_i\ k\times E\cdot e_i']e_i$$

multiplying by e_i, dividing by α_i and bringing the interaction term to the left:

$$\sum_j \mu_j \cdot e_j \left[\frac{\delta_{ij}}{\alpha_i} + G_{ij}\right] = E(r_i)\cdot e_i - ib_i\ k\times E\cdot e_i'$$

solving this set of equations

$$\mu_i \cdot e_i = \sum_j A_{ij} \left[E(r_j) \cdot e_j - \frac{i b_j n \omega}{c} k \times E \cdot e_j' \right] \qquad (7)$$

where the solution matrix is

$$A_{ij} = \left[\frac{\delta_{ij}}{\alpha_i} + G_{ij} \right]^{-1} \qquad (8)$$

δ_{ij} is the Kroneker delta. Substituting equations (7) and (1) into (2):

$$\langle \mu_j \, e^{ik \cdot r_j} \rangle = \langle \sum_i A_{ij} \left[e_i \cdot E_o \, e_j - \frac{i b_i n \omega}{c} k \times E_o \cdot e_i' \, e_j \right] e^{ik \cdot (r_j - r_i)} \rangle \qquad (9)$$

To do the space averaging we will assume that all intra-polymer distances are small compared to the wavelength of light:

$$k \cdot (r_j - r_i) = k \cdot r_{ij} << 1; \quad e^{ik \cdot r_{ij}} \simeq 1 + ik \cdot r_{ij}$$

This allows us to use equations I.10a and I.10b. We could, however, extend the theory to arbitrarily large polymers by using equations I.11 and I.12 which average over the entire exponential. Upon averaging:

$$\langle \mu_j \, e^{ik \cdot r_j} \rangle =$$

$$\frac{1}{3} \sum_i A_{ij} \left[e_i \cdot e_j \, E_o + \left(\frac{1}{2} e_i \times e_j \cdot r_{ij} - i b_i \, e_i' \cdot e_j \right) k \times E_o \right] \qquad (10a)$$

$$\langle m_j \, e^{ik \cdot r_j} \rangle = \frac{i \omega}{3c} \sum_i A_{ij} \, e_j' \cdot e_i \, b_j \, E_o \, . \qquad (10b)$$

When we substitute into equation I.6 the contribution from $(c/\omega) k \times M$ will be identical to the contribution from the

magnetic dipoles in equation (10a):

$$n^2-1 = \frac{4\pi}{3} \sum_{i,j} A_{ij}[e_i\cdot e_j + (\frac{1}{2} e_i\times e_j\cdot r_{ij} - 2ib_i\, e_i'\cdot e_j) \frac{k\times E_o}{|E_o|}]. \quad (11)$$

To find the absorption we take the imaginary part of both sides ignoring terms first order or higher in k (the absorption is zero order in k)

$$2n'n'' = \frac{4\pi}{3} \sum_{i,j} Im(A_{ij})e_i\cdot e_j$$

we will assume that $n' = 1$. (This is part of the environmental solvent influence so we will drop it.)

$$n'' = \frac{4\pi}{6} \sum_{i,j} A_{ij}\, e_i\cdot e_j$$

and using equation I.17:

$$\varepsilon = \frac{-4\pi N_o}{6909N} \frac{\omega}{c} Im(A_{ij})e_i\cdot e_j \,. \quad (12)$$

To analyze the CD $= \varepsilon_L-\varepsilon_R = \varepsilon_- - \varepsilon_+$, we must find $n_\pm^2-1$ where $\pm$ refers to right and left circular polarization (see Chapter II section I).

$$E_\pm = \varepsilon_\pm |E_o| \qquad k\times E_\pm = \mp ikE_\pm$$

where $k = |k|$. With these substitutions equation (11) is:

$$n_\pm^2-1 = \frac{4\pi k}{3} \sum_{i,j} A_{ij}[e_i\cdot e_j \pm (\frac{1}{2} e_i\times e_j\cdot r_{ij} - 2b_i\, e_i'\cdot e_j)k] \quad (12a)$$

and

$$n_-^2-n_+^2 = \frac{4\pi k}{3} \sum_{i,j} A_{ij}(4b_i\, e_i'\cdot e_j - e_i\times e_j\cdot r_{ij}) \,.$$

Dividing by $n_- + n_+ = 2n$ and using $k = n\omega/c$:

$$n_- - n_+ = \frac{4\pi}{6}\frac{\omega}{c}\sum_{i,j} A_{ij}(4b_i\, e_i'\cdot e_j - e_i\times e_j\cdot r_{ij}). \quad (13)$$

Again with equation I.17,

$$\varepsilon_L - \varepsilon_R = \frac{4\pi N_o}{6909N}\frac{\omega^2}{2}\sum_{i,j} \mathrm{Im}(A_{ij})(e_i\times e_j\cdot r_{ij} - 4b_i\, e_i'\cdot e_j) \quad (14)$$

We have chosen to calculate the absorptive optical properties of our polymer, but by a completely similar method we can derive (see Chapter I section V and Chapter II section I):

$$[R] = \frac{4\pi N_o}{9N}\sum_{i,j} \mathrm{Re}(A_{ij})e_i\cdot e_j \quad (15)$$

$$[\phi] = \frac{6N_o}{N}\frac{\omega^2}{c^2}\sum_{i,j} \mathrm{Re}(A_{ij})(4b_i\, e_i'\cdot e_j - e_i\times e_j\cdot r_{ij}). \quad (16)$$

There is an optical activity contribution from the coupling between electronic transitions, (as in the Kirkwood and Johnson-Tinoco theories) and a contribution from coupling between electric and magnetic transitions.

These equations give us another method of calculating polymer optical activity from monomer properties. First the monomer absorption spectrum must be resolved into bands with characteristic directions. Each such band is assigned an oscillator. The complex polarizability of this oscillator is determined from equations (4) and I.15a. We determine α data for the far UV transitions from the real refractive index corrected for the near UV bands:

$$\frac{n^2-1}{n^2+2} = \frac{4\pi\alpha'(\omega)}{9} .$$

The assignment of these far UV polarizabilities is discussed in more detail in Chapter V. For a given geometry, G_{ij} may be calculated from the empirical transition dipoles, or from ab initio molecular orbital transition densities. Although G_{ij} is frequency independent, the matrix, A in equation (8) must be inverted at each frequency.

The De Voe theory is all order in the intermonomer interactions. Also, the use of complex frequency dependent polarizabilities is a consistent treatment of both absorption and dispersion. In other words, ignoring electron exchange and overlap,[3] this theory is time dependent and self consistent. This is just the time dependent Hartree approximation.[4]

II. Comparison with the Kirkwood and Johnson-Tinoco Results

For comparison with perturbation theories we will expand A_{ij} to first order in G_{ij}. Let $[\alpha]_{ij} = \delta_{ij}\alpha_i$, $[\alpha^{-1}]_{ij} = \delta_{ij}/\alpha_i$, $A = [\alpha^{-1} + G]^{-1}$, $[\alpha^{-1} + G]\cdot[\alpha + x] = 1$ where x is some matrix first order in G:

$$1 + (\alpha^{-1}\cdot x + G\cdot x) + \cdots = 1$$

we have included only the terms first order in G. This implies that

$$\alpha^{-1}x = - G\alpha$$

or

$$x = \alpha G \alpha .$$

Thus

$$A_{ij} = \alpha_i[\delta_{ij} - \alpha_j G_{ij}]. \tag{16}$$

With this result and dropping the magnetic terms in equation (14):

$$\varepsilon_L - \varepsilon_R = \frac{-4\pi N_o}{6909N} \frac{\omega^2}{c^2} \sum_{i,j} G_{ij}\, \mathrm{Im}(\alpha_i \alpha_j) e_i \times e_j \cdot r_{ij}. \tag{17}$$

Now,

$$\mathrm{Im}(\alpha_i \alpha_j) = \alpha_i' \alpha_j'' + \alpha_j' \alpha_i''$$

and

$$G_{ij} = G_{ji} \qquad e_i \times e_j \cdot r_{ij} = e_j \times e_i \cdot r_{ji}.$$

Using these and equation I.17,

$$\varepsilon_L - \varepsilon_R = \frac{2\omega}{c} \sum_i \varepsilon_i(\omega) \sum_j \alpha_j'(\omega)\, G_{ij}\, e_i \times e_j \cdot r_{ij} \tag{18}$$

$$[\phi] = \frac{-6N_o}{N} \frac{\omega^2}{c^2} \sum_i \sum_j (\alpha_i'(\omega)\, \alpha_j'(\omega) + \alpha_i''(\omega)\, \alpha_j''(\omega)) G_{ij} e_i \times e_j \cdot r_{ij} \tag{19}$$

from the Kronig-Kramers transform we see:

$$\alpha'(\omega) = -\frac{2}{\pi} \int_0^\infty \frac{\omega'\, \alpha''(\omega')\, d\omega'}{(\omega')^2 - \omega^2}.$$

For comparison with Kirkwood we take:

$$\varepsilon_i = \frac{8\pi^3 N_o}{6909N} \frac{\omega_i}{c} \frac{1}{h} |\mu_{io}|^2$$

or

$$\alpha_i'' = \frac{2\pi^2}{h} |\mu_{io}|^2 .$$

The transform gives

$$\alpha_i' = \frac{4\pi}{h} \frac{\omega'}{\omega_i^2 - \omega^2} |\mu_{io}|^2 . \qquad (20)$$

Far from any absorption $\alpha_i'\alpha_j' >> \alpha_i''\alpha_j''$, and

$$[\phi] = \frac{-6No}{N} \frac{\omega^2}{c} \frac{(4\pi)^2}{h} \sum_i \frac{R_i}{\omega_i^2 - \omega^2}$$

where

$$R_i = \frac{-\omega_i}{c} \sum_j G_{ij} |\mu_{io}|^2 \left(\frac{\omega_j |\mu_{jo}|^2}{(\omega_j^2 - \omega^2)}\right) e_i \times e_j \cdot r_{ij} .$$

If we place all the μ_j at a single far UV frequency, ω_o, this result is identical to Kirkwood's theory. Thus if we are interested in rotations far from any absorption, we need no information about the bandshape.

For comparison with the Johnson-Tinoco (J-T) theory, we again place all the far UV transitions at ω_o and place all the near UV transitions at ω_a. In the J-T theory, the CD consisted of 2 parts. The first part, due to coupling with the far UV transitions had the shape of the near UV absorption spectrum of the monomer. We can substitute equation (20) into equation (18)

$$\varepsilon_L - \varepsilon_R = \frac{2\omega}{c} \sum_i \varepsilon_i(\omega) \sum_j \frac{4\pi}{h} |\mu_{jo}|^2 \left(\frac{\omega_o}{\omega_1^2 - \omega^2}\right) G_{ij}\, e_i \times e_j \cdot r_{ij}$$

instead of including the frequency dependence of the far UV polarizability $\alpha'(\omega)$, Johnson and Tinoco assumed that $\alpha'(\omega) = \alpha'(\omega_a)$. Also they used a monopole field interaction for G_{ij}. However, these differences are rather minor and the prediction of bandshape is very similar: far UV transitions coupling with the near UV will give rise to CD with bandshape similar to the near UV extinction.

For the totally degenerate near UV transitions, Johnson and Tinoco took the derivative of the absorption curve as the CD bandshape. According to our derivation the bandshape should be the product of the near UV extinction and its own Kronig-Kramers transform. The use of the derivative bandshape rather than equation (20) becomes more questionable if we consider non-degenerate transitions. Thus De Voe theory, even in first order, gives a much better description of coupling between transitions at different frequencies intermediate between the totally degenerate and widely seperated cases considered by Johnson and Tinoco. If the coupling is sufficiently weak, the first order De Voe theory may be useful in interpreting experimental CD spectra (see Chapter VI). In this order of approximation the frequency dependence and the geometry dependence of the CD are well separated.

Chapter III Bibliography

1. H. De Voe, J. Chem. Phys. 41, 393 (1964).

2. H. De Voe, J. Chem. Phys. 43, 3199 (1965).

3. W. Rhodes and M. Chase, Rev. Mod. Physics 348 (1967).

4. R.A. Harris, J. Chem. Phys. 43, 959 (1965).

Chapter IV

Classical Theory for Infinite Helical Polymers

I. Introduction

In this chapter we will apply helical symmetry and periodic boundary conditions to the classical theory derived in Chapter III. The classical result as it stands cannot be applied to extended systems. Recall that we assumed that all intrapolymer dimensions were small compared with the wavelength of light. This assumption will be bad for a very long helix, and we will base our symmetry arguments on an infinite helix. We will therefore rederive the classical theory for large helices.

II. Helix Geometry and Helical Symmetry

Helical geometry and the helical point subgroup are discussed thoroughly by Rhodes.[1] The emphasis here is developing the bare essentials necessary for our purposes.

Consider a right handed orthogonal system of coordinates with unit vectors:

$$\varepsilon_3 = \varepsilon_1 \times \varepsilon_2 \ .$$

A right-handed helical lattice is described by a translation along ε_3 by Δz and a rotation about ε_3 through θ. This primitive screw operation may be abbreviated:

$$[R(\theta)|\Delta z]$$

where $R(\theta)$ is the rotational part and Δz is the translational part of the screw operation. Figure 1 shows such a helical lattice. The ε_1, ε_2, ε_3 coordinate system will be referred to as the molecular reference frame.

If all the lattice points are equivalent, then the screw operator is a symmetry operator. For all the lattice sites to be equivalent, they must all be equidistant from the ends of the helix. This implies that the helix is unlimited in length or has an arbitrarily large number of lattice points N. It is presumed that the N+1 lattice point is identical to the first lattice point. This is the periodic boundary condition. Another way to envision the periodic boundary condition for a long lattice is to begin with a circular array with lattice points equally spaced on its circumference. This system is strictly periodic. If there are N lattice points, the N+1 lattice point is identical to the first lattice point. If we allow the radius of the circle to grow, the circumference will include more and more lattice points and the curvature of the circumference will decrease. We can make the curvature between lattice points arbitrarily small by allowing the radius (and thus the number of points) to grow arbitrarily large. So we can make our circular periodic array identical to a linear periodic array if the number of lattice points is sufficiently large.

In the language of group theory, there are N operators forming the helical point symmetry group whose typical

Figure 1: Relationship between unit cells in the molecular reference frame.

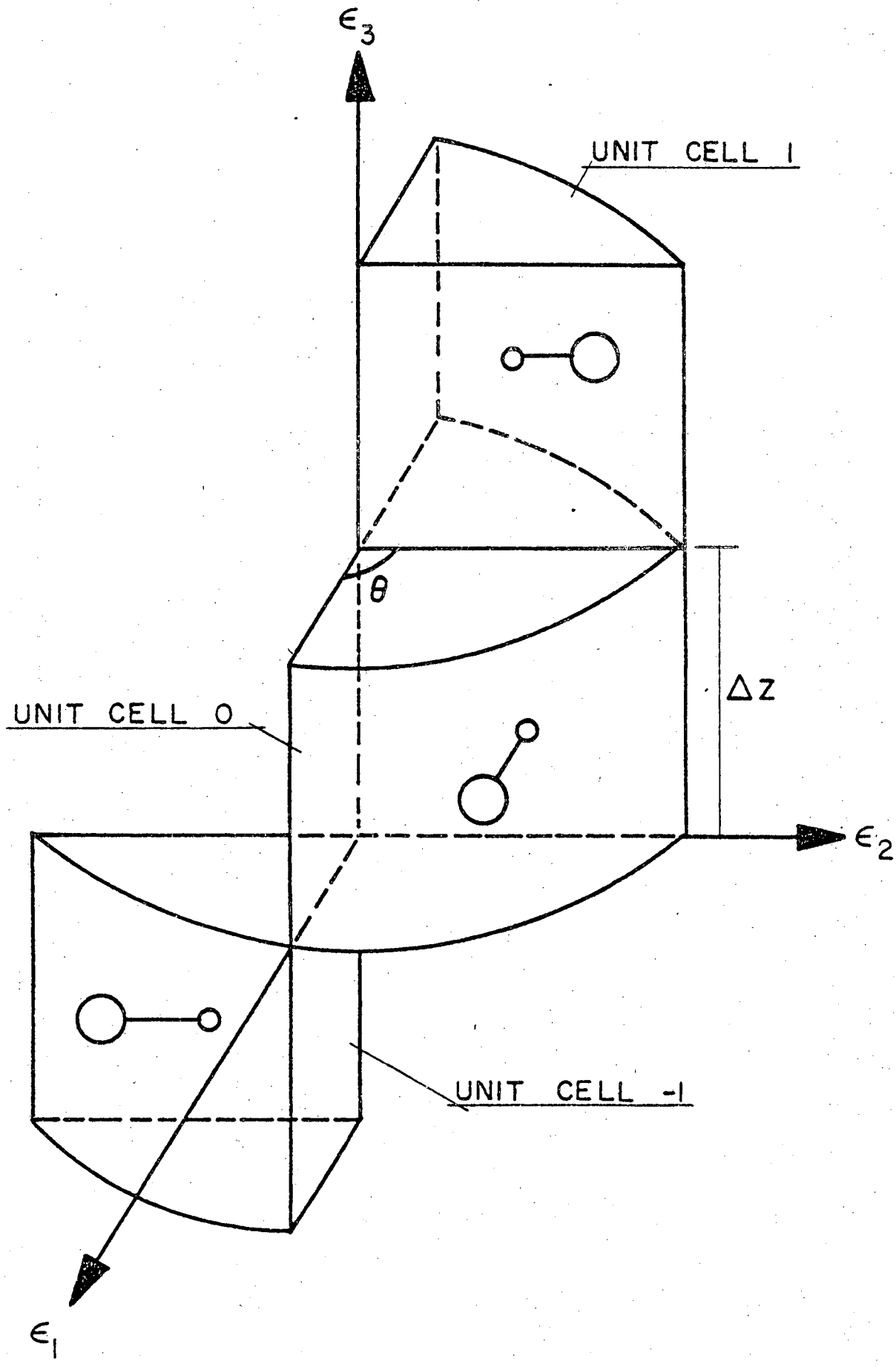
ϵ_3
UNIT CELL 1
θ
Δz
UNIT CELL 0
ϵ_2
UNIT CELL -1
ϵ_1

element is:

$$[R(\theta)|\Delta z]^{\ell} = [R(\ell\theta)|\Delta \ell z] \qquad \ell = \{1,2,3,\cdots,N\} .$$

All the operators commute, and the periodic boundary condition is:

$$[R(\theta)|\Delta z]^{N} = E$$

where E is the identity operator. More succinctly, the group is Abelian and cyclic. These group attributes insure that there are N one-dimensional representations of each group operation, namely the N Nth roots of one;

$$\exp(2\pi i j/N) \qquad j = \{1,2,3,\cdots,N\}.$$

The representative of the ℓth operator in the jth representation is:

$$\Gamma_j[R(\theta)|\Delta z] = \exp(2\pi i j\ell/N).$$

These irreducible representations will be used to construct normal modes.

Consider the two-dimensional vector in figure 2. We will examine what happens to its components when the x and y axes are rotated through θ. According to the figure:

$$x' = x\cos\theta - y\sin\theta$$
$$y' = x\sin\theta + y\cos\theta.$$

Instead of viewing this as resulting from a counter clockwise rotation of the axes we may regard it from the equivalent standpoint of a clockwise rotation of the vector itself. With this result we see that a spatial representation of the

Figure 2: A change in coordinates caused by rotating the axes through θ.

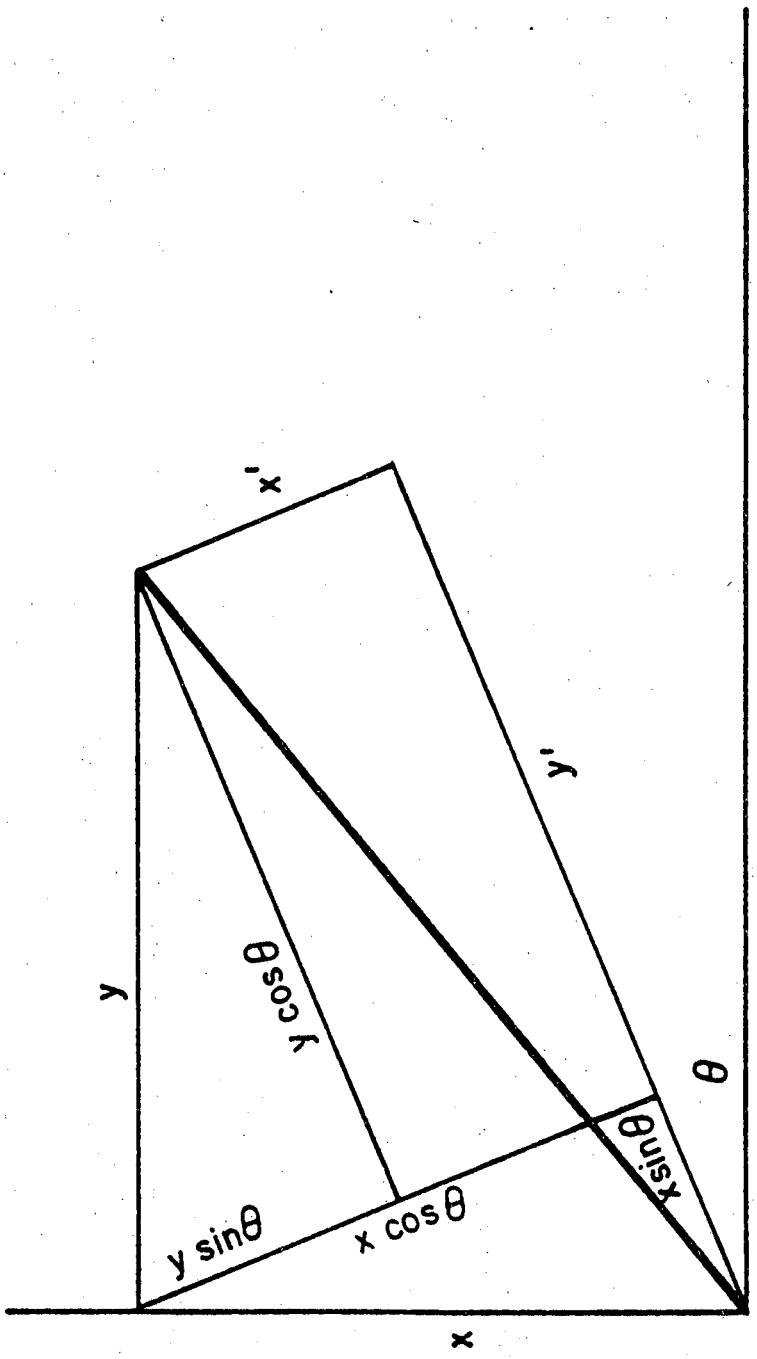

rotation operator in the molecular reference frame is:

$$R(\theta) = \begin{vmatrix} \cos\theta & -\sin\theta & 0 \\ \sin\theta & \cos\theta & 0 \\ 0 & 0 & 1 \end{vmatrix} .$$

An equivalent but more convenient form for our purpose is:

$$R(\theta) = e^{i\theta}\, \varepsilon_- \varepsilon_+ + e^{-i\theta}\, \varepsilon_+ \varepsilon_- + \varepsilon_3 \varepsilon_3$$

where:

$$\varepsilon_\pm = \frac{1}{\sqrt{2}} (\varepsilon_1 \pm i\varepsilon_2) \qquad \varepsilon_\pm^2 = 0 \qquad \varepsilon_\pm \cdot \varepsilon_\mp = 1$$

are the right and left circular unit vectors. We will consider more than one transition per monomer and perhaps more than one monomer at each lattice point. It is more reasonable, therefore, to speak of some volume with an origin and coordinate system defined for each lattice point. For the rotation operator in the representations given above, the origin in each unit cell must lie on the ε_3 axis. We will choose the coordinate system in unit cell 0 to coincide with the molecular reference frame. The coordinate system for unit cell ℓ will have its origin at the point $(0,0,\ell\Delta z)$ and the system will be rotated through $\ell\cdot\theta$ about the ε_3-axis. for any direction vector $\mathbf{v}_o$ in unit cell 0 there is a corresponding vector $\mathbf{v}_\ell$ in unit cell ℓ. With respect to the molecular reference frame;

$$\mathbf{v}_\ell = R^\ell \mathbf{v}_o .$$

Similarly for any corresponding position vectors $\mathbf{r}_\ell$ and $\mathbf{r}_o$:

$$\mathbf{r}_\ell = \mathbf{R}^\ell \mathbf{r}_o + \ell\Delta z\ \boldsymbol{\varepsilon}_3.$$

III. Derivation

As we mentioned earlier (see Chapter III), in deriving ε and $\varepsilon_L-\varepsilon_R$ we will assume that the internal field is equal to the external field. This amounts to ignoring solvent effects in the extinction and CD:

$$\varepsilon_s = \frac{(n_s^2 + 2)^2}{9n_s}\,\varepsilon$$

$$(\varepsilon_L-\varepsilon_R)_s = \frac{n_s^2 + 2}{3}\,(\varepsilon_L-\varepsilon_R)$$

where n_s is the solvent refractive index and ε_s and $(\varepsilon_L-\varepsilon_R)_s$ are the extinction and CD of the solution.

We first relabel equation III.6a with Arabic unit cell indices and Greek indices labeling transitions within the cell, e.g. $\mu_{\ell\sigma}$ is transition σ in unit cell ℓ. This gives:

$$\boldsymbol{\mu}_{\ell\sigma}\cdot\mathbf{e}_{\ell\sigma} = \alpha_\sigma\{\mathbf{E}(\mathbf{r}_{\ell\sigma})\cdot\mathbf{e}_{\ell\sigma} - ib_\sigma\ \mathbf{k}\times\mathbf{E}(\mathbf{r}_{\ell\sigma})\cdot\mathbf{e}'_{\ell\sigma} - \sum_{m\tau}^{N\eta\,\prime} G_{\ell\sigma m\tau}\boldsymbol{\mu}_{m\tau}\cdot\mathbf{e}_{m\tau}\}.$$

There are $N\eta$ equations in the $N\eta$ unknowns $\mu_{\ell\sigma}$. Note that α and b do not depend on unit cell but only on the nature of the transition. Taking linear combinations of these equations according to the irreducible representations we obtain the normal mode equations:

$$\frac{1}{N}\sum_{\ell}\exp[2\pi i j\ell/N]\mu_{\ell\sigma}\cdot e_{\ell\sigma} =$$

$$\frac{\alpha_\sigma}{N}\sum_{\ell}\exp[2\pi i j\ell/N]\{E(r_{\ell\sigma})\cdot e_{\ell\sigma} - ib_\sigma\, k\times E(r_{\ell\sigma})\cdot e'_{\ell\sigma} - \sum_{m\tau}^{N\eta}\sum G_{\ell\sigma m\tau}\mu_{m\tau}\cdot e_{m\tau}\}$$

dividing both sides by α_σ and bringing the interaction term to the left:

$$\frac{1}{N}\sum_{\ell}\exp(2\pi i j\ell/N)[\frac{\mu_{\ell\sigma}\cdot e_{\ell\sigma}}{\alpha_\sigma} + \sum_{m\tau}\sum G_{\ell\sigma m\tau}\mu_{m\tau}\cdot e_{m\tau}] =$$

$$\frac{1}{N}\sum_{\ell}\exp(2\pi i j\ell/N)[E(r_{\ell\sigma})\cdot e_{\ell\sigma} - ib_\sigma\, k\times E(r_{\ell\sigma})\cdot e'_{\ell\sigma}]$$

examination of the normal modes shows that:

$$\mu_{m\tau}\cdot e_{m\tau} = \exp[2\pi i j(m-\ell)/N]\mu_{\ell\tau}\cdot e_{\ell\tau}$$

with this substitution:

$$\frac{1}{N}\sum\exp[2\pi i j\ell/N]\sum_{\tau}\mu_{\ell\tau}\cdot e_{\ell\tau}\{\frac{\delta_{\sigma\tau}}{\alpha_\sigma} + \sum_{m} G_{\ell\sigma m\tau}\exp[2\pi i j(m-\ell)/N]\} =$$

$$\frac{1}{N}\sum_{\ell}\exp[2\pi i j\ell/N]\{E(r_{\ell\sigma})\cdot e_{\ell\sigma} - ib_\sigma\, k\times E(r_{\ell\sigma})\cdot e'_{\ell\sigma}\}\ .$$

Solving this set of $N\eta$ equations we obtain:

$$\mu_\tau(j)\cdot e_\tau = \frac{1}{N}\sum_{\ell}\exp[2\pi i j\ell/N]\mu_{\ell\tau}\cdot e_{\ell\tau} = \frac{1}{N}\sum\exp[2\pi i j\ell/N]\sum_{\sigma}A^j_{\tau\sigma}[E(r_{\ell\sigma})\cdot e_{\ell\sigma} - ib_\sigma\, k\times E(r_{\ell\sigma})\cdot e'_{\ell\sigma}\ ].$$

The coefficients $A^j_{\tau\sigma}$ are obtained by inverting the following $\eta\times\eta$ matrix:

$$A^{j}_{\tau\sigma} = \{\frac{\delta_{\sigma\tau}}{\alpha_\sigma} + \sum_m G_{\ell\sigma m\tau}\exp[2\pi i j(m-\ell)/N]\}^{-1}. \qquad (1)$$

At this point we will introduce the helical geometry explicitly using the rotation operator to express $\mathbf{e}_{\ell\sigma}$ in terms of $\mathbf{e}_{0\sigma}$. Also the unit cell subscript will be dropped for the 0 unit cell:

$$\mu_\tau(j)\cdot\mathbf{e} = \frac{1}{N}\sum_\ell \exp[2\pi i j\ell/N] \sum_\sigma A^{j}_{\tau\sigma}[\mathbf{E}(\mathbf{r}_{\ell\sigma})\cdot\mathbf{R}^{\ell}\cdot\mathbf{e}_\sigma - i b_\sigma\ k\times\mathbf{E}(\mathbf{r}_{\ell\sigma})\cdot\mathbf{R}^{\ell}\cdot\mathbf{e}'_\sigma] \qquad (2)$$

We can write a similar expression for the magnetic dipole moment $\mathbf{m}_\tau(j)$. The macroscopic electric polarization for the j normal mode, P(j), and the macroscopic magnetic polarization for the j normal mode, M(j), are related to the microscopic dipoles by the following equations:

$$P(j) = \sum_\tau \langle \mu_\tau(j)\ \exp[i\mathbf{k}\cdot\mathbf{r}_\tau]\rangle$$

$$M(j) = \sum_\tau \langle \mathbf{m}_\tau(j)\ \exp[i\mathbf{k}\cdot\mathbf{r}_\tau]\rangle \qquad (3)$$

The refractive index of the j normal mode is:

$$n^2(j)-1 = 4\pi\mathbf{E}^*\cdot[P(j) - \frac{c}{\omega}\ k\times M(j)]/\mathbf{E}^*\cdot\mathbf{E}$$

where * denotes the complex conjugate. We are interested in the refractive index for incident circularly polarized light:

$$n^2_\pm - 1 = \frac{4\pi}{N}\sum_j\sum_\ell \exp(2\pi i j\ell/N) \sum_{\ell,\tau} A^{j}_{\tau\sigma}[\varepsilon'_\pm\cdot\mathbf{R}^{\ell}\cdot\mathbf{e}_\sigma - i2\ b_\sigma\ k\times\varepsilon'_\pm\cdot\mathbf{R}^{\ell}\cdot\boldsymbol{\varepsilon}'_\sigma]$$

$$\times \exp(i\mathbf{k}\cdot(\mathbf{r}_\tau-\mathbf{r}_{\ell\sigma}))\mathbf{e}_\tau\cdot\varepsilon'_\mp \qquad (4)$$

where $n_{\pm}$ are the refractive indices for right and left circularly polarized light propagating in the k direction, and $\varepsilon'_{\pm}$ are the unit vectors for right and left circular polarization in the plane perpendicular to k. The space averaging indicated by the angle brackets in equation (3) is done by calculating the refractive index along each axis in the molecular reference frame and averaging:

$$\langle n^2-1\rangle = \frac{1}{3}\langle n^2-1\rangle_{33} + \frac{2}{3}\langle n^2-1\rangle_{\perp}$$

$$\langle n^2-1\rangle_{\perp} = \frac{1}{2}[\langle n^2-1\rangle_{11} + \langle n^2-1\rangle_{22}] .$$

We have now shown that a matrix of dimension $\eta\times\eta$ must be inverted rather than the original $\eta N\times\eta N$ matrix. However according to equation (1) we must invert a different matrix for each normal mode j. Fortunately, the sum over ℓ in equation (4) leads to selection rules (in the limit of large N). These selection rules determine which of the polymer transition normal modes is excited, and for each allowed transition we must solve η equations in η unknowns.

As an example consider light propagating along the helix or ε_3 axis:

$$\mathbf{k} = k\varepsilon_3 \qquad \varepsilon'_{\pm} = \varepsilon_{\pm}$$

$$\mathbf{k}\cdot\mathbf{r}_{\ell\sigma} = k\ell\Delta z + \mathbf{k}\cdot\mathbf{r}_{\sigma}$$

the sum over ℓ in equation (4) includes the product:

$$\frac{1}{N}\sum_{\ell}\exp[2\pi i j\ell/N]\exp[-ik\ell\Delta z][\exp(i\ell\theta)\varepsilon_-\varepsilon_+ + \exp(-i\ell\theta)\varepsilon_+\varepsilon_- + \varepsilon_3\varepsilon_3]$$

then the selection rules are:

$$\delta(\frac{2\pi j}{N} - k\Delta z + \theta)\varepsilon_-\varepsilon_+ + \delta(\frac{2\pi j}{N} - k\Delta z - \theta)\varepsilon_+\varepsilon_- + \delta(\frac{2\pi j}{N} - k\Delta z)\varepsilon_3\varepsilon_3.$$

These selection rules are for right and left circular polarization in the ε_1, ε_2 plane and linear polarization in the ε_3 direction. We must solve three $\eta\times\eta$ matrices corresponding to the three selection rules. In fact as we will show later, to first order in $k\Delta z$ only two matrices need be inverted.

To find the CD = $\varepsilon_L - \varepsilon_R$ of the system, $n_- - n_+$, the difference between the refractive indices for left and right cilcularly polarized light will be calculated. For light propagating along ε_3,:

$$(n_-^2 - n_+^2)_{\|} = 4\pi\sum_{\sigma,\tau}(A^+_{\tau\sigma}\,\mathbf{e}_\tau\cdot(\varepsilon_+\varepsilon_-)\cdot\mathbf{e}_\sigma - A^-_{\tau\sigma}\mathbf{e}_\sigma\cdot(\varepsilon_+\varepsilon_-)\cdot\mathbf{e}_\tau)\exp[ik\cdot r_{\sigma\tau}]$$

$$+ 8\pi\sum_{\sigma,\tau} kb_\sigma(A^+_{\tau\sigma}\mathbf{e}_\tau\cdot(\varepsilon_+\varepsilon_-)\mathbf{e}'_\sigma + A^-_{\tau\sigma}\mathbf{e}'_\sigma\cdot(\varepsilon_+\varepsilon_-)\cdot\mathbf{e}_\tau)\exp[ik\cdot r_{\sigma\tau}] \quad (5)$$

where

$$A^{\pm}_{\tau\sigma} = A^{(N/2\pi)(k\Delta z\pm\theta)}_{\tau\sigma} \qquad \mathbf{r}_{\sigma\tau} = \mathbf{r}_\tau - \mathbf{r}_\sigma .$$

We want this difference expressed to first order in k. The magnetic contribution is already first order in k, so that the k dependence in $A^{\pm}_{\tau\sigma}$ and $\exp[ik\cdot r_{\sigma\tau}]$ can be ignored for these terms. In the electric contribution both $A^{\pm}_{\tau\sigma}$ and $\exp(ik\cdot r_{\sigma\tau})$ must be expanded to first order in k. Expanding

the exponential:

$$\exp(ik\cdot r_{\sigma\tau}) = 1 + ik\cdot r_{\sigma\tau} \quad .$$

To first order in k:

$$A^{\pm}_{\tau\sigma} = A^{(N/2\pi)(k\Delta z\pm\theta)}_{\tau\sigma} =$$

$$[\frac{\delta_{\sigma\tau}}{\alpha_\sigma} + \sum_{m=-nc}^{nc} G_{0\sigma m\tau}\exp(\pm im\theta) + ik\Delta z \sum_{m=-nc}^{nc} G_{0\sigma m\tau}\exp(\pm im\theta)]^{-1} \quad .$$

The sums over m run over positive and negative values to convergence. We will use the same procedure we used in Chapter III to expand A_{ij} to first order in G_{ij}. In general:

$$(C + k\Delta zD)(C^{-1} + k\Delta zF) = I$$

$$I + k\Delta z(DC^{-1} + CF) + \cdots = I$$

and:

$$F = -C^{-1}DC^{-1}.$$

To first order in $k\Delta z$:

$$(C + k\Delta zD)^{-1} = C^{-1} - k\Delta zC^{-1}DC^{-1}$$

$$A^{\pm} = A^{\pm\theta}_{\tau\sigma} - k\Delta z\ [A^{\pm\theta}]_{\tau\sigma}$$

where:

$$A^{\pm\theta} = [\frac{\delta_{\sigma\tau}}{\alpha_\sigma} + \sum_m G_{o\sigma m\tau}\exp(\pm im\theta)]^{-1}.$$

Since $\sum_m G_{o\sigma m\tau}\exp(im\theta) = \sum_m G_{o\tau m\sigma}\exp(-im\theta)$

$$A^{-\theta}_{\tau\sigma} = A^{\theta}_{\sigma\tau} \quad .$$

Therefore only two matrices need be inverted, namely A^{θ} and $A^{0} = A^{(N/2\pi)(0)}$. Finally,

$$[A^{\pm\theta}]_{\tau\sigma} = i \sum_{\gamma,\varepsilon} A^{\pm\theta}_{\tau\gamma}[\sum_{m} mG_{0\gamma m\varepsilon}\exp(\pm im\theta)]A^{\pm\theta}_{\varepsilon\sigma}$$

and

$$[A^{-\theta}]_{\tau\sigma} = -[A^{\theta}]_{\sigma\tau}$$

therefore,

$$A^{+}_{\tau\sigma} = A^{\theta}_{\tau\sigma} - k\Delta z[A^{\theta}]_{\tau\sigma}$$

$$A^{-}_{\tau\sigma} = A^{\theta}_{\sigma\tau} + k\Delta z[A^{\theta}]_{\sigma\tau} .$$

Using these results and dividing equation (5) by $n_{-}+n_{+} = 2kc/\omega$, we find:

$$(n_{-}-n_{+})_{\|} = \frac{4\pi\omega}{c}[a_{\|} + b_{\|} + c_{\|}]$$

$$a_{\|} = -\Delta z \sum_{\sigma,\tau} [A^{\theta}]_{\tau\sigma}\mathbf{e}_{\tau}\cdot(\varepsilon_{+}\varepsilon_{-})\cdot\mathbf{e}_{\sigma}$$

$$b_{\|} = i \sum_{\sigma,\tau} A^{\theta}_{\tau\sigma}\ \mathbf{e}_{\tau}\cdot(\varepsilon_{+}\varepsilon_{-})\cdot\mathbf{e}_{\sigma}\ \boldsymbol{\varepsilon}_{3}\cdot\mathbf{r}_{\sigma\tau} \qquad (6)$$

$$c_{\|} = \sum_{\sigma,\tau} A^{\theta}_{\tau\sigma}\ [\mathbf{e}_{\tau}\cdot(\varepsilon_{+}\varepsilon_{-})\cdot\mathbf{e}'_{\sigma}\ b_{\sigma} + \mathbf{e}'_{\tau}\cdot(\varepsilon_{+}\varepsilon_{-})\cdot\mathbf{e}_{\sigma}\ b_{\tau}]$$

For light propagating perpendicular to the helix axis:

$$\exp[i\mathbf{k}\cdot(\mathbf{r}_{\tau}-\mathbf{r}_{\ell\sigma})] = \exp[-i\mathbf{k}\cdot\mathbf{R}^{\ell}\cdot\mathbf{r}_{\sigma}]\exp[i\mathbf{k}\cdot\mathbf{r}_{\tau}].$$

Since the exponential may be written as a power series in $-i\mathbf{k}\cdot\mathbf{R}^{\ell}\cdot\mathbf{r}_{\sigma}$ this would imply selection rules including θ, 2θ,

3θ, etc. However, R is unitary and we assume that all radial distances are small compared to the wavelength of light, therefore:

$$\exp[ik\cdot(r_\theta - r_{\ell\sigma})] = 1 - ik\cdot R^\ell \cdot r_\sigma + ik\cdot r_\tau .$$

Substituting this into equation (4):

$$n_\pm^2 - 1 = \frac{4\pi}{N} \sum_j \sum_\ell \exp[2\pi i j\ell/N] \sum_{\sigma,\tau} A^j_{\tau\sigma} \times$$

$$(\varepsilon'_\pm \cdot R^\ell \cdot e_\sigma - 2ib_\sigma\, k\times\varepsilon'_\pm \cdot R^\ell \cdot e'_\sigma] \times$$

$$(1 - ik\cdot R^\ell \cdot r_\sigma + ik\cdot r_\tau) e_\tau \cdot \varepsilon'_\mp .$$

For the ε_1 and ε_2 direction we will expand each of three terms to first order in k. The three terms are $b_\sigma k\times\varepsilon'_\pm$, $k\cdot R^\ell \cdot r_\sigma$, and $k\cdot r_\tau$. For light incident along ε_1:

$$k = k\varepsilon_1$$

$$\varepsilon'_\pm = \frac{1}{\sqrt{2}} (\varepsilon_2 \pm i\varepsilon_3)$$

$$k\times\varepsilon_\pm = \mp ik\varepsilon_\pm .$$

The magnetic term is

$$n_\pm^2 - 1 = \frac{4\pi}{N} \sum_j \sum_\ell \exp(2\pi i\ell j/N) \sum_{\sigma,\tau} A^j_{\tau\sigma} (\mp 2k) b_\sigma\, \varepsilon'_\pm \cdot R^\ell \cdot e'_\sigma\, e_\tau \cdot \varepsilon'_\mp .$$

The selection rules are

$$(j + \frac{N\theta}{2\pi})\varepsilon'_\pm \cdot \varepsilon_- \varepsilon_+ + (j - \frac{N\theta}{2\pi})\varepsilon'_\pm \cdot \varepsilon_+ \varepsilon_- + \delta(j)\varepsilon'_\pm \cdot \varepsilon_3 \varepsilon_3$$

and

$$n_{\pm}^2-1 = \mp 8\pi k \sum_{\sigma,\tau} b_\sigma[(\tfrac{-i}{2})A_{\tau\sigma}^{-\theta}\varepsilon_+\cdot e'_\sigma + (\tfrac{i}{2})A_{\tau\sigma}^{\theta}\varepsilon_-\cdot e'_\sigma \pm$$

$$(\tfrac{i}{\sqrt{2}})A_{\tau\sigma}^{\theta}\varepsilon_3\cdot e'_\sigma]e_\tau\cdot\varepsilon'_{\mp}$$

$$\varepsilon'_{\pm}\cdot\varepsilon_- = -i/2, \quad \varepsilon'_{\pm}\cdot\varepsilon_+ = i/2, \quad \varepsilon'_{\pm}\cdot\varepsilon_3 = \pm i/\sqrt{2}$$

since:

$$\varepsilon'_- + \varepsilon'_+ = \frac{2}{\sqrt{2}}\,\varepsilon_2 \qquad \varepsilon'_+ - \varepsilon'_- = \frac{2i}{\sqrt{2}}\,\varepsilon_3$$

$$(n_-^2-n_+^2) = 8\pi k \sum_{\sigma,\tau} b_\sigma[(\tfrac{-i}{2})A_{\tau\sigma}^{-\theta}\varepsilon_+\cdot e'_\sigma + (\tfrac{i}{2})A_{\tau\sigma}^{\theta}\varepsilon_-\cdot e'_\sigma](\tfrac{2}{\sqrt{2}})\varepsilon_2\cdot e_\tau$$

$$+ 8\pi k \sum_{\sigma,\tau} b_\sigma A_{\tau\sigma}^{0}\varepsilon_3\cdot e'_\sigma\ \varepsilon_3\cdot e_\tau. \qquad (7)$$

We will now examine the magnetic contribution for light incident along ε_2:

$$k = k\varepsilon_2 \qquad \varepsilon'_{\pm} = \frac{1}{\sqrt{2}}(\varepsilon_3 \pm i\varepsilon_1) \qquad k\times\varepsilon'_+ = \mp i\varepsilon'_{\pm}\ .$$

The selection rules are the same but now

$$\varepsilon_{\pm}\cdot\varepsilon'_+ = \frac{i}{2} \qquad \varepsilon'_-\cdot\varepsilon_{\pm} = \frac{-i}{2} \qquad \varepsilon'_{\pm}\cdot\varepsilon_3 = \frac{1}{\sqrt{2}}$$

so that:

$$(n_{\pm}^2-1) = \mp 8\pi k \sum_{\sigma,\tau} b_\sigma[(\tfrac{\pm i}{2})(A_{\tau\sigma}^{-\theta}\varepsilon_+\cdot e'_\sigma + A_{\tau\sigma}^{\theta}\varepsilon_-\cdot e'_\sigma) +$$

$$(\tfrac{1}{\sqrt{2}})A_{\tau\sigma}^{0}\varepsilon_3 e'_\sigma]\varepsilon'_{\mp}\cdot e_\tau$$

since:

$$\varepsilon_+' + \varepsilon_- = \frac{2}{\sqrt{2}}\varepsilon_3 \qquad \varepsilon_+' - \varepsilon_-' = \frac{2i}{\sqrt{2}}\varepsilon_1 ,$$

$$(n_-^2 - n_+^2) = 8\pi k \sum_{\sigma,\tau} b_\sigma \left(\frac{-i}{2}\right)\left(A_{\tau\sigma}^{-\theta}\varepsilon_+\cdot e_\sigma' + A_{\tau\sigma}^{\theta}\varepsilon_-\cdot e_\sigma'\right)\left(\frac{2i}{\sqrt{2}}\right)\varepsilon_1\cdot e_\tau$$

$$+ 8\pi k \sum_{\sigma,\tau} b_\sigma A_{\tau\sigma}^{0}\varepsilon_3\cdot e_\sigma'\ \varepsilon_3\cdot e_\tau . \qquad (8)$$

Combining equations (7) and (8) and remembering that

$$\varepsilon_\pm = \frac{1}{\sqrt{2}}(\varepsilon_1 \pm i\varepsilon_2),$$

$$(n_-^2 - n_+^2) = 8\pi k \sum_{\sigma,\tau} b_\sigma [A_{\tau\sigma}^{-\theta}\varepsilon_+\cdot e_\sigma'\ \varepsilon_-\cdot e_\tau + A_{\tau\sigma}^{\theta}\varepsilon_-\cdot e_\sigma'\ \varepsilon_+\cdot e_\tau$$

$$+ 2A_{\tau\sigma}^{0}\varepsilon_3\cdot e_\sigma'\ \varepsilon_3\cdot e_\tau] . \qquad (9)$$

This will be our technique for the other two terms as well. We will calculate the contributions along ε_1 and ε_2, and by summing them, express the contribution perpendicular to the helix in terms of ε_+ and ε_-.

Next we consider the $ik\cdot r_\tau$ terms. The selection rules are the same as those for the magnetic terms. For light incident along ε_1:

$$n_\pm^2 - 1 = 4\pi i k \sum_{\sigma,\tau} \left[\left(\frac{-}{2}\right)A_{\tau\sigma}^{-\theta}\varepsilon_+\cdot e_\sigma + \left(\frac{-}{2}\right)A_{\tau\sigma}^{\theta}\varepsilon_-\cdot e_\sigma \frac{\pm}{\sqrt{2}}\varepsilon_3\cdot e_\sigma A_{\tau\sigma}^{0}\right] \times$$

$$e_\tau\cdot\varepsilon_\mp'\ \varepsilon_1\cdot r_\tau$$

$$n_-^2 - n_+^2 = 4\pi ik \sum_{\sigma,\tau} [(\frac{-i}{2})A^{-\theta}_{\tau\sigma}\varepsilon_+\cdot e_\sigma + (\frac{i}{2})A^{\theta}_{\tau\sigma}\varepsilon_-\cdot e_\sigma](\frac{2i}{\sqrt{2}})e_\tau\cdot\varepsilon_3\ \varepsilon_1\cdot r_\tau$$

$$-4\pi ik \sum_{\sigma,\tau} A^0_{\tau\sigma}\varepsilon_3\cdot e_\sigma\ e_\tau\cdot\varepsilon_2\ \varepsilon_1\cdot r_\tau\ . \qquad (10)$$

For light incident along ε_2:

$$n_\pm^2 - 1 = 4\pi ik \sum_{\sigma,\tau} [(\frac{\pm i}{2})(A^{-\theta}_{\tau\sigma}\varepsilon_+\cdot e_\sigma + A^{\theta}_{\tau\sigma}\varepsilon_-\cdot e_\sigma) + \frac{1}{\sqrt{2}} A^0_{\tau\sigma}\varepsilon_3\cdot e_\sigma] \times$$

$$\varepsilon'_\pm\cdot e_\tau\ \varepsilon_2\cdot r_\tau$$

$$n_-^2 - n_+^2 = 4\pi ik \sum_{\sigma,\tau} [(\frac{-i}{2})(A^{-\theta}_{\tau\sigma}\varepsilon_+\cdot e_\sigma + A^{\theta}_{\tau\sigma}\varepsilon_-\cdot e_\sigma)(\frac{2}{\sqrt{2}})\varepsilon_3\cdot e_\tau\ \varepsilon_2\cdot r_\tau$$

$$+4\pi ik \sum_{\sigma,\tau} (i)A^0_{\tau\sigma}\varepsilon_3\cdot e_\sigma\ \varepsilon_1\cdot e_\tau\ \varepsilon_2\cdot r_\tau\ . \qquad (11)$$

Combining equations (10) and (11):

$$(n_-^2 - n_+^2) = 4\pi ik \sum_{\sigma,\tau} [A^{-\theta}_{\tau\sigma}\varepsilon_+\cdot e_\sigma\ \varepsilon_-\cdot r_\tau\ \varepsilon_3\cdot e_\tau$$

$$- A^{\theta}_{\tau\sigma}\varepsilon_-\cdot e_\sigma\ \varepsilon_+\cdot r_\tau\ \varepsilon_3\cdot e_\tau]$$

$$+ 4\pi ik \sum_{\sigma,\tau} A^0_{\sigma\tau}\ e_\sigma\cdot\varepsilon_3(\varepsilon_+\cdot r_\tau\ \varepsilon_-\cdot e_\tau - \varepsilon_-\cdot r_\tau\ \varepsilon_+\cdot e_\tau) \qquad (12)$$

where in the last term we used the identity:

$$a\cdot(\varepsilon_+\varepsilon_- - \varepsilon_-\varepsilon_+)\cdot b = ib\times a.$$

Finally, the contribution of $-ik\cdot R\cdot r_\sigma$, will have new selection rules:

$$\delta(\tfrac{2\pi j}{N} + \theta)\varepsilon'_{\pm}\cdot\varepsilon_3\ \varepsilon_3\cdot e_\sigma\ k\cdot\varepsilon_-\ \varepsilon_+\cdot r_\sigma$$

$$+\delta(\tfrac{2\pi j}{N} - \theta)\varepsilon'_{\pm}\cdot\varepsilon_3\ \varepsilon_3\cdot e_\sigma\ k\cdot\varepsilon_+\ \varepsilon_-\cdot r_\sigma$$

$$+\delta(\tfrac{2\pi j}{N})[\varepsilon'_{\pm}\cdot\varepsilon_-\ \varepsilon_+\cdot e_\sigma\ k\cdot\varepsilon_+\ \varepsilon_- r_\sigma\ +\ \varepsilon'_{\pm}\cdot\varepsilon_+\ \varepsilon_-\cdot e_\sigma\ k\cdot\varepsilon_-\ \varepsilon_+\cdot r_\sigma]$$

$$+\delta(\tfrac{2\pi j}{N} + 2\theta)\varepsilon'_{\pm}\cdot\varepsilon_-\ \varepsilon_+\cdot e_\sigma\ k\cdot\varepsilon_-\ \varepsilon_+\cdot r_\sigma$$

$$+\delta(\tfrac{2\pi j}{N} - 2\theta)\varepsilon'_{\pm}\cdot\varepsilon_+\ \varepsilon_-\cdot e_\sigma\ k\cdot\varepsilon_+\ \varepsilon_-\cdot r_\sigma\ .$$

With these selection rules along ε_1

$$n^2-1 = -4\pi i k \sum_{\sigma,\tau}(\tfrac{\pm i}{2})[A^{-\theta}_{\tau\sigma}\varepsilon_3\cdot e_\sigma\ \varepsilon_+\cdot r_\sigma + A^{\theta}_{\tau\sigma}\varepsilon_3\cdot e_\sigma\ \varepsilon_-\cdot r_\sigma]\varepsilon'_{\mp}\cdot e_\tau$$

$$+4\pi k \sum_{\sigma,\tau}(\tfrac{1}{2})A^0_{\tau\sigma}[\varepsilon_-\cdot e_\sigma\ \varepsilon_+\cdot r_\sigma - \varepsilon_+\cdot e_\sigma\ \varepsilon_-\cdot r_\sigma](\tfrac{1}{\sqrt{2}})\varepsilon'_{\mp}\cdot e_\tau$$

$$+4\pi k \sum_{\sigma,\tau}(\tfrac{1}{2})[A^{2\theta}_{\tau\sigma}\varepsilon_-\cdot e_\sigma\varepsilon_-\cdot r_\sigma - A^{-2\theta}_{\tau\sigma}\varepsilon_+\cdot e_\sigma\ \varepsilon_+\cdot r_\sigma](\tfrac{1}{\sqrt{2}})\varepsilon'_{\mp}\cdot e_\tau$$

$$n_-^2-n_+^2 = -4\pi i k \sum_{\sigma,\tau}\{\tfrac{-i}{\sqrt{2}}[A^{-\theta}_{\tau\sigma}\varepsilon_3\cdot e_\sigma\ \varepsilon_+\cdot r_\sigma + A^{\theta}_{\tau\sigma}\varepsilon_3\cdot e_\sigma\ \varepsilon_-\cdot r_\sigma]\varepsilon_2\cdot e_\tau$$

$$-\tfrac{1}{2}A^0_{\tau\sigma}[\varepsilon_-\cdot e_\sigma\ \varepsilon_+\cdot r_\sigma - \varepsilon_+\cdot e_\sigma\ \varepsilon_-\cdot r_\sigma]\varepsilon_3\cdot e_\tau$$

$$-\tfrac{1}{2}[A^{2\theta}_{\tau\sigma}\varepsilon_-\cdot e_\sigma\ \varepsilon_-\cdot r_\sigma - A^{-2\theta}_{\tau\sigma}\varepsilon_+\cdot e_\sigma\ \varepsilon_+\cdot r_\sigma]\varepsilon_3\cdot e_\tau\} \qquad (13)$$

For light along ε_2:

$$n_{\pm}^2-1 = 4\pi ik \sum_{\sigma,\tau}[(\tfrac{-i}{2})A_{\tau\sigma}^{-\theta}\varepsilon_3\cdot e_\sigma\ \varepsilon_+\cdot r_\sigma + (\tfrac{i}{2})A_{\tau\sigma}^{\theta}\varepsilon_3\cdot e_\sigma\ \varepsilon_-\cdot r_\sigma]\varepsilon_{\mp}'\cdot e_\tau$$

$$+4\pi ik \sum_{\sigma,\tau}(\tfrac{\pm 1}{2})[A_{\tau\sigma}^{0}(\varepsilon_+\cdot e_\sigma\ \varepsilon_-\cdot r_\sigma - \varepsilon_-\cdot e_\sigma\ \varepsilon_+\cdot r_\sigma)(\tfrac{1}{\sqrt{2}})]\varepsilon_{\mp}'\cdot e_\tau$$

$$+4\pi ik \sum_{\sigma,\tau}(\tfrac{\pm 1}{2})[A_{\tau\sigma}^{2\theta}\varepsilon_-\cdot e_\sigma\ \varepsilon_-\cdot r_\sigma - A_{\tau\sigma}^{-2\theta}\varepsilon_+\cdot e_\sigma\ \varepsilon_+\cdot r_\sigma](\tfrac{1}{\sqrt{2}})\varepsilon_{\mp}'\cdot e_\tau$$

$$n_-^2-n_+^2 = -2\pi ik\{\tfrac{-1}{\sqrt{2}}[A_{\tau\sigma}^{\theta}\varepsilon_3\cdot e_\sigma\ \varepsilon_-\cdot r_\sigma - A_{\tau\sigma}^{-\theta}\varepsilon_3\cdot e_\sigma\ \varepsilon_+\cdot r_\sigma]\varepsilon_1\cdot e_\tau$$

$$-\tfrac{1}{2}A_{\tau\sigma}^{0}[\varepsilon_-\cdot e_\sigma\ \varepsilon_+\cdot r_\sigma - \varepsilon_+\cdot e_\sigma\ \varepsilon_-\cdot r_\sigma]\varepsilon_3\cdot e_\tau$$

$$+\tfrac{1}{2}[A_{\tau\sigma}^{2\theta}\varepsilon_-\cdot e_\sigma\ \varepsilon_-\cdot r_\sigma - A_{\tau\sigma}^{-2\theta}\varepsilon_+\cdot e_\sigma\ \varepsilon_+\cdot r_\sigma]\varepsilon_3\cdot e_\tau\}. \qquad (14)$$

Combining equations (13) and (14):

$$(n_-^2-n_+^2) = -2\pi ik \sum_{\sigma,\tau}[A_{\tau\sigma}^{-\theta}r_\sigma\cdot(\varepsilon_+\varepsilon_-)\cdot e_\tau\ \varepsilon_3\cdot e_\sigma - A_{\tau\sigma}^{\theta}\varepsilon_\tau\cdot(\varepsilon_+\varepsilon_-)\cdot r_\sigma\varepsilon_3\cdot e_\sigma]$$

$$-4\pi ik \sum_{\sigma,\tau}A_{\tau\sigma}^{0}[e_\sigma\cdot(\varepsilon_+\varepsilon_-)\cdot r_\sigma\ \varepsilon_3\cdot e_\tau - r_\sigma\cdot(\varepsilon_+\varepsilon_-)\cdot e_\sigma\ \varepsilon_3\cdot e_\tau]. \qquad (15)$$

Notice that the terms involving selection rules of 2θ for incident light along ε_1 cancel those for incident light along ε_2. In other words, upon averaging around ε_3 there are no contributions from selection rules including multiples of θ (to first order in k). Comparing equations (12) and (15) we see that the $ik\cdot r_\tau$ and $-ik\cdot R^{\ell}\cdot r$ phase differences make the same contribution to the CD. The perpendicular CD has equal contributions from inter- and intra-unit cell phase differences. This is because both were expanded to

first order in k before the selection rules were taken. The sum of the three contributions, equations (9), (12) and (15) is:

$$(n_- - n_+)_\perp = \frac{2\pi\omega}{c} [b_\perp + c_\perp]$$

$$b_\perp = i \sum_{\sigma,\tau} A^{\theta}_{\tau\sigma} [e_\tau \cdot (\varepsilon_+ \varepsilon_-) \cdot r_\sigma \; \varepsilon_3 \cdot e_\sigma - r_\tau \cdot (\varepsilon_+ \varepsilon_-) \cdot e_\sigma \; \varepsilon_3 \cdot e_\tau]$$

$$+ i \sum_{\sigma,\tau} A^{0}_{\tau\sigma} [r_\tau \cdot (\varepsilon_+ \varepsilon_-) \cdot e_\tau \; \varepsilon_3 \cdot e_\sigma - e_\tau \cdot (\varepsilon_+ \varepsilon_-) \cdot r_\tau \; \varepsilon_3 \cdot e_\sigma]$$

$$c_\perp = \sum_{\sigma,\tau} A^{\theta}_{\tau\sigma} [e_\tau \cdot (\varepsilon_+ \varepsilon_-) \cdot e'_\sigma \; b_\sigma + e'_\tau \cdot (\varepsilon_+ \varepsilon_-) \cdot e_\sigma \; b_\tau]$$

$$+ 2 \sum_{\sigma,\tau} A^{0}_{\tau\sigma} \; e_\tau \cdot (\varepsilon_3 \varepsilon_3) \cdot e'_\sigma \; b_\sigma \qquad (16)$$

The extinction coefficient is related to the refractive index by:

$$\varepsilon = C_1 \; \mathrm{Im}\{n\} \qquad C_1 = \frac{-2N_o\omega}{2303cN} . \qquad (17)$$

N_o is Avogadro's number and N is the number of molecules per unit volume. The parallel and perpendicular CD are:

$$(\varepsilon_L - \varepsilon_R)_\parallel = \frac{4\pi\omega}{c} C_1 \; \mathrm{Im}[a_\parallel + b_\parallel + c_\parallel]$$

and

$$(\varepsilon_L - \varepsilon_R)_\perp = \frac{2\pi\omega}{c} C_1 \; \mathrm{Im}[b_\perp + c_\perp]. \qquad (18)$$

The total average CD is:

$$CD = \frac{1}{3} CD_{\parallel} + \frac{4}{3} \frac{\pi\omega}{c} C_1 \, Im\{b_{\perp} + c_{\perp}\}. \qquad (19)$$

Similarly for the optical rotary dispersion (ORD) in deg-cm^2-decimole^{-1}:

$$[\phi]_{\perp} = \frac{9N_o}{N} \frac{\omega}{c} Re(n_- - n_+)_{\perp} = 18\frac{N_o}{N} \frac{\omega^2}{c^2} [b_{\perp} + c_{\perp}]$$

$$[\phi]_{\parallel} = \frac{9N_o}{N} \frac{\omega}{c} Re(n_- - n_+)_{\parallel} = 36\frac{N_o}{N} \frac{\omega^2}{c^2} [a_{\parallel} + b_{\parallel} + c_{\parallel}]$$

$$[\phi] = \frac{1}{3} [\phi]_{\parallel} + \frac{2}{3} [\phi]_{\perp}. \qquad (20)$$

There are three contributions to the optical activity for light propagating along ε_3. $a_{\parallel}$, the helical contribution, is due to the difference in the selection rules for right and left circularly polarized light propagating parallel to a helix. It is proportional to Δz, the distance between unit cells. $a_{\parallel}$ is called the helical term because it derives from the helical arrangement between unit cells. $b_{\parallel}$, the residual contribution is due to phase differences within the unit cell. It is proportional to the distances between electric dipoles within the unit cell projected on the ε_3 axis: $\varepsilon_3 \cdot r_{\sigma\tau}$. $c_{\parallel}$, the magnetic contribution, is due to coupling between electric and magnetic moments within the unit cell.

For light propagating perpendicular to the helix axis there is no term corresponding to $a_{\parallel}$. $b_{\perp}$ is due to phase

differences within the unit cell projected on the plane perpendicular to the helix axis. There is also a magnetic contribution for light propagating perpendicular to the helix axis, $c_{\perp}$.

To determine the average extinction coefficient $\varepsilon = (\varepsilon_L + \varepsilon_R)/2$ we can ignore the k dependence in equation (4). To zero order in k equation (4) is:

$$n_{\pm}^2 - 1 = \frac{4\pi}{N} \sum_j \sum_\ell \exp(2\pi i j \ell / N) \sum_{\sigma,\tau} A_{\tau\sigma}^j \, \varepsilon_{\pm}' \cdot R^\ell \cdot e_\sigma \, e_\tau \cdot \varepsilon_{\mp}' \,. \qquad (21)$$

Thus, for absorption the selection rules are:

$$\delta(\tfrac{2\pi j}{N} + \theta)\varepsilon_- \varepsilon_+ + \delta(\tfrac{2\pi j}{N} - \theta)\varepsilon_+ \varepsilon_+ + \delta(\tfrac{2\pi j}{N})\varepsilon_3 \varepsilon_3$$

for light along ε_3

$$n_{\pm}^2 - 1 = 4\pi \sum_{\sigma,\tau} A_{\tau\sigma}^{\mp\theta} \, \varepsilon_{\pm} \cdot e_\sigma \, \varepsilon_{\mp} \cdot e_\tau$$

$$n_+^2 + n_-^2 - 2 = 4\pi \sum_{\sigma'\tau} [A_{\tau\sigma}^{-\theta} \, \varepsilon_+ \cdot e_\sigma \, \varepsilon_- \cdot e_\tau + A_{\tau\sigma}^{\theta} \, \varepsilon_- \cdot e_\sigma \, \varepsilon_+ \cdot e_\tau]$$

$$= 8\pi \sum_{\sigma,\tau} A_{\tau\sigma}^{\theta} \varepsilon_- \cdot e_\sigma \, \varepsilon_+ \cdot e_\tau \qquad (22)$$

for light along ε_1:

$$n_{\pm}^2 - 1 = 4\pi \sum_{\sigma,\tau} [(\tfrac{-i}{2}) A_{\tau\sigma}^{-\theta} \varepsilon_+ \cdot e_\sigma + (\tfrac{i}{2}) A_{\tau\sigma}^{\theta} \varepsilon_- \cdot e_\sigma \pm (\tfrac{i}{\sqrt{2}}) A_{\tau\sigma}^{0} \varepsilon_3 \varepsilon_3] \varepsilon_{\mp}' \cdot e_\tau$$

$$n_+^2 + n_-^2 - 2 = 4\pi \sum_{\sigma,\tau} [A_{\tau\sigma}^{\theta} (\tfrac{i}{2}) \varepsilon_- \cdot e_\sigma - (\tfrac{i}{2}) A_{\tau\sigma}^{-\theta} \varepsilon_+ \cdot e_\sigma] \, \frac{2}{\sqrt{2}} \, \varepsilon_2 \cdot e_\tau$$

$$+ 4\pi \sum_{\sigma,\tau} A_{\tau\sigma}^{0} \, \varepsilon_3 \cdot e_\tau \, \varepsilon_3 \cdot e_\sigma \qquad (23)$$

for light along ε_2:

$$n_{\pm}^2-1 = 4\pi \sum_{\sigma,\tau} (\tfrac{\pm i}{2})[A_{\tau\sigma}^{-\theta}\varepsilon_+\cdot e_\sigma + A_{\tau\sigma}^{\theta}\varepsilon_-\cdot e_\sigma) + \frac{1}{\sqrt{2}} A_{\tau\sigma}^{0}\varepsilon_3\cdot e_\sigma\ ]e_\tau\cdot\varepsilon_{\pm}'$$

$$n_+^2+n_-^2-2 = 4\pi \sum_{\sigma,\tau} (\tfrac{-i}{2})[A_{\tau\sigma}^{-\theta}\varepsilon_+\cdot e_\sigma + A_{\tau\sigma}^{\theta}\varepsilon_-\cdot e_\sigma](\tfrac{2i}{\sqrt{2}})\varepsilon_1\cdot e_\tau$$

$$+ 4\pi \sum_{\sigma,\tau} A_{\tau\sigma}^{0}\varepsilon_3\cdot e_\tau\ \varepsilon_3\cdot e_\sigma. \qquad (24)$$

Combining equations (23) and (24) and using the facts that $A_{\tau\sigma}^{\theta} = A_{\tau\sigma}^{-\theta}$ and $\varepsilon_{\pm} = \varepsilon_1 \pm i\varepsilon_2$:

$$(n_+^2+n_-^2-2) = 8\pi \sum_{\sigma,\tau} [A_{\tau\sigma}^{\theta} e_\tau\cdot(\varepsilon_+\varepsilon_-)\cdot e_\sigma + A_{\tau\sigma}^{0} e_\tau\cdot(\varepsilon_3\varepsilon_3)\cdot e_\sigma].$$

Combining this with equation (22) and dividing by 3 gives the total average:

$$\langle n_+^2+n_-^2-2\rangle = \frac{16\pi}{3} \sum_{\sigma,\tau} A_{\tau\sigma}^{\theta}\ e_\tau\cdot(\varepsilon_+\varepsilon_-)\cdot e_\sigma + \frac{8\pi}{3} \sum_{\sigma,\tau} A_{\tau\sigma}^{0} e_\tau\cdot(\varepsilon_3\varepsilon_3)\cdot e_\sigma.$$

Taking the imaginary part of the both sides we find:

$$\mathrm{Im}(n_+^2+n_-^2-2) = 2(n_+'n_+'' + n_-'n_-'').$$

We assume $n_+=n_-=1$ (this is a solvent influence assumption as in Chapter III) and $n_+''+n_-''=2n''$. Thus:

$$n'' = \frac{4\pi}{3} \sum_{\sigma,\tau} A_{\tau\sigma}^{\theta} e_\tau\cdot(\varepsilon_+\varepsilon_-)\cdot e_\sigma + \frac{2\pi}{3} \sum_{\sigma,\tau} A_{\tau\sigma}^{0}\ e_\tau\cdot(\varepsilon_3\varepsilon_3)\cdot e_\sigma\ .$$

Using equation (17) we find:

$$\varepsilon_{\parallel} = 4\pi C_1 \, \mathrm{Im}[A^{0}_{\tau\sigma} \, e_\tau \cdot (\varepsilon_3 \varepsilon_3) \cdot e_\sigma]$$

$$\varepsilon_{\perp} = 4\pi C_1 \, \mathrm{Im}[A^{\theta}_{\tau\sigma} \, e_\tau \cdot (\varepsilon_+ \varepsilon_-) \cdot e_\sigma]$$

$$\varepsilon = \frac{1}{3} \varepsilon_{\parallel} + \frac{2}{3} \varepsilon_{\perp} \quad .$$

Note that subscripts in the extinction coefficient refer to polarization direction rather than propagation direction. $\varepsilon_{\parallel}$ is the extinction coefficient for light polarized along the helix axis, and $\varepsilon_{\perp}$ is the extinction coefficient for light polarized in the plane perpendicular to the helix axis.

IV. Discussion

The major advantage of polarizability theory over the equivalent time dependent Hartree[1,2] theory lies in its ease of application without ab initio wavefunctions. For most polymers of interest accurate wavefunctions are very difficult to obtain. The present equations allow useful calculations to be made in terms of experimental monomer optical properties and calculated interaction energies. CNDO CI calculations[3] have been used to obtain transition monopoles for estimating the interaction energies. In suitable systems where the monomers are sufficiently separated to use a dipole-dipole interaction, polymer calculations may be based entirely on empirical monomer optical properties.[4] While the resolution of the absorption spectrum and assignment of the transition directions is not

unequivocal, the use of empirical monomer properties is much more practical than ab initio calculations on real polymer systems. Satisfactory results have been obtained for oligonucleotides using polarizability theory;[5,6] this work allows extension to polynucleotides and other polymers of biological interest. The limitations of the method should be kept in mind, however. No electron exchange or overlap can be considered and the interactions between transitions are expressed in terms of local fields. Static field effects are omitted, but they can easily be added by using the properties of the monomer in the static field of the polymer. Intermolecular interactions and specific solvent interactions were not explicitly considered.

In De Voe's original formulation, the maximum dimensions of the aggregate were assumed to be small compared to the wavelength of light, λ, and $\exp[i\mathbf{k}\cdot\mathbf{r}]$ was expanded to first order in $\mathbf{k}\cdot\mathbf{r}$. This is the classical analog of the Rosenfeld approximation.[7] Clearly this approximation is not good along the axis of a very long helix. At two stages in the present derivation this expansion is in fact made; it is important to note the different assumptions involved. To obtain the selection rules for light incident parallel and perpendicular to the helix axis, we expanded the exponential and assumed that the size of the unit cell was small compared to the wavelength of light.

$$\frac{|\mathbf{r}_{\sigma\tau}|}{\lambda} \text{ and } \frac{|\mathbf{r}_{\sigma}|}{\lambda} \ll 1$$

In the $(\varepsilon_L-\varepsilon_R)_{\parallel}$ we have the expansion

$$\sum_m G_{o\sigma m\tau}\exp[ikm\Delta z] = \sum_m G_{o\sigma m\tau} + ik\Delta z \sum_{m=-n_c}^{n_c} mG_{0\sigma m\tau}.$$

Here we assume that the sum over interactions converges in a distance small compared with λ:

$$\frac{n_c\Delta z}{\lambda} << 1$$

where n_c is the number of unit cells necessary for convergence and Δz is the rise along the helix axis per unit cell. This last expansion is made to express the difference between $\mathbf{A}^+_{\tau\sigma}$ and $\mathbf{A}^-_{\tau\sigma}$ to first order in k. $\mathbf{A}^+_{\tau\sigma}$ and $\mathbf{A}^-_{\tau\sigma}$ are different because there are different selection rules for right and left circular polarization and both selection rules are a function of $k\Delta z$.

In equation (6) the perpendicular CD appears to be origin dependent whereas the parallel terms contain only the differences Δz and $\mathbf{r}_{\sigma\tau}$. However, as we pointed out in the geometry section, the origin in each unit cell must be on the helix axis. This follows from the definition of the rotation operator **R**. In equation (16) the $\mathbf{r}_\sigma$ is projected into the plane perpendicular to the helix axis and is just the radial distance of the transition from the helix axis. This obviously will not change if the molecule is rotated or translated in space.

In contrast with the quantum theories,[8-15] which are based on a scattering formalism, we treat both the absorptive and dispersive behavior of the polymer with a complex

frequency dependent polarizability. Thus, the classical theory is a consistent treatment of the CD bandshape in terms of the absorption spectra of the monomers in solution. In our formalism the frequency dependent polymer CD is calculated directly in terms of the monomer extinction and its Kronig-Kramers transform

$$\alpha = \alpha' + i\alpha''$$

$$\alpha''(\omega) = \frac{3}{4\pi C_1}\,\varepsilon(\omega)$$

$$\alpha'(\omega) = -\frac{2}{\pi}\int_0^\infty \frac{\omega'\,\alpha''(\omega')\,d\omega'}{(\omega')^2 - \omega^2}\,.$$

Also, we are the first to consider explicitly a complex unit cell containing several monomers. We consider numerous transitions located throughout the unit cell. The optical activity of this unit cell is expressed directly in terms of electric-electric and electric-magnetic optical activity.

As a simple example and for comparison with previous work we consider a unit cell consisting of a single transition with no magnetic moment. The unit direction vector $\mathbf{e} = \mathbf{e}_{\parallel} + \mathbf{e}_{\perp}$ where $\mathbf{e}_{\parallel}$ is the vector projected onto the helix axis and $\mathbf{e}_{\perp}$ is the vector projected into the plane perpendicular to the helix axis. We will give the results in terms of the simplified coordinate system in figure 3: $\mathbf{e}_{\perp} = \mathbf{e}_r + \mathbf{e}_t$. For this simple system $\mathbf{A}^{\theta}$ is a scalar and there is no matrix inversion, merely division:

Figure 3: Simplified coordinate system for 1 transition per unit cell.

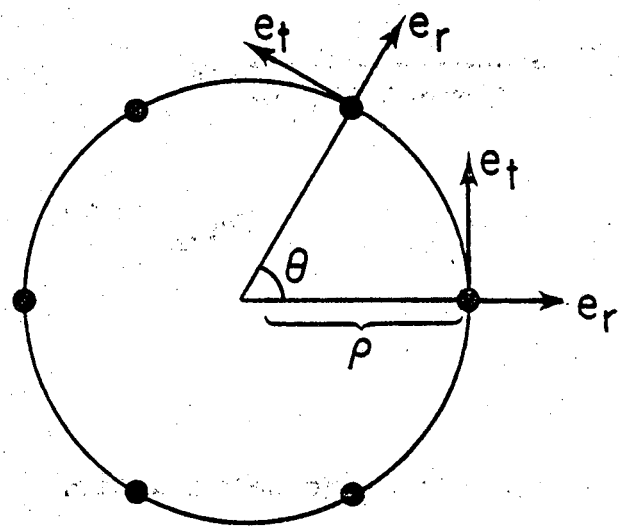

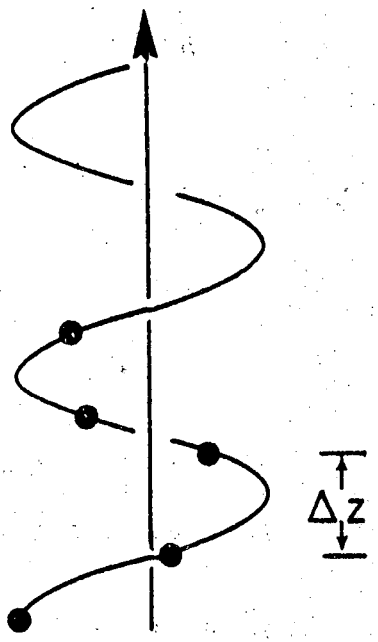

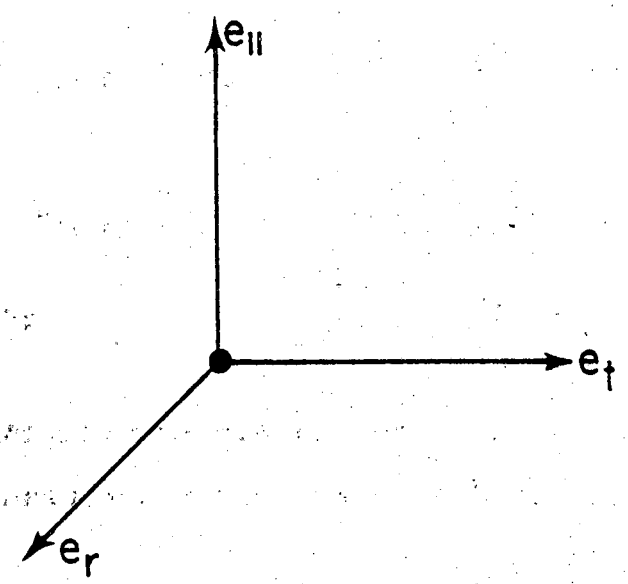

$$CD_{\parallel} = \frac{2\pi\omega}{c} C_1 e_{\perp}^2 \, \mathrm{Im}\, A^{\theta} \, \Delta z$$

$$CD_{\perp} = \frac{4\pi\omega}{c} C_1 \rho \, e_t e_{\parallel} \, (\mathrm{Im}\, A^{0} - \mathrm{Im}\, A^{\theta})$$

$$A^{\theta} = (\frac{1}{\alpha} + \sum_n G_{on} e^{in\theta})^{-1} = \frac{\alpha}{1 + \alpha \sum_n G_{on} e^{in\theta}}$$

$$[A^{\theta}] = i(A^{\theta})^2 \sum_n nG_{on} e^{in\theta} = (\frac{i\alpha^2}{(1+\alpha \sum_n G_{no} e^{in\theta})^2}) \sum_n nG_{on} e^{in\theta}$$

$\rho \equiv$ radius of transition.

For comparison with the results of first order perturbation theory we expand the result to first order in G_{on}:

$$A^{\theta} = (1 - 2\alpha \sum_{n=0}^{n_c} G_{on} \cos n\theta$$

$$[A^{\theta}] = -2 \alpha^2 \sum_{n=0}^{n_c} nG_{on} \sin n\theta$$

where we used the fact that: $G_{on} = G_{o-n}$. Now we examine $\mathrm{Im}(\alpha^2)$:

$$\mathrm{Im}(\alpha^2) = \mathrm{Im}(\alpha' + i\alpha'')^2 = 2\alpha'\alpha''$$

$$\varepsilon_m = \frac{4\pi}{3} C_1 \alpha'' \qquad\qquad \alpha_m = \alpha''$$

where ε_m and α_m are the monomer extinction and (real) polarizability. Thus the first order result is:

$$CD_{\parallel} = \frac{4\omega}{c} \varepsilon_m \alpha_m \Delta z e_{\perp}^2 \sum_{n=0}^{n_c} nG_{on} \sin n\theta$$

$$CD_{\perp} = \frac{-8\omega}{c} \varepsilon_m \alpha_m \rho \, e_{\parallel} e_t \sum_{n=0}^{n_c} G_{on} \sin^2(n\theta/2)$$

which is exactly analogous to the Moffitt Fitts and Kirkwood result for the ORD of an infinite helix.[15]

Chapter IV Bibliography

1. W. Rhodes, J. Chem. Phys. 37, 2433 (1962).
2. R.A. Harris, J. Chem. Phys. 43, 959 (1965).
3. W. Hug and I. Tinoco, Jr., J. Amer. Chem. Soc. 95, 2803 (1973).
4. W. Hug, F. Ciardelli and I. Tinoco, Jr., J. Amer. Chem. Soc. 96, 3407 (1974).
5. C. Cech, W. Hug and I. Tinoco, Jr., Biopolymers 15, 131 (1976).
6. C. Cech, Ph.D. Thesis, Berkeley (1975).
7. Rosenfeld, Z. Physik 52, 161 (1928).
8. W. Rhodes and M. Chase, Rev. Mod. Phys. 39, 348 (1967).
9. D.G. Barnes and W. Rhodes, J. Chem. Phys. 48, 817 (1968).
10. W. Rhodes, J. Chem. Phys. 53, 3650 (1970).
11. A.R. Ziv and W. Rhodes, J. Chem. Phys. 57, 5354 (1972).
12. F.M. Loxsom, J. Chem. Phys. 51, 4899 (1969).
13. C.S. Deutsche, J. Chem. Phys. 52 3703 (1970)
14. W. Moffitt, J. Chem. Phys. 25, 467 (1956).
15. W. Moffitt, D.D. Fitts and J.G. Kirkwood, Proc. Nat. Acad. Sci. 43, 723 (1957).

Chapter V

Calculations of Polynucleotide Circular Dichroism

I. Polynucleotide Conformation

The theoretical tools developed in the previous chapters were motivated in great part by the discovery of the importance of helical structure in biological macromolecules.[1,2] In particular we will be interested in calculating the CD of double and single stranded polynucleotides.[2] To do these calculations we will need information about the polymer geometry as well as monomer properties.

The basic structural unit of a double stranded polynucleotide is the base pair. Each base pair contains a purine, adenine (A), or guanine (G) hydrogen bonded to a pyrimidine, uracil (U), thymine (T), or cytosine (C). To describe the conformation of the base pair[3] we will define two axes perpendicular to the helix axis. (See figure 1.) The first, the tilt or dyad axis, is a twofold symmetry axis which relates the glycosidic links in the base-pair. The second, the twist axis, is perpendicular to both the helix and dyad axes and passes through pyrimidine C6. The conformation of the base-pair is determined by three parameters, D_x, the tilt, and the twist. Looking along the dyad or tilt axis from the minor groove to the helix axis, the tilt is the angle measured counterclockwise from the twist axis to the base plane. (Although the bases are not

Figure 1: Base pair conformation parameters.

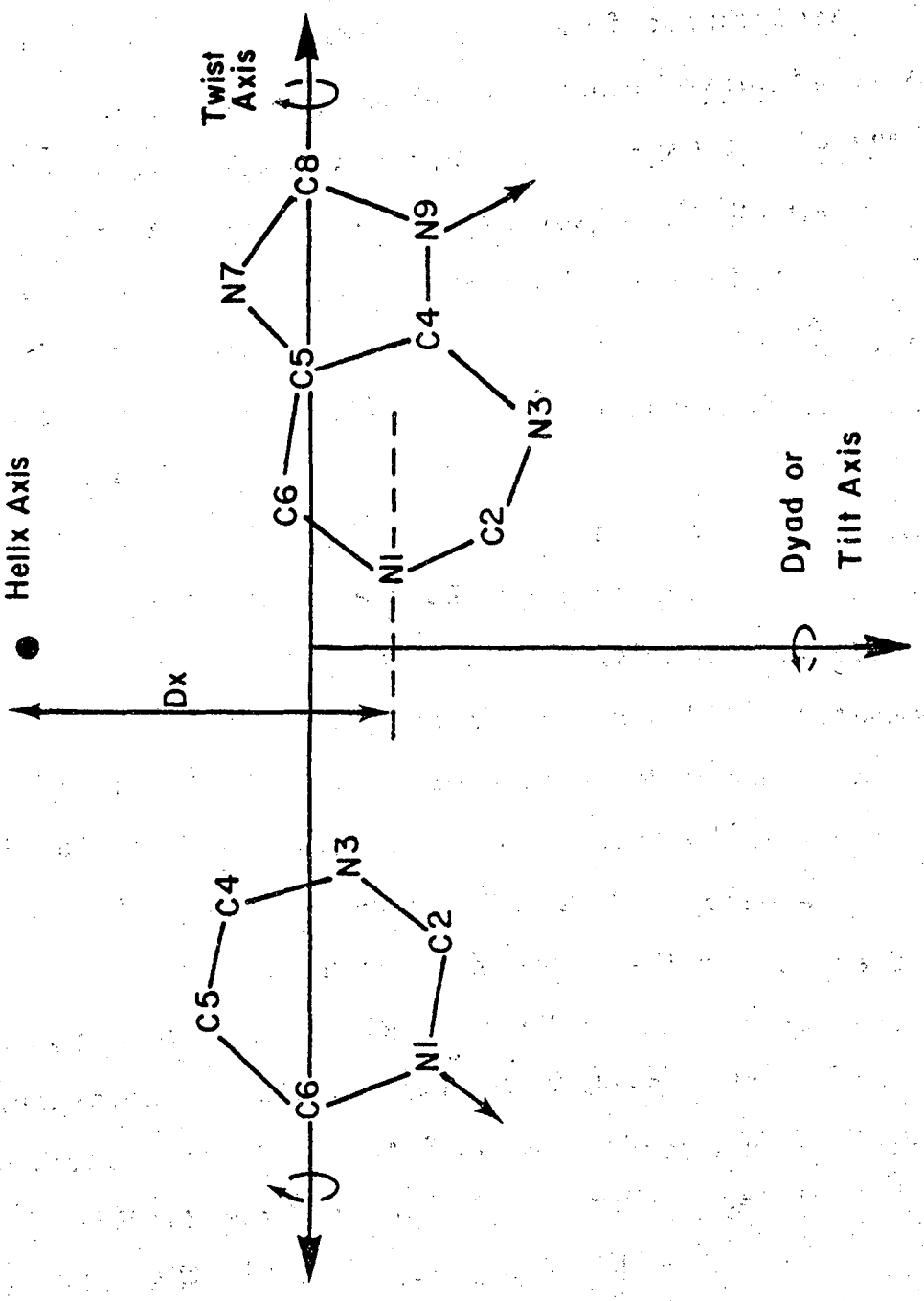

strictly planar, the best least squares plane is fit to the base atoms). Looking along the twist axis, the twist is the angle between the base plane and the dyad axis measured counterclockwise from the dyad axis. In figure 1 a positive value of twist brings the purine glycosidic link above the plane of the page and the pyrimidine glycosidic link below the plane of the page. D_x is defined in figure 1. We have not specified the conformation of the sugar phosphate backbone. We will assume it has no influence on the CD in the region of interest (200 nm - 300 nm).[5] Once the base pair conformation is specified, the double helix is generated by translating the base pair along the helix axis by Δz and rotating the base pair around the helix axis by θ.

Table I and figures 2, 3 and 4 give the geometrical parameters[6,7,8] and experimental CD spectra[11,12] of natural double stranded deoxyribonucleic acid (DNA) in the so called B[6] and C-DNA[7] conformations, and ribonucleic acid (RNA) in A-RNA[8] geometry. These geometries are determined from X-ray diffraction studies. X-ray scattering from fibers[11] under varying conditions of humidity gives A, B or C type patterns. The CD of these films is measured under the identical conditions of temperature and humidity.[11] These studies demonstrate the sensitivity of the CD to these conformational changes. Along with solution studies,[12] the film CD studies indicate that both synthetic and native polynucleotides have a wide and relatively continuous range of conformational analogues to the X-ray crystal structures. The CD of a

Table I

	Δz (Å)	θ (°)	bases per turn
A-RNA	2.81	32.7	11
B-DNA	3.38	36.0	10
C-DNA	3.32	38.6	9.3
Poly(I)	3.41	31.3	11.5
Poly(A)	2.82	40.0	9

Figure 2: Geometric parameters and CD of RNA.
With permission from D. Moore, Ph.D. Thesis,
Ohio University (1974).

VIEW DOWN HELIX AXIS (RNA)

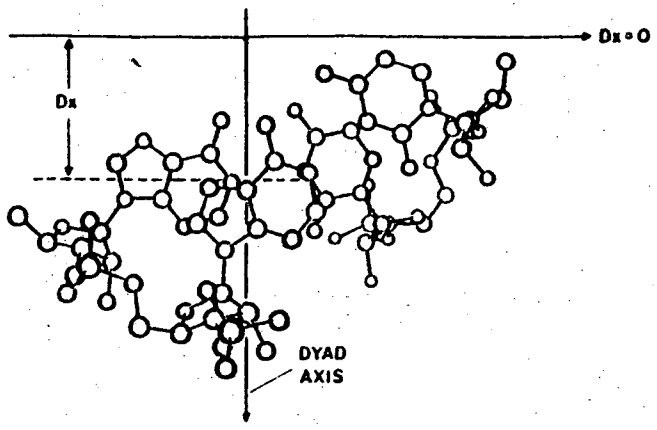

VIEW DOWN HELIX DYAD (RNA)

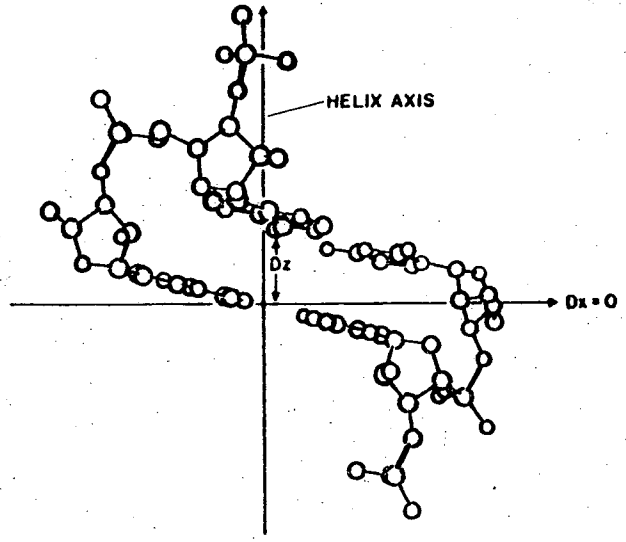

CD SPECTRUM (RNA)

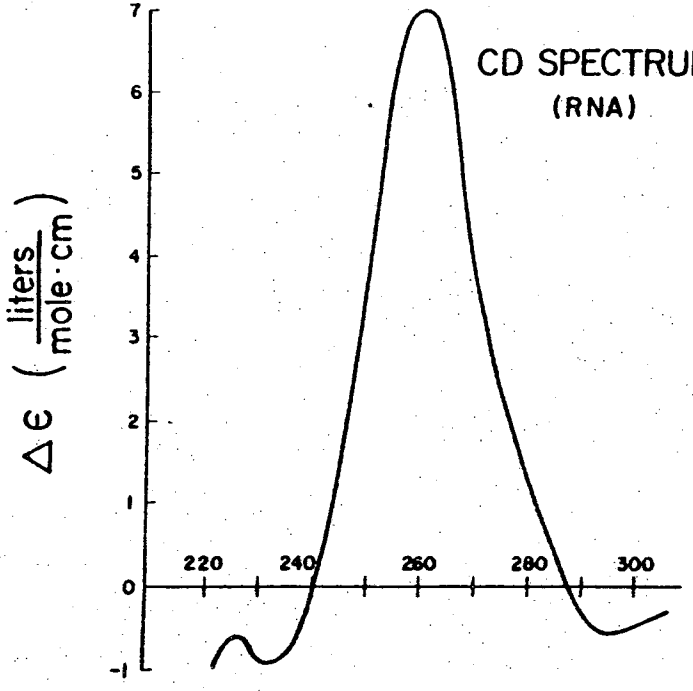

GEOMETRIC PARAMETERS (RNA)

Dx	4.9 Å
TILT	-14°
TWIST	0°
Dz	2.73Å
θ	32.7°

(Pitch = 30.0Å, 11 Residues / Turn)

Figure 3: Geometric parameters and CD of B-DNA
With permission from D. Moore, Ph.D. Thesis, Ohio University (1974).

VIEW DOWN HELIX AXIS (DNA-B)

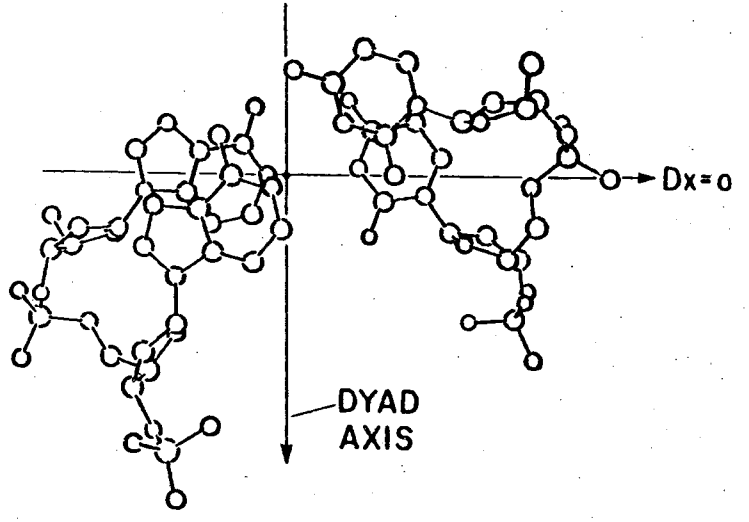

VIEW DOWN DYAD AXIS (DNA-B)

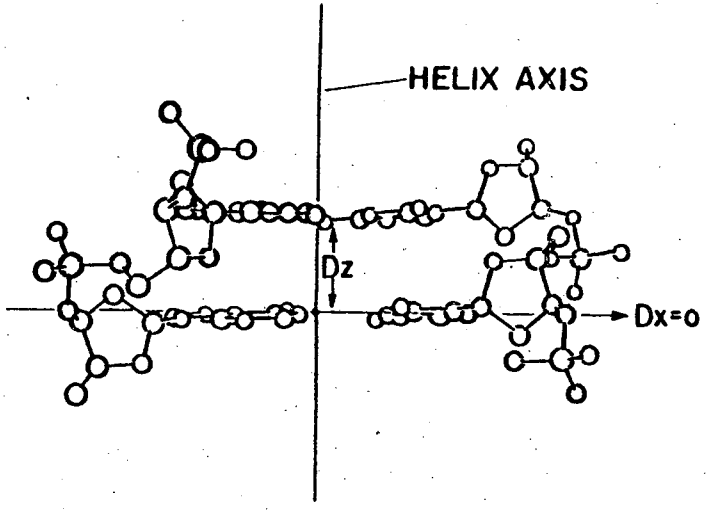

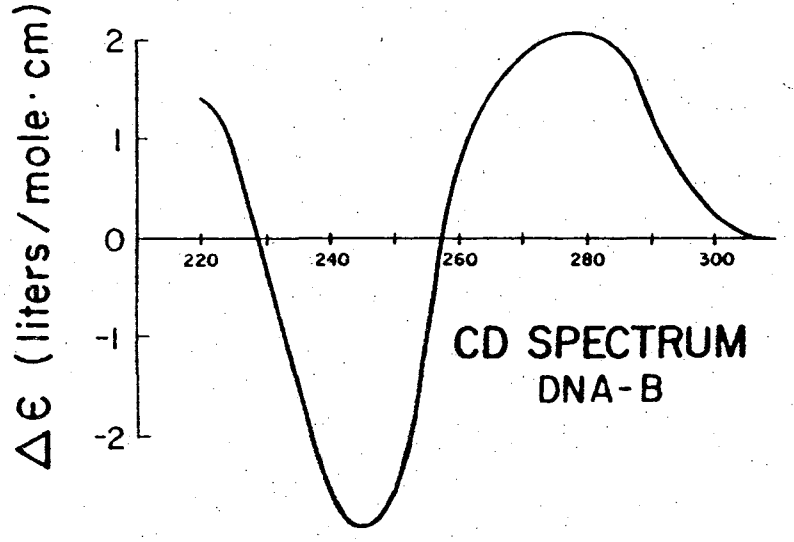

GEOMETRIC PARAMETERS (DNA-B)

Dx	0 Å
TILT	2°
TWIST	5°
Dz	3.36 Å
θ	36.0°

(PITCH = 33.6 Å
10 Residues/Turn)

Figure 4: Geometric parameters and CD of C-DNA
With permission from D. Moore, Ph.D. Thesis,
Ohio University (1974).

VIEW DOWN HELIX AXIS (DNA-C)

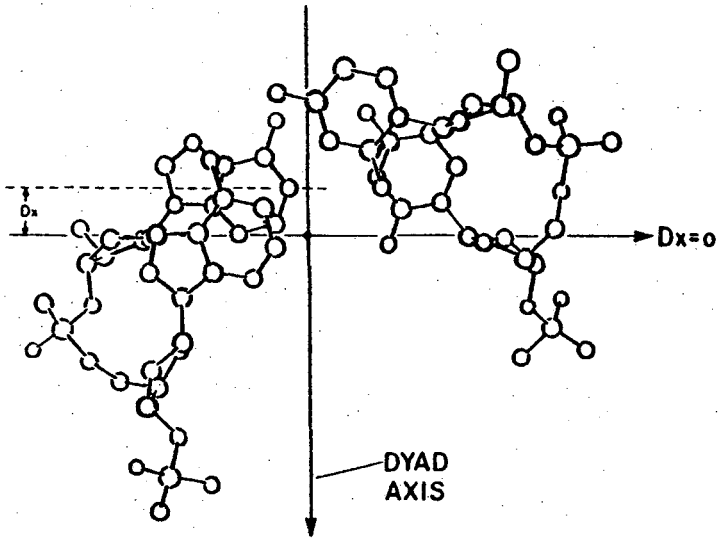

VIEW DOWN DYAD AXIS (DNA-C)

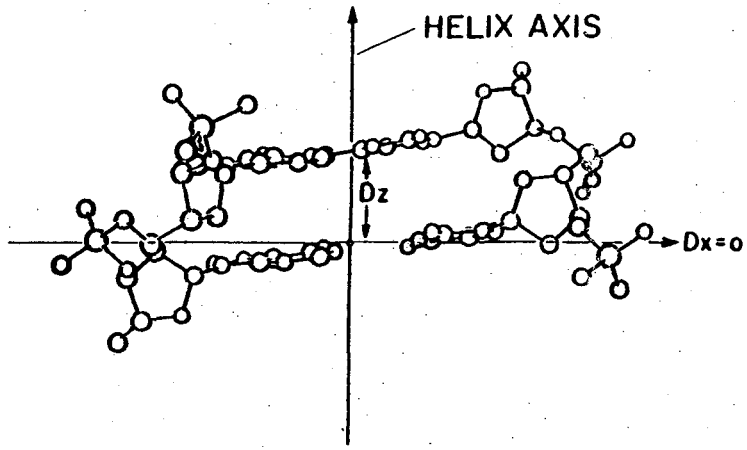

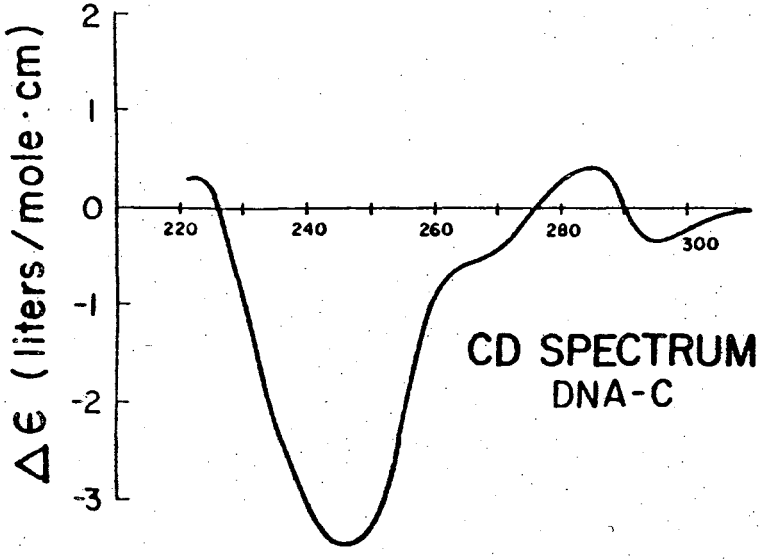

GEOMETRIC PARAMETERS (DNA-C)

Dx	1.5 Å
TILT	6°
TWIST	5°
Dz	3.32 Å
θ	38.6°

(PITCH = 31.0 Å
9.3 Residues/Turn)

polynucleotide in solution is sensitive to the temperature, ionic strength, and solvent conditions as well as the presence of proteins. In fact the CD is an important probe of the organization of DNA into compact or condensed phase structures in phage heads[14] and ψ DNA.[15] With a reliable and practical method of calculating the CD, these measured spectral changes could be interpreted in terms of specific geometrical parameters and proposed conformational changes.

Moore and Wagner[16] took an important step in this direction with the discovery that D_x is the most important factor in determining whether the CD spectrum is A-like or B-like. Prior to their work, base tilt in the A conformation was thought to be responsible for the "non-conservative" A-RNA CD spectrum. Moore and Wagner used the Johnson-Tinoco theory to calculate the CD.

II. Monomer Properties

The monomer properties necessary for our calculations are the transition directions and polarizabilities and the CNDO monopoles of each transition. The resolution of absorptions spectra into single transition absorptions and the determination of transition directions is discussed in detail by Cech.[17] Cech made a rather extensive study of monomer properties. Because one of our aims is to continue previous oligomer studies of chain length to the polymer limit, we used her monomer properties unless otherwise specified. These monomer properties are discussed in the

following pages.

The purines were resolved into four $\pi \rightarrow \pi^*$ transitions plus three background transitions, the pyrimidines were resolved into three $\pi \rightarrow \pi^*$ transitions plus three background transitions. The bandshapes of the absorptions above 200 nm were determined from measured spectra and were generally close to Gaussian in shape. The three background transitions were taken to be Lorentzian bands centered at 119 nm. All transitions except one background transition are in the plane of the base (thus no $n \rightarrow \pi^*$ transitions were included).

Transition monopoles for the first two long wavelength transitions in each base were calculated using a CNDO-CI molecular orbital approach.[22] Monopoles for the other transitions were calculated using program BASES (see appendix A). Although this placement of monopoles is not unequivocal, the transition is delocalized by this procedure, and the monopoles give the proper empirical transition direction. The transition locations, $\mathbf{R}$, are determined according to:

$$\mathbf{R} = \frac{\sum_s |q^s| \mathbf{r}_s}{\sum_s |q^s|}$$

where the $\mathbf{r}_s$ are the atom position vectors of the base on which oscillator i is located. Program BASES determines these positions as well as calculating transition directions relative to the molecular reference frame from the atomic

X-ray coordinates of any geometry. All single strands were assumed to have the geometry corresponding to half a double strand unless otherwise specified. No monomer CD was included in any of the following calculations.

III. Computational Considerations

Program ROTOPI was written to calculate the Absorption and CD of an infinite polymer based on the equations IV.19 and IV.25. Only $\pi \rightarrow \pi^*$ transitions are considered in these calculations. While the magnetic contributions to the CD have been programmed, $b_\sigma = 0$ is always used. For consistency with previous oligomer calculations, the subroutines which read in the reference base data and polarizability data have been altered as little as possible. These input routines were developed by C.M. Cech. These routines also generate a section of double or single helix (an oligomer). This section of helix is taken as the unit cell for the infinite polymer calculation. The helical parameters relating one unit cell to another are calculated from the parameters used to generate the unit cell. As an example, in A-RNA geometry $\theta = 32.7°$ and $\Delta z = 2.81$ Å. If the unit cell contains the sequence r(AAU) the next unit cell is found by rotating through $\theta = 3 \times 32.7°$ and translating $\Delta z = 3 \times 2.81$ Å $= 8.43$ Å. The same would apply for any single strand containing three bases or any double strand containing three base-pairs. Each would contain three helical steps per unit cell.

The interaction terms in equations IV.1 must be calculated for n_c unit cells to either side of the 0 unit cell. This

means generating the atomic coordinates of the bases in the other cells from $-n_c$ to n_c. However since $G_{o\sigma m\tau} = G_{o\tau m\sigma}$, only half the interactions need be calculated. The proper choice of n_c depends on sequence and complexity of the unit cell as well as geometry. However, convergence to within 1% in the final CD calculations was always obtained by considering 20 helical steps to either side. Unless otherwise specified all calculations were done for 20 unit cells to either side of the 0 unit cell. A dipole-dipole interaction was used to calculate interactions between transitions more than ten unit cells apart. An effective dielectric constant of 2 is used in all calculations. The present program which runs in 100 k on the LBL CDC 7600 can accomodate 42 oscillators per unit cell, and 101 frequency points. With 7 oscillators per unit cell a 14 frequency point calculation takes 11 central processor (CP) seconds; with 39 oscillators a 14 point calculation takes 120 (CP) seconds. In comparison, with 130 oscillators a 14 point oligomer calculation takes 150 CP seconds (program ROTOPM is given in appendix A).

The internal consistency of the theory and the ROTOPI program were tested in a number of ways. A calculation for a linear array of adenine gave no CD. A hand calculation using only the 260 nm transition of adenine in A-RNA geometry was compared with the computer calculation. Calculations were done in A-RNA geometry for unit cells containing 1, 2 and 3 A's. The results were identical. (For these

calculations n_c = 30 was used for (A_1), n_c = 15 was used for (A_2), and n_c = 10 was used for (A_3). Thus each calculation included precisely the same number of interactions.) The CD and absorption calculated for these three were identical. Finally infinite polymer calculations with only the 260 nm transition of adenine were compared with oligomer calculations containing 140 bases (the upper limit of the ROTOPM program). In all three geometries the CD agreed to better than 1%. Infinite polymer calculations have been carried out for the sequences: poly (A), poly(T), poly(A·T), poly[(A-T)·(A-T)], poly (G), poly(C), poly(G·C), poly[(G-C)·(G-C], poly[(A-G)·(C-T)], poly[(A-C)·(G-T)], poly(A-T), poly(G-C), poly(A-C), poly(G-T), poly(A-G), poly(C-T) in the A, B, and C form geometries. (The results of these calculations in both digitalized and graphical forms, for the parallel and perpendicular components of the CD and extinction are given in appendix B.)

IV. Chainlength Dependence

Chainlength dependence studies are crucial in evaluating previous polynucleotide calculations done with the De Voe theory.[17,18,19] With the results of Chapter IV we can extend the chainlength studies to the infinite polymer limit. With the earlier program core space limited us to 20 bases (10 base-pairs). Thus it was necessary to assume that one turn of the helix was sufficient to determine the polymer CD.

Oligomer chainlength studies were compared with the infinite polymer result for the following sequences: poly(A), poly(A·T), poly[(A-T)·(A-T)], poly(G·C) and poly[(G-C)·(G-C)] in all three geometries. We will only present the results for the A-RNA geometry. While the spectra were different in the other geometries, the convergence of the chainlength was very similar and generally dependent on sequence rather than the particular geometry chosen. In figures 5 and 6 the infinite polymer calculation is compared to the oligomer containing 20 bases for the sequences poly(A) and poly[(G-C)·(G-C)]. Poly(A) is an example of only minor changes in magnitude in going from the oligomer to the infinite polymer. In poly[(G-C)·(G-C)] both the magnitude and the locations of the maxima and minima are changing. This is the worst case of convergence that was found. Thus, most of the polymer CD are very similar in shape and peak location with only minor changes in magnitude. For those polymers which showed only changes in magnitude but no shifts or shape changes the results are presented in figure 7. The magnitude of the first long wavelength maximum is plotted vs. chainlength. Note that we actually plot the ratio of the maximum at any chainlength to the maximum of the dimer.

The infinite polymer studies indicate that the general conclusions of previous studies are justified, and that considering ten base-pairs (or 20 bases) gives a good approximation to the polymer shape and magnitude (± 20%).

Figure 5: Comparison of oligo$(A)_{20}$----, and infinite poly(A) calculation ———.

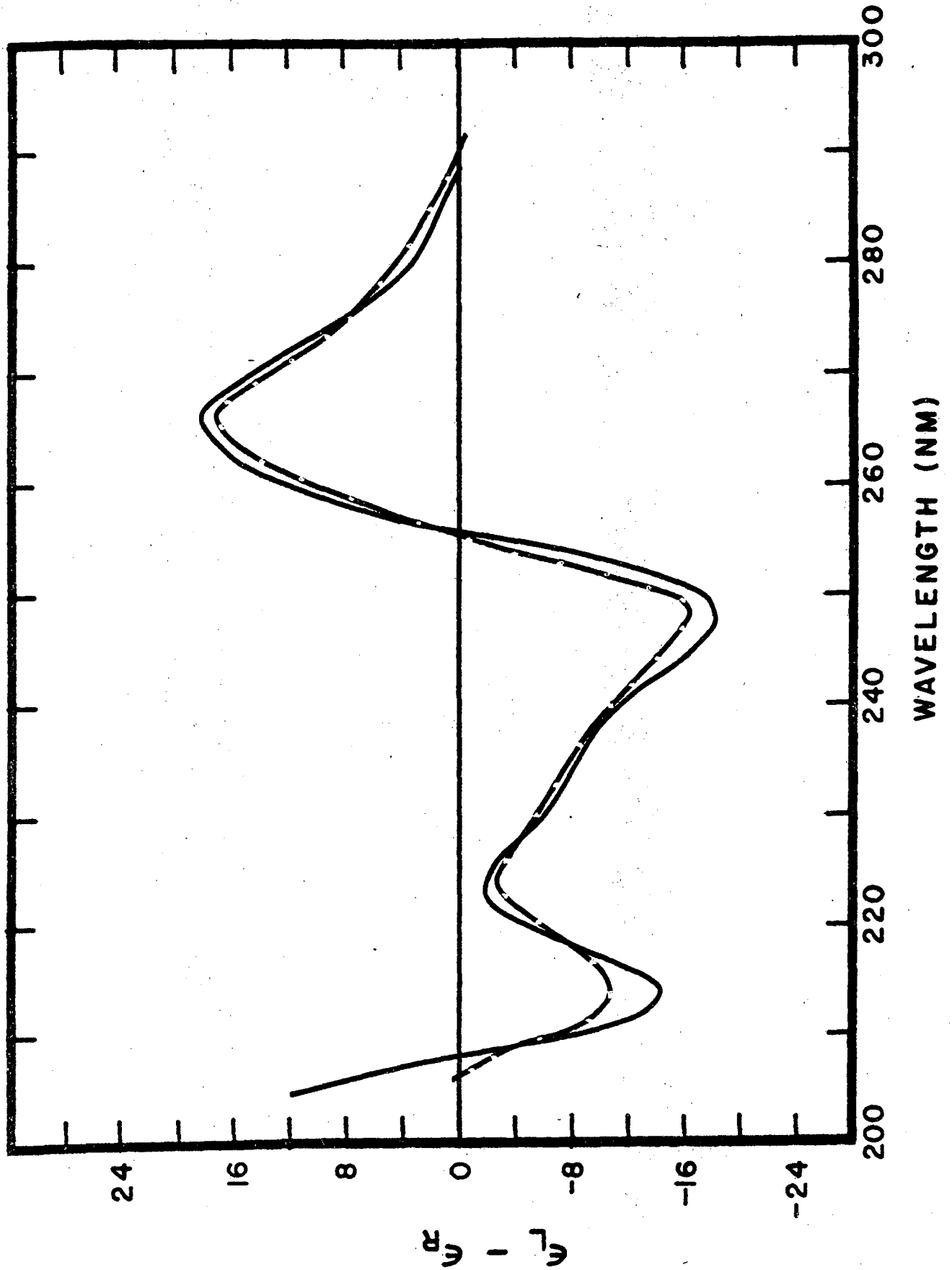

Figure 6: Comparison of oligo[$(G\text{-}C)_5 \cdot (G\text{-}C)_5$] -----, and poly[(G-C)·(G-C)] calculations.

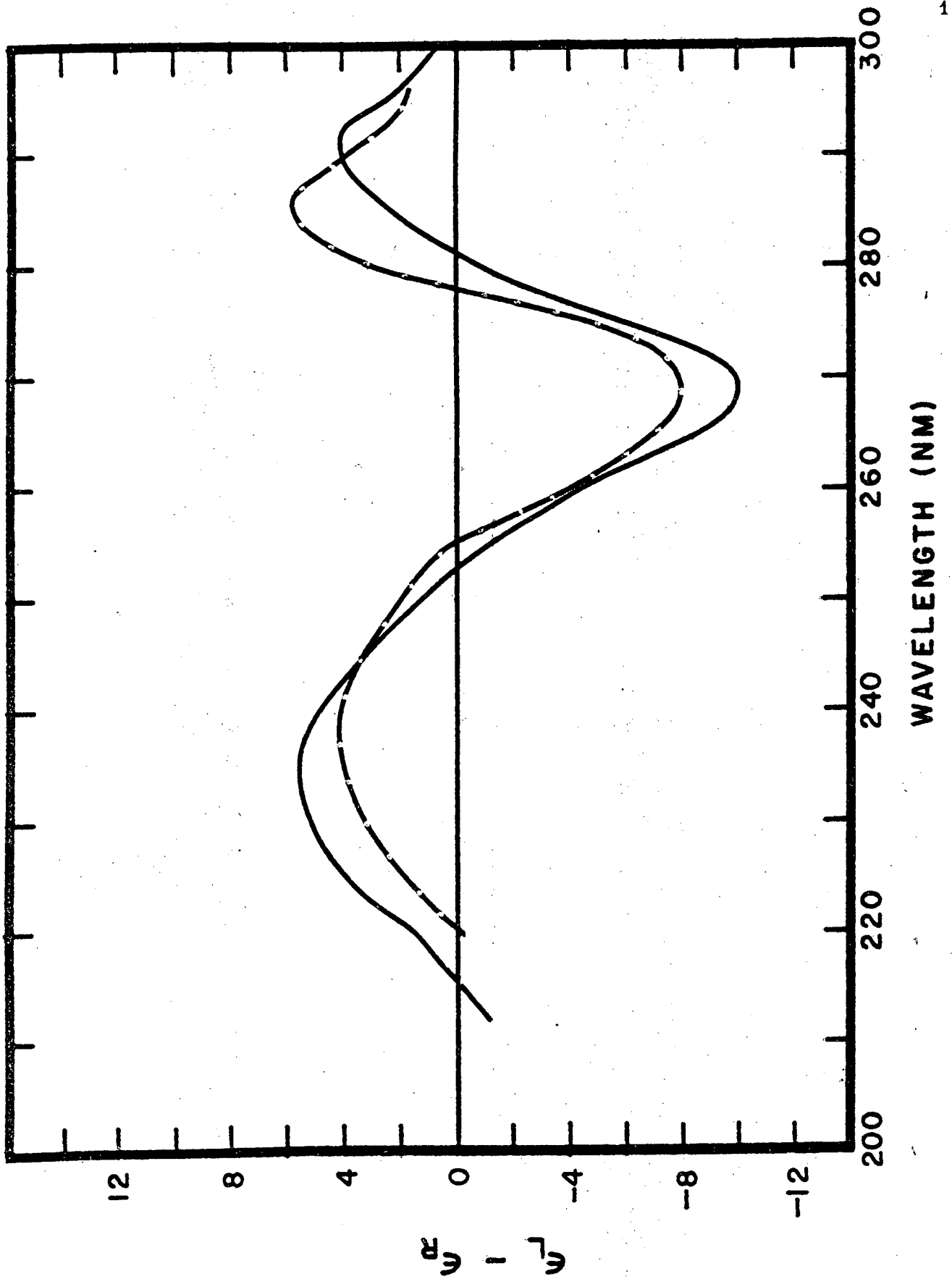

Figure 7: Chainlength dependence of A, A·U, dA and dA·dT. $(CD^{N}_{max})/(CD^{2}_{max})$ is the ratio of the maximum of the first long wavelength band in the N-mer to the first long wavelength maximum in the dimer. N is the number of bases in the single strand or the number of base pairs in the double strand.

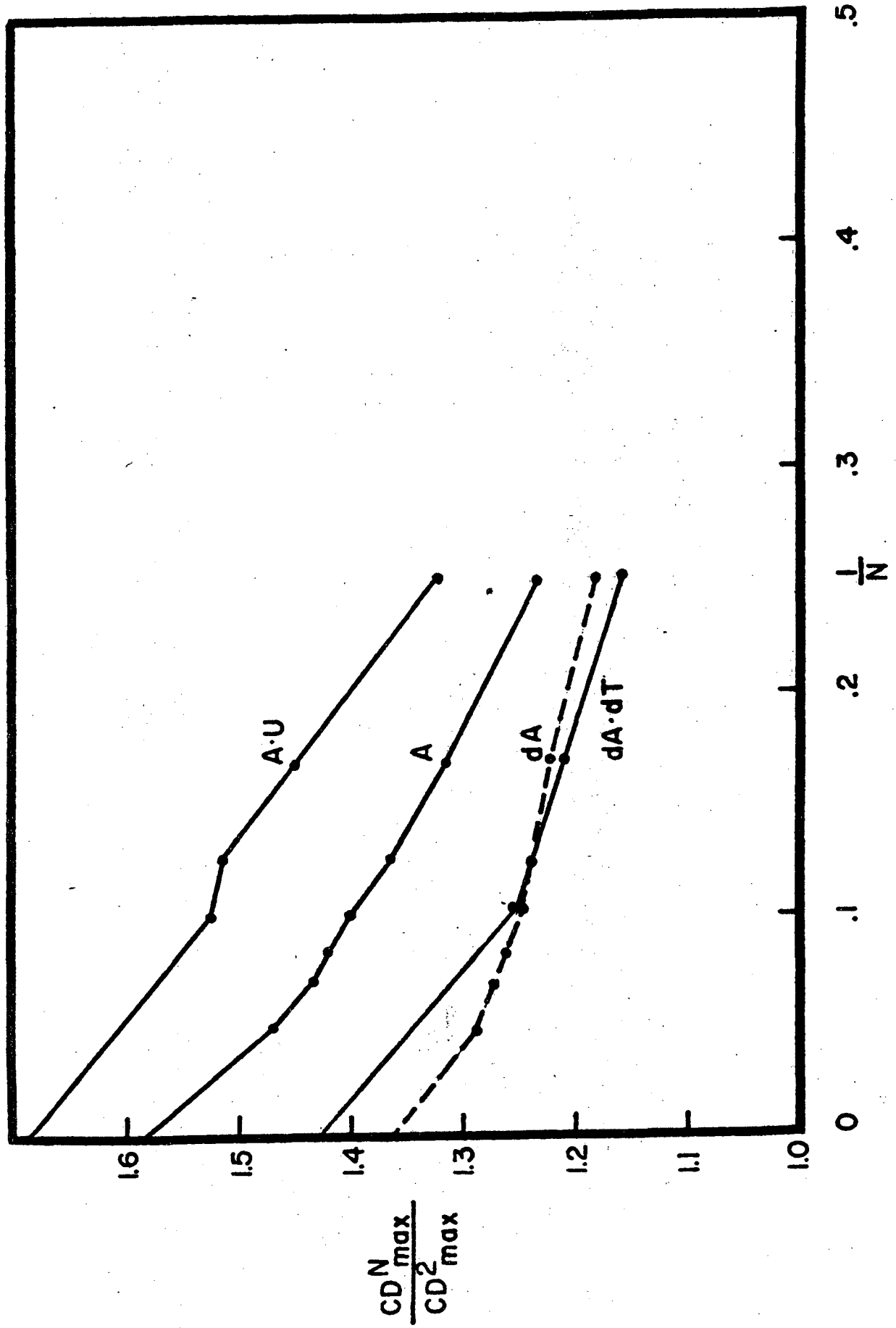

This statement is of course based on the present level of agreement between theory and experiment. With improvement in our understanding of monomer properties and polymer conformations these differences will be more important. Also, these more accurate polymer calculations use less computer time for any repeating sequence less complex than 8 bases (4 base-pairs).

Finally, these studies indicate that the theory developed in Chapter IV for the infinite polymer is correct, in the sense that the oligomers always tend to converge to the calculated polymer limit.

V. New Calculations

A number of new calculations have been done prompted by recent crystallographic and CD data. Saenger[21] et al have proposed X-ray coordinates for poly(A) based on the X-ray structure of ApApA under acidic conditions. The crystal contained the zwitter ionic base paired dimer: $Ap^{-}AH^{+}p^{-}AH^{+}\cdot Ap^{-}AH^{+}p^{-}AH^{+}$. This dimer contains a helical region and a looped region. The model coordinates of a poly(A) helix are obtained from the helical sections of this structure. This helix contains 9 bases per turn compared with 11 bases per turn for A-RNA. The other parameters of the structure are compared in table I.

It was hoped that this structure might give improved agreement between calculation and experiment. This is particularly important since adenine containing oligomers

were used to assess the polarizability theory calculations.[17,18] As is shown in figure 8, this structure does not give improved agreement with experiment when compared with standard A-RNA geometry. While the differences between the calculated CD are too small to rule out either geometry, it seems likely that poly(A) has a structure closer to A-RNA than that suggested by Saenger et al.

Recently Gray[22] has measured the CD of poly[d(A-C)·d(G-T)] and poly[(A-C)·(G-U)]. Calculations have been done for this sequence in A-RNA and B-DNA geometries. The comparison between calculation and experiment is shown in figures 9 and 10. Although the magnitude of the DNA calculation is too large, and the bands of the RNA calculation are too far to the red, the general trends for the change from B to A conformation are seen: The first maximum increases and shifts to the blue. The difference in magnitude of the B-DNA calculation is not serious. Our calculation assumes a perfectly rigid polymer, where as there is thermal motion in the solution which tends to decrease the CD. If the polymer CD was measured at lower temperature, the agreement would improve. The shifted bands and the failure to predict the negative band at long wavelength for the RNA calculation are less easily rationalized.

In figures 11 and 12 measured[23] poly[d(A-G-C)·d(G-C-T)] and poly[(A-G-C)·(G-C-U)] spectra are compared with calculation. The two calculated spectra are very similar and neither agrees well with experiment. We will not endeavor to place blame

Figure 8: Comparison of measured poly(A) (0°, 0.1M NaCl, 0.01 Tris, pH 7.4) - - - - -, calculation based on data of Saenger et. al, -·-·-, and calculation based on standard RNA geometry ———.

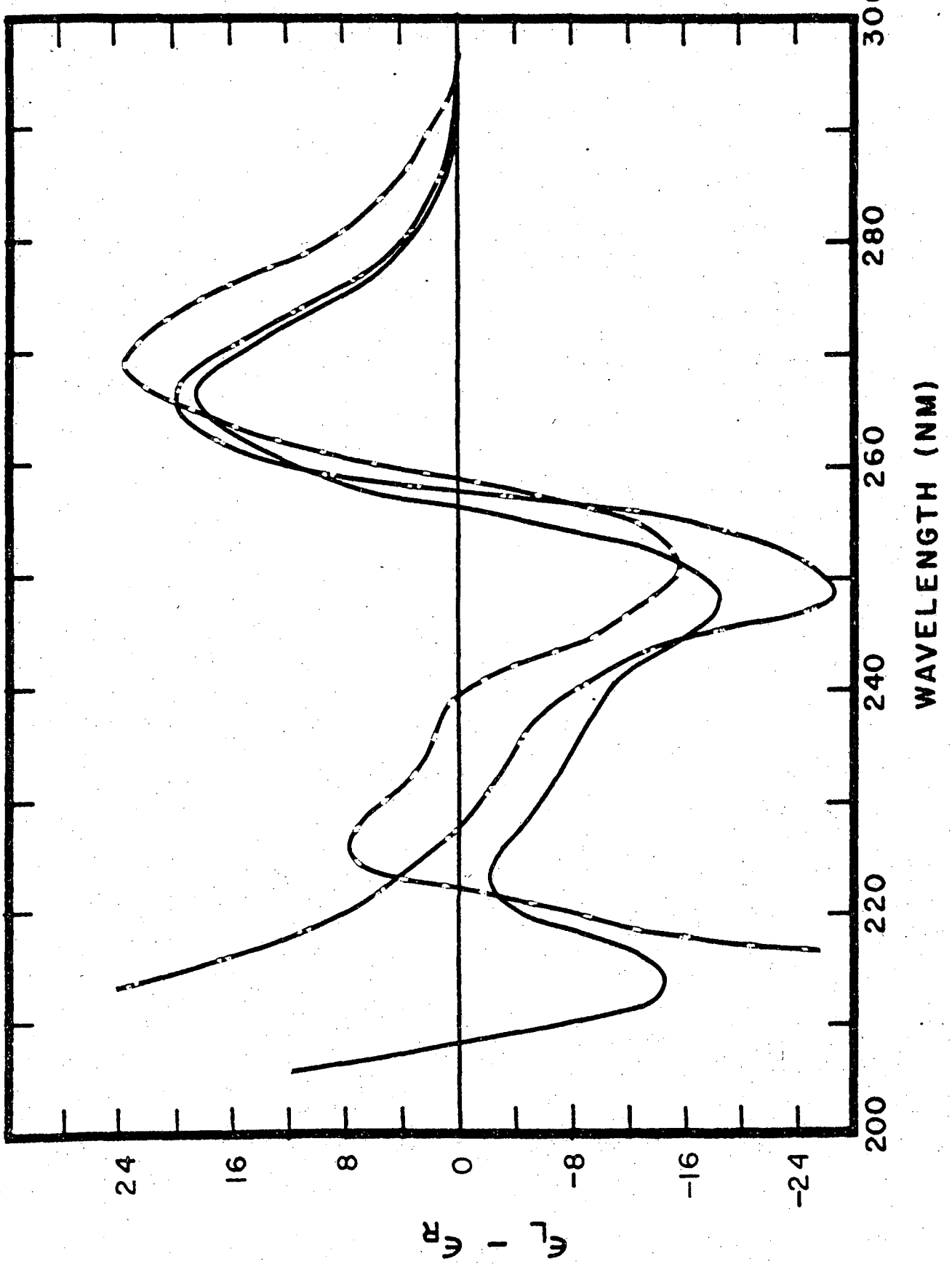

Figure 9: Poly [(A-C)·(G-T)] 20°, .02 M Na^+ phosphate buffer, pH 7.0. Measured -----, calculated ——.

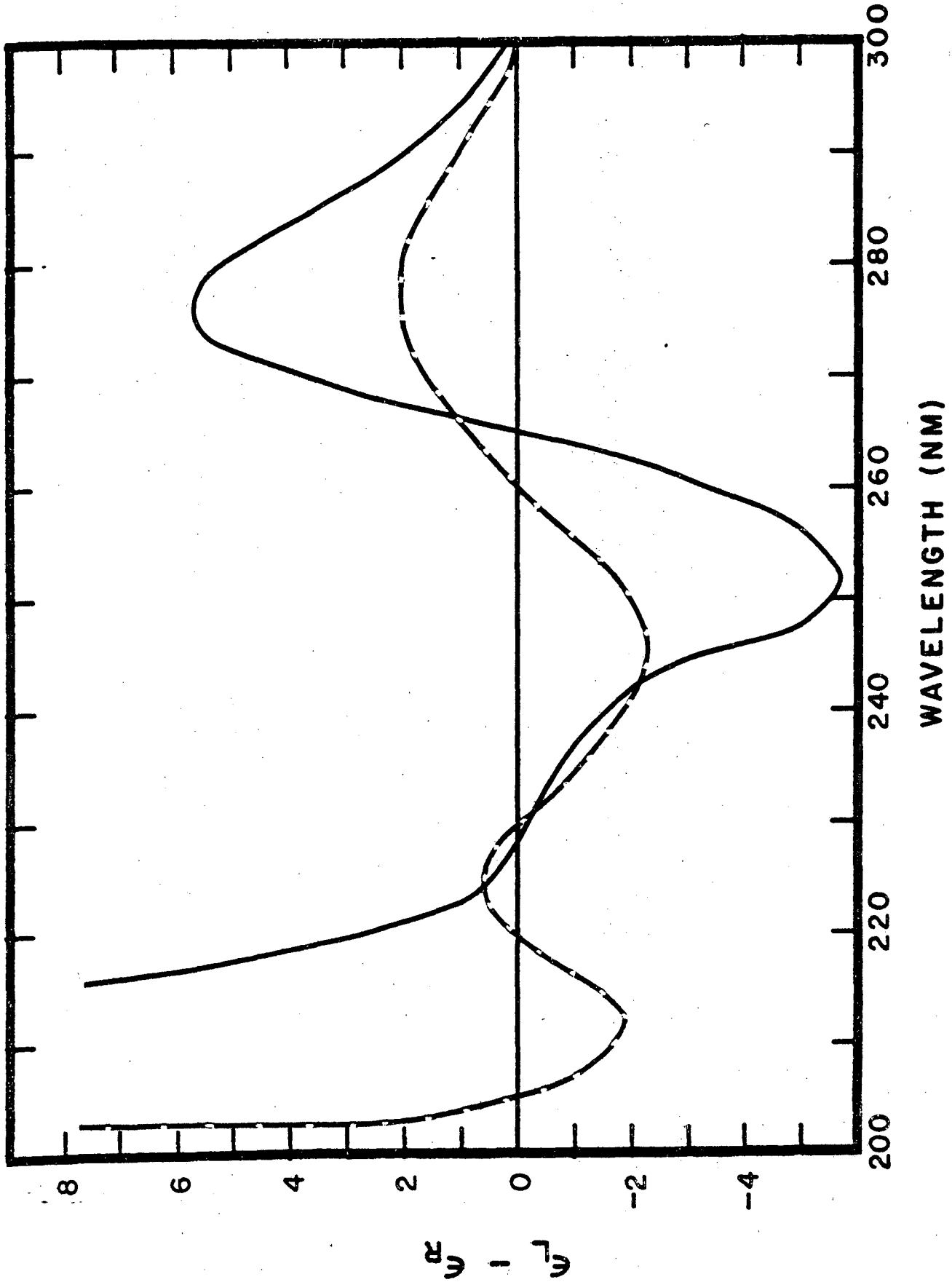

Figure 10: Poly[d(A-C)·d(G-T)]. 20°, .02 M Na^+ phosphate buffer, pH 7.0. Measured -----, calculated ———.

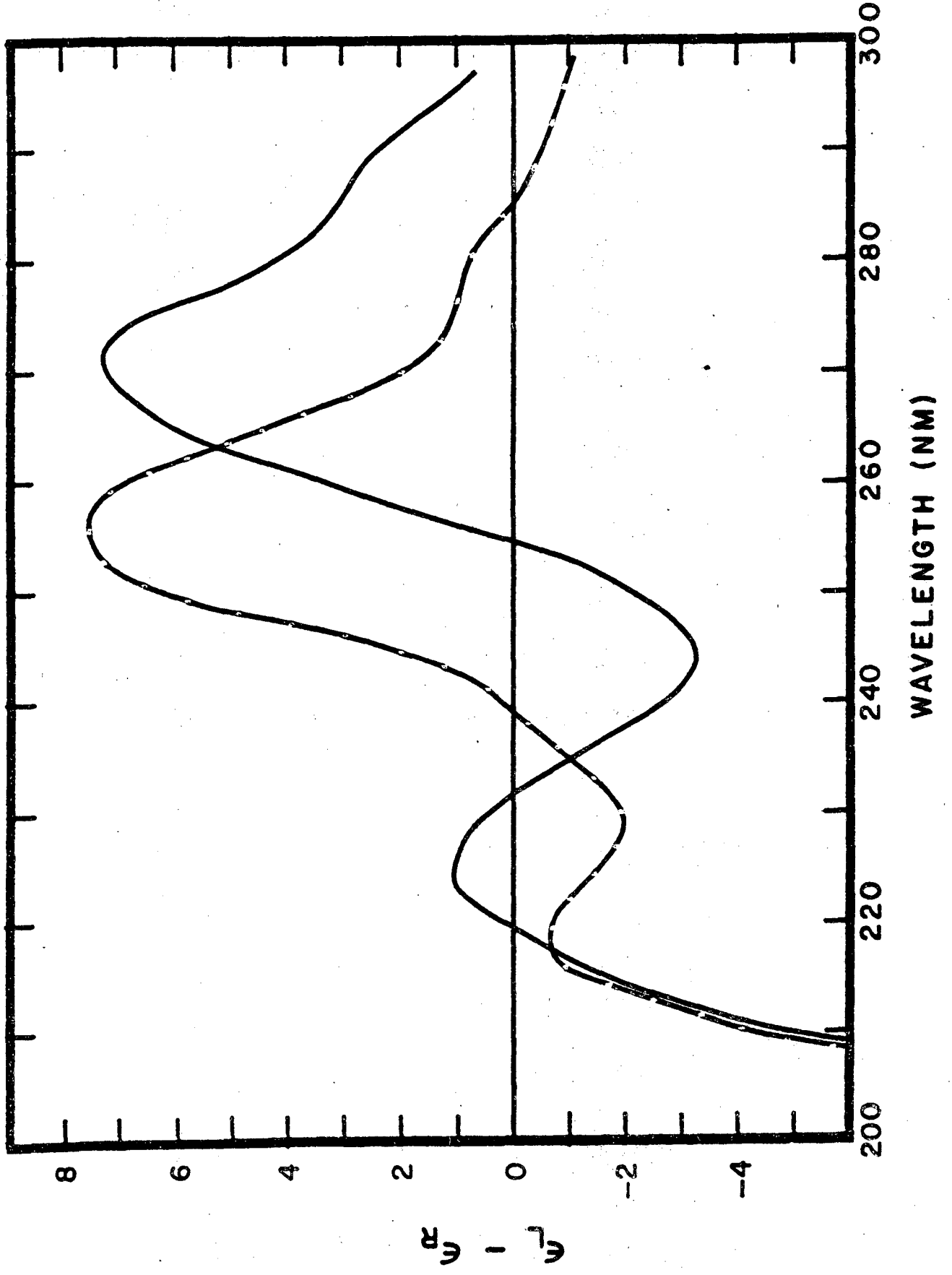

Figure 11: Poly[(A-G-C)·(G-C-T)]. 20°, .01 M Na^+ phosphate buffer, pH 7.0. Measured -----. calculated ———.

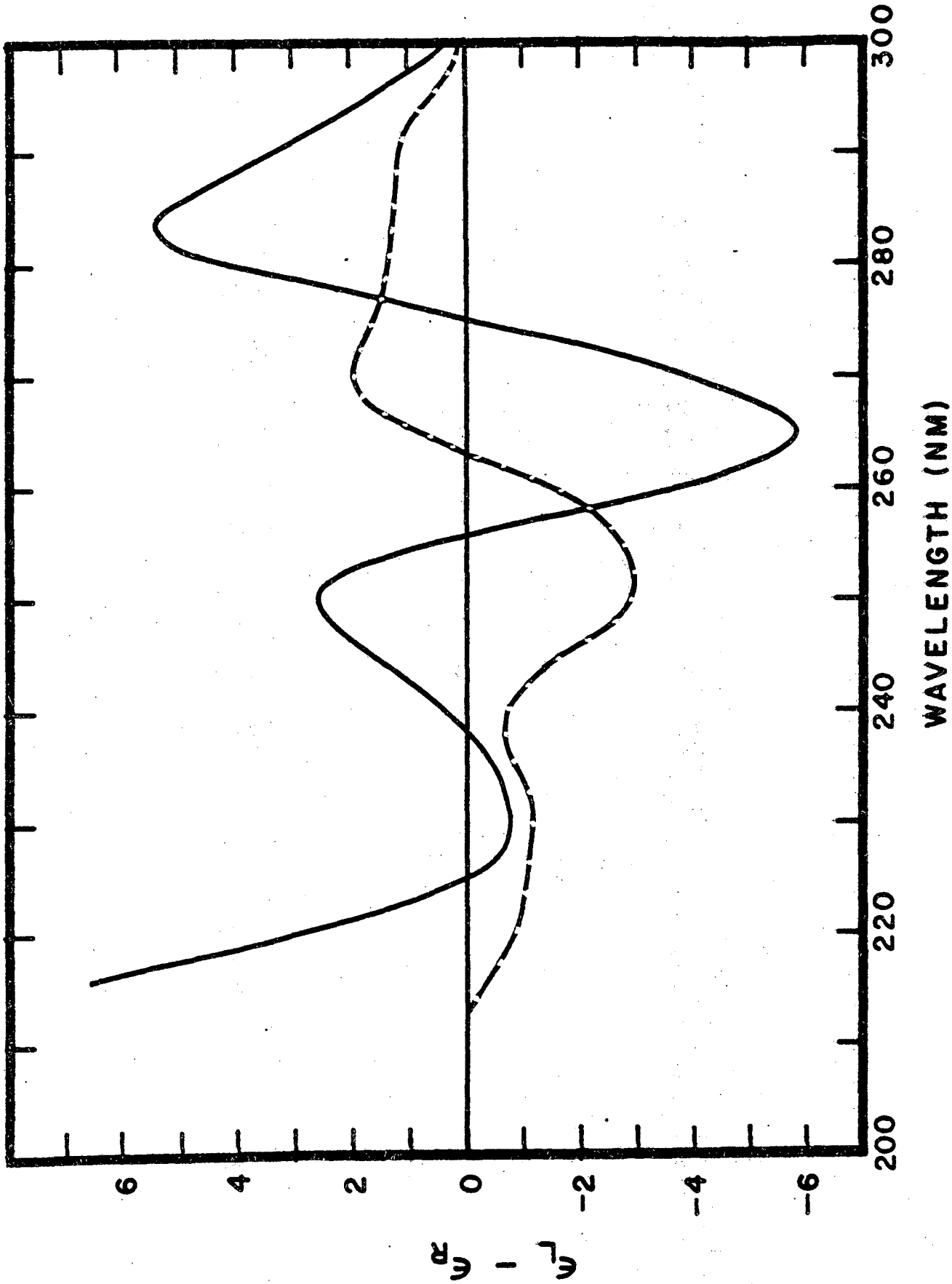
300
280
260
240
220
200
WAVELENGTH (NM)
6
4
2
0
-2
-4
-6
$\alpha_\nu - \Gamma_\nu$

Figure 12: Poly[d(A-G-C)·d(G-C-T)]. 20°, .01 M Na^+ phosphate buffer, pH 7.0. Measured -----, calculated ———.

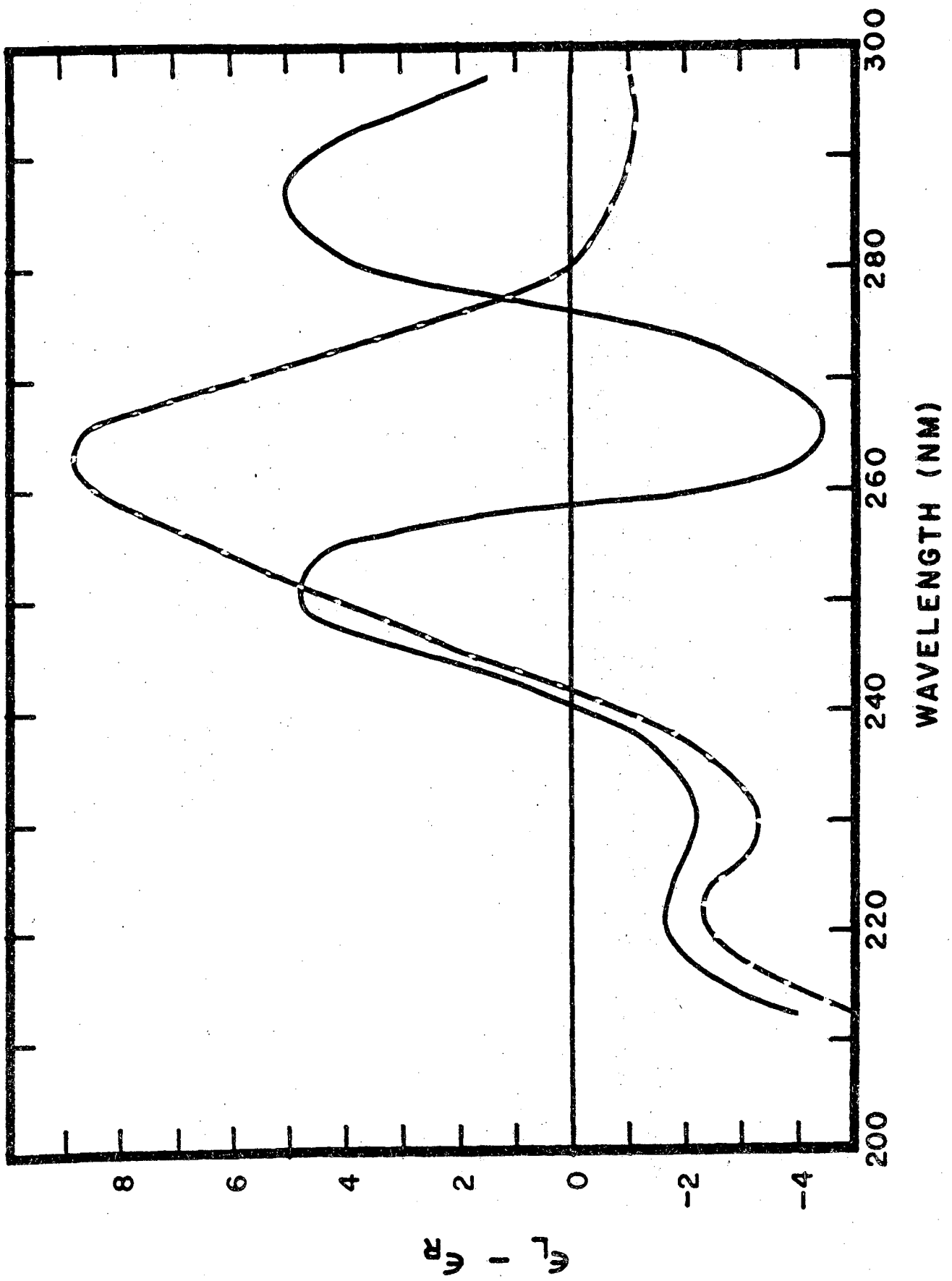

for the failure of these calculations. The success of other calculations seems to suggest that the monomer properties for some of the bases are still in doubt, however failure of the theory or a special geometry for these polymers cannot be ruled out.

In figures 13 and 14 poly[d(A-A-T)·d(A-T-T)] and poly[(A-A-U)·(A-U-U)] calculations are compared with experiment.[24] Except for the fine structure of the maximum at 265 nm, the agreement is fairly good for the ribo polymer. Here again, the difference in magnitude is not serious. For the deoxypolymer we see a very characteristic discrepancy between calculation and experiment for deoxy A·T containing polymers. Both polyd(A) and poly(dA·dT) have similar peak structure in the 260 nm to 280 nm region. It has been suggested that these deoxypolymers do not have standard B-form DNA geometry. Although there is poor agreement between measured and calculated spectra in this series of A·T containing polymers, we will discuss improved methods of analyzing the experimental data in chapter VI. This analysis and and model calculations help locate rotational strengths, and resolve polymer transitions.

VI. Four Stranded Polyinosinic Acid

We have extended previous calculations on polyinosinic acid (poly(I)).[17,19] Since the model geometries for poly(I) contain 3 or 4 bases per helical step,[25] and 11.5 helical

Figure 13: Poly[d(A-A-T)·d(A-T-T)]. 20°, .02 M Na^+ phosphate buffer, pH 7.0. Measured × 5 -----, calculated ———.

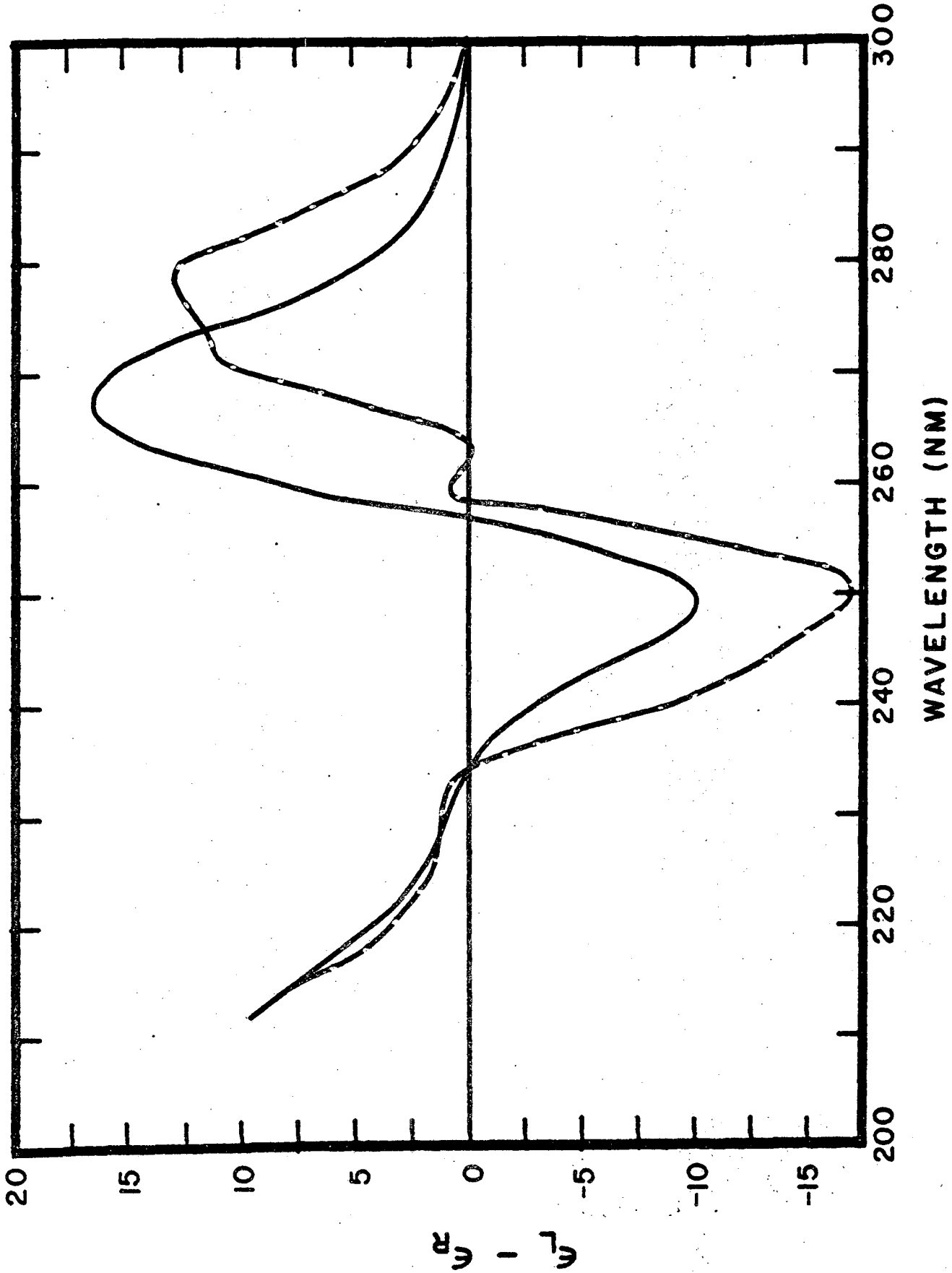
20
15
10
5
0
-5
-10
-15
$\varepsilon_L - \varepsilon_R$
200
220
240
260
280
300
WAVELENGTH (NM)

Figure 14: Poly[(A-A-T)·(A-T-T)] 20°, .02 M Na^+ phosphate buffer pH 7.0. Measured -----, calculated ———.

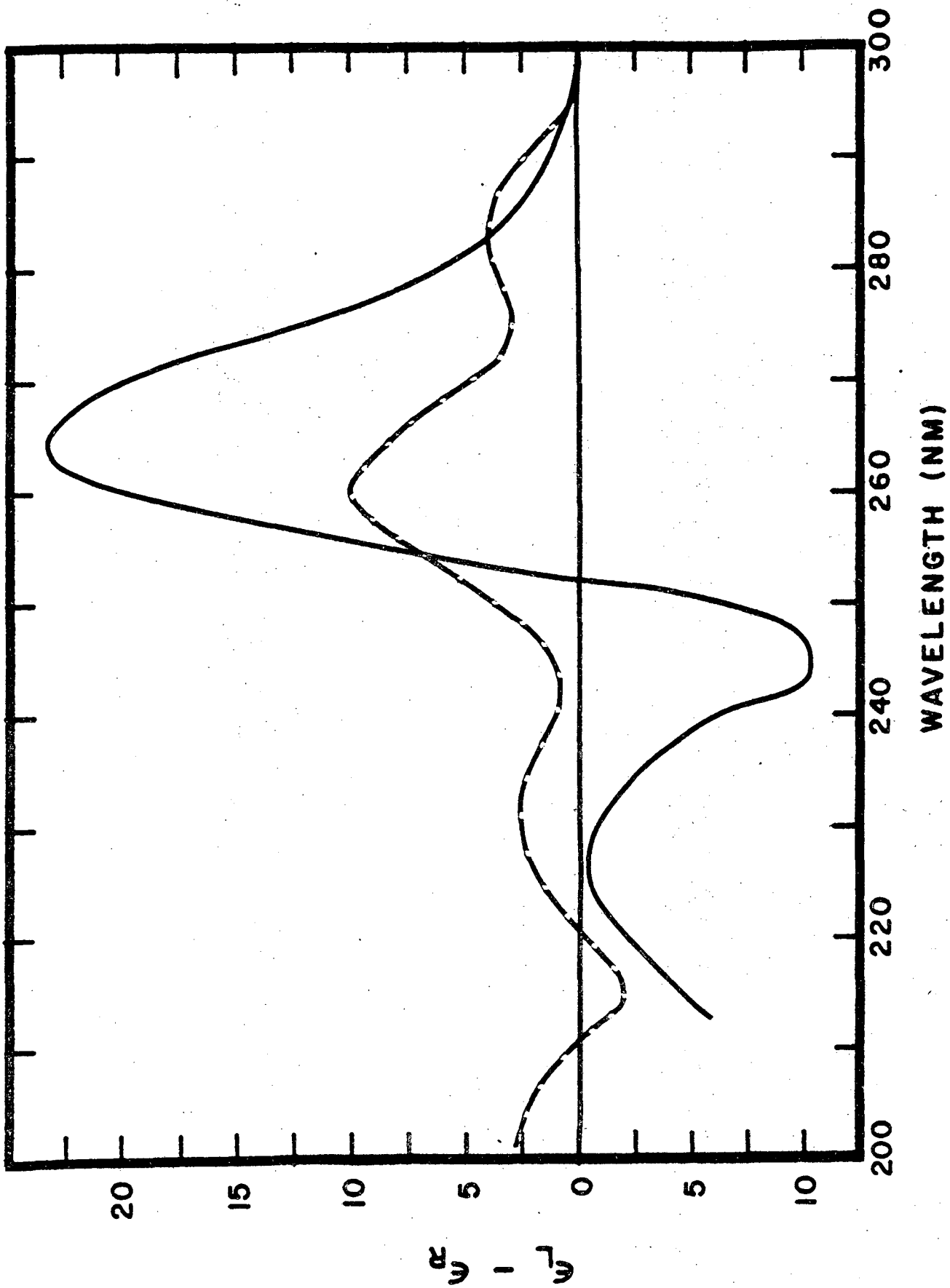
200
220
240
260
280
300
WAVELENGTH (NM)
20
15
10
5
0
5
10
$\varepsilon_L - \varepsilon_R$

steps per turn of the helix, oligomer calculations were extremely difficult. Previous calculations[17] on the 4 stranded poly(I) structure were done including only the 2 longest wavelength transitions of inosine with 68 bases. The infinite polymer calculation with only 2 transitions is very similar to the oligomer calculation with 68 bases and 2 transitions per base. The infinite polymer calculation is compared with experiment[26] in figure 15. Since only 2 transitions were used, the sum rule had to be obeyed in the 200 nm to 300 nm region. Thus without including background transitions, the negative peak at 233 nm can not be avoided.

Cech estimated the effect of the other transitions in inosine by calculating the CD of three of the four strands using the 7 transitions of guanine and only 12 bases in the oligomer. In this calculation, the CD no longer had the minimum at 233 nm, and the maximum at 260 nm and the minimum at 268 nm were increased. She therefore assumed that including the other transitions in the poly(I) calculation would have a similar effect.

To test this hypothesis we have done the infinite polymer calculations on 4 stranded poly(I) with 7 transitions. The inosine absorption spectrum below 220 nm was approximated by using guanine transition directions, polarizabilities, and monopoles. The use of guanine parameters, where necessary, was considered justified since both the short wavelength absorption and the CNDO calculations of the two bases are

Figure 15: Poly(I) CD at 3° in 1.0 M NaCl after gradual addition of NaCl -----. Infinite polymer calculation with only 2 transitions per base ———.

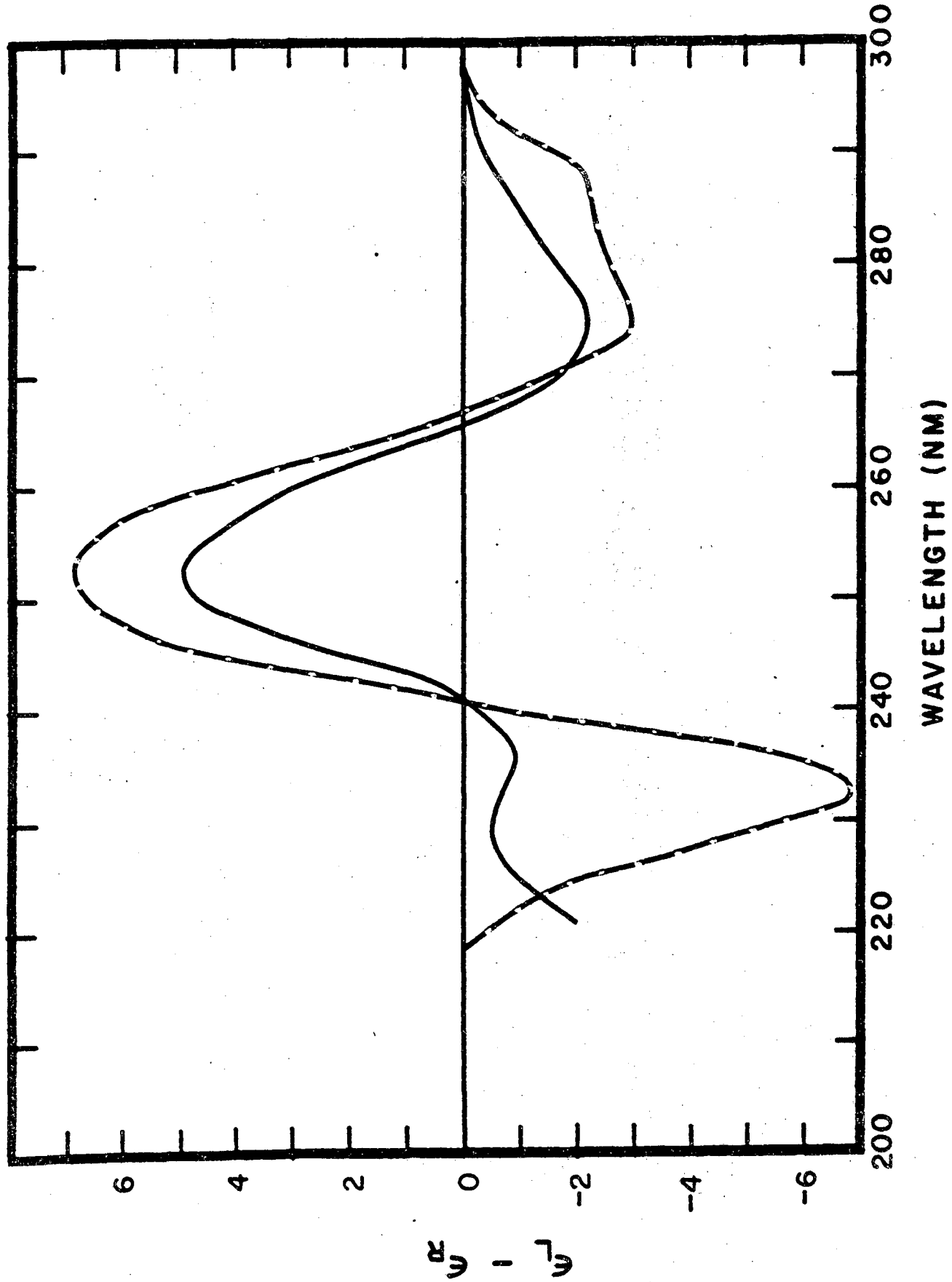

very similar. The calculated CD is shown in figure 16. The negative peak at 280 nm is relatively unaffected, but the maximum at 255 nm is greatly increased. There is no longer a minimum at 233 nm. In general, the agreement with experiment is poorer when the background transitions are included. This suggests that the monomer properties of inosine (and probably guanine) are in error.

Figure 16: Poly(I) calculation with 7 transitions per base.

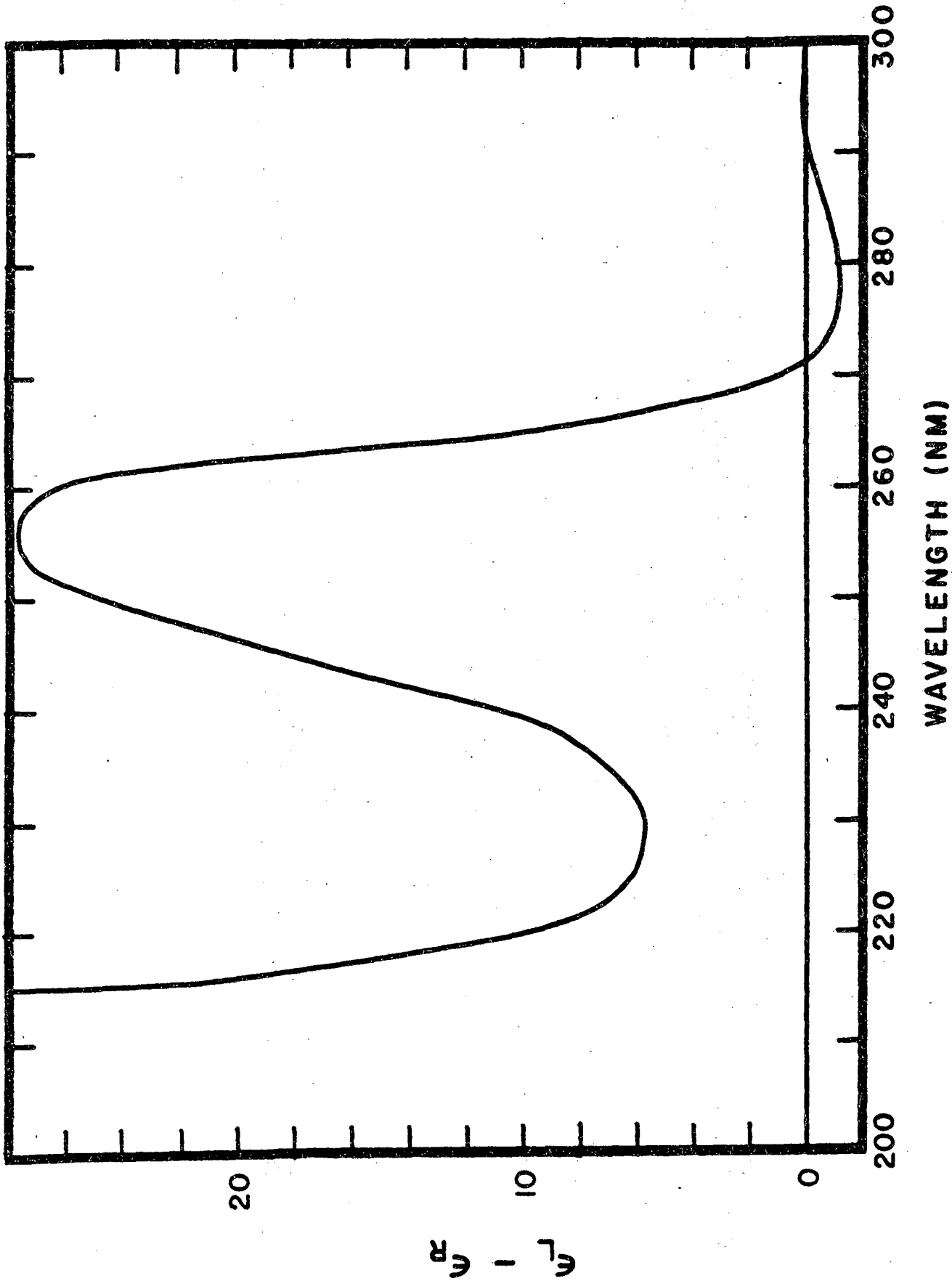
300
280
260
240
220
200
WAVELENGTH (NM)
0
10
20
$\epsilon_L - \epsilon_R$

Chapter V Bibliography

1. J.D. Watson and F.H.C. Crick, Nature 171, 737 (1953).
2. V.A. Bloomfield, D.M. Crothers, and I. Tinoco, Jr., Harper and Row, Publishers, Inc., New York (1974). The Physical Chemistry of Nucleic Acids
3. S. Arnott, S.D. Dover, and A.J. Wonacott, Acta Cryst. B25, 2192 (1969).
4. D. Moore, Ph.D. Thesis, Ohio University (1974).
5. D. Moore and T.E. Wagner, Biopolymers 13, 977 (1974).
6. R. Langridge, D.A. Marvin, W.E. Seeds, H.R. Wilson, C.W. Cooper, M.H.F. Wilkins, and L.D. Hamilton, J. Mol. Biol. 2, 38 (1960).
7. D.A. Marvin, M. Spencer, M.H.F. Wilkins, and L.D. Hamilton, J. Mol. Biol. 3, 547 (1961).
8. S. Arnott and D.W.L. Hukins, Biochem. Biophys. Res. Comm. 47, 1504 (1972).
9. W. Fuller, M.H.F. Wilkins, H.R. Wilson, and L.D. Hamilton, J. Mol. Biol. 12, 60 (1965).
10. S. Arnott, D.W.L. Hukins, and S.D. Dover, Biochem. Biophys. Res. Comm. 48, 1392 (1972).
11. M.J.B. Tunis-Schneider and M.F. Maestre, J. Mol. Biol. 52, 521 (1970).
12. C.A. Bush and I. Tinoco, Jr., J. Mol. Biol. 23, 601 (1967).
13. V.I. Ivanov, L.E. Minchenkova, A.K. Schulkina, and A.I. Poletayev, Biopolymers, 12, 89 (1973).

14. B.P. Dorman and M.F. Maestre, Proc. Nat. Acad. Sci., U.S.A. 70, 255 (1973).

15. L.S. Lerman, Proc. Nat. Acad. Sci., U.S.A. 68, 1886 (1971).

16. D.S. Moore and T.E. Wagner, Biopolymers, 12, 201 (1973).

17. C. Cech, Ph.D. Thesis, University of California, Berkeley (1975).

18. C. Cech, W. Hug, and I. Tinoco, Jr., Biopolymers, 15, 131 (1976).

19. C. Cech, and I. Tinoco, Jr., Nucleic Acids Research 3, 399 (1976).

20. W. Hug and I. Tinoco, Jr., J. Amer. Chem. Soc. 95, 2803 (1973).

21. W. Saenger, J. Riecke, and D. Suck, J. Mol. Biol. 93, 529 (1975).

22. D.M. Gray, Biopolymers 14, 487 (1975).

23. R.L. Ratliff, D.E. Hoard, F.N. Hayes, D.A. Smith, and D.M. Gray, Biochemistry 15, 168 (1976).

24. D.M. Gray, R.T. Ratliff, and D.L. Williams, Biopolymers 12, 1233 (1973).

25. S. Arnott, R. Chandrasekaran, and C.M. Martilla, Biochem. J. 141, 537 (1974).

26. D. Thiele and W. Guschlbauer, Biophysik 9, 261 (1973).

Chapter VI

Circular Dichroism of Adenine and Thymine Containing Synthetic Polynucleotides*

I. Introduction

From X-ray diffraction studies[1-3] it is well-known that DNA can assume a number of distinct structures, the main types being the A, B, C and D structures. The A, B and C conformations were related to circular dichroism (CD) by measuring CD spectra of DNA films.[4-6] When these film spectra are compared to solution spectra,[7,8] it becomes clear that both DNA and synthetic polynucleotides in solution do not occur in one well-defined conformation. Instead, more or less continuous transitions occur due to changes in salt concentration,[8] solvent composition,[9] and temperature.[10,11] In this paper we describe the temperature dependence of the adenine (A) and thymine (T) containing synthetic polymers polyd(A), polyd(T), poly[d(A)·d(T)] and poly[d(A-T)·d(A-T)].

The reasons for this study are numerous. It was hoped to get information about premelting conformational changes which occur in the double stranded polymers. It is not clear which structural transitions are involved and whether they are the same for poly[d(A)·d(T)] and poly[d(A-T)·d(A-T)].

---

* The material in this chapter has been submitted to Biopolymers for publication with coauthors Jan Greve and Marcos F. Maestre.

From theory[12,13] it is clear that the CD of polynucleotides is determined by the structure of the polymer and the optical transitions of the bases. Any change in CD brought about by a conformation change occurs at wavelengths determined by the location of the polymer rotational strength bands. By studying polymers containing only A and T, information about the location of the polymer bands due to A and T should be obtained. Such data are badly needed[14-17] to improve calculations of polynucleotide spectra.

II. Materials and Method

CD spectra were measured with a Cary 60 spectrophotometer equipped with a 6001 unit. The computerized data-collecting system has been described before.[18] Temperatures were measured with a thermocouple inserted in a water-filled cuvet which was in an identical position as the sample cuvet. Absorption measurements were made on a Cary 14 or Gilford spectrophotometer. All polymers were purchased from P.L. Biochemicals. The data provided by the manufacturer are:

	λ max(nm)	$\varepsilon(\ell mol^{-1})$	$s_{20}w(s)$	Cat. No.	Batch No.
polyd(A)	258.5	8,600	6.8	7,836	526-35
polyd(T)	264	8,520	8.5	7,834	508-68
poly[d(A)·d(T)]	258	6,000	-	7,860	526-26
poly[d(A-T)·d(A-T)]	262	6,600	7.8	7,870	508-101

The lyophilized polymers were dissolved in buffer solution and stored frozen. The buffers used were: Buffer I; 10 mM KCl, 2 mM Tris pH 7.8, 0.1 mM EDTA; Buffer II; Buffer I plus 10 mM $MgSO_4$.

Poly[d(A)·d(T)] in buffer I showed a 4 percent increase in absorption in raising the temperature from 20° C to 40° C and then melted at 47° C. Poly[d(A-T)·d(A-T)] in buffer I melted at 44° C, in buffer II at 67.5° C.

CD data are presented as the CD per mole of monomer $\varepsilon_L - \varepsilon_R$ where ε_L and ε_R are the extinction coefficients for left and right circularly polarized light respectively.

III. Results

CD spectra of polyd(A), polyd(T), poly[d(A)·d(T)] and poly[d(A-T)·d(A-T)] have been published before.[10,11,19,20] Our spectra are in good agreement with these data, provided the comparison is made between spectra measured under similar conditions.

CD Spectra

Poly[d(A-T)·d(A-T)]. CD spectra of poly[d(A-T)·d(A-T)] in buffer II are shown in figure 1. The premelting changes (figure 1a) involve mainly changes in amplitude of the extrema. Upon melting (figure 1b) both amplitude and position of the extrema change. A similar premelting behavior was found in buffer I. The CD spectra of melted poly[d(A-T)·d(A-T)] in buffer I at 53°C and in buffer II at 71.5°C have extrema at the same wavelengths but the amplitudes are greater in buffer I.

Polyd(A)·d(T). The temperature dependence of the polyd(A)·d(T) CD spectrum is shown in figures 2 and 3. In buffer I (figure 2) an isosbestic point is detected at 264 nm. The changes in $\Delta\varepsilon$ observed in going from 1° C (double stranded) to 48.2° C (melted) occur in only one direction at each particular wavelength. A similar behavior is found in buffer II between 2.5° C and 65° C (figure 3. Above 65° C, however, the CD spectrum behaves differently in this buffer. At 260 nm $\Delta\varepsilon$ decreases upon raising the temperature from 2.5° C to 65° C, increases in going from 65°C to 76° C and then decreases upon denaturation. As shown in figure 4, the spectrum measured at 71.1° C resembles the low temperature spectrum measured for poly[d(A-T)·d(A-T)].

Polyd(A) and polyd(T). CD spectra of polyd(A) and polyd(T) measured in buffer I are shown in figures 5 and 6.

Difference CD Spectra

The spectral changes observed upon varying the temperature look complicated and it is not clear what the relation is between the spectral changes of poly[d(A-T)·d(A-T)] and poly[d(A)·d(T)]. To change this situation we calculated difference spectra by subtracting the CD spectrum measured at low temperature from the spectra obtained at higher temperatures.

Poly[d(A)·d(T)]. Difference spectra obtained for poly[d(A)·d(T)] in buffer I are shown in figure 7. They all have a characteristic appearance with maxima at 288 nm,

272 nm and 246 nm and minima at 257 nm and 214 nm. The difference spectra obtained for poly[d(A)·d(T)] in buffer II (figure 8) have extrema at the same wavelengths. Moreover, the magnitudes of the difference spectra obtained after melting are almost the same for buffer I and buffer II except for the 214 nm trough which is a factor of two deeper in buffer II.

Poly[d(A-T)·d(A-T)]. In figure 9 the difference spectra for poly[d(A-T)·d(A-T)] in buffer II are shown. Up until 60° C the difference spectra have a maximum at 264 nm and minima at 283 and 217 nm. After melting the difference spectrum looks like the one obtained for poly[d(A)·d(T)] after melting. Above 220 nm all extrema have the same sign and occur at the same wavelength. The only difference is that the magnitudes of the poly[d(A-T)·d(A-T)] difference spectrum are smaller. The difference spectra for poly [d(A-T)·d(A-T)] in buffer I (figure 10) are similar to those found in buffer II.

Polyd(A) and polyd(T). Difference spectra for polyd(A) and polyd(T) are shown in figures 11 and 12. The polyd(T) spectra have extrema at 273 nm, 254 nm and 216 nm. The polyd(A) difference spectra show extrema at 282 nm, 265 nm, 254 nm and 232 nm.

IV. Discussion

Theory

From De Voe's[13] classical coupled oscillator theory it follows that the CD of a polynucleotide to first order

(weak interaction) is:

$$(\varepsilon_L - \varepsilon_R) = \frac{2\omega}{c} \sum_i \varepsilon_i \sum_j \alpha_j G_{ij} e_i e_j r_{ij} \qquad (1)$$

where ε_i and α_j refer to extinction and (real) polarizability of oscillators i and j and the bases; e_i and e_j are the oscillator directions, and r_{ij} is the vector from transition i to transition j; and G_{ij} contains the interaction parameters.

Equation (1) shows that in first order the frequency and geometry dependence of the CD spectrum is separated. This follows also from first order Quantum Mechanical theory.[12] Therefore, a rotational strength band arising from interaction of two transitions i and j should always be seen at the same frequency no matter what the geometry of the polynucleotide is. The geometry determines the relative amplitudes of the different bands in the CD spectrum. In particular, any rotational strength band present in the CD spectrum should occur at the same wavelength in a difference spectrum. It is, however, possible that not all rotational strength bands present in the original spectrum are seen in the difference spectrum. Those due to interactions which are left unchanged by the temperature induced conformational change are subtracted. Moreover, it is clear that each distinct structural change will yield a different difference spectrum as the structural parameters are different.

To determine frequencies of the near UV transitions from the spectra, it should be kept in mind that according to equation (1) each transition may give rise to either one or two peaks. One peak (non-conservative), centered at the same frequency as the maximum of ε_i, will be observed if transition j is so far from i that α_j is almost constant at frequencies where $\varepsilon_i \neq 0$. Two peaks of opposite sign (conservative) will be observed if transition j is the same as i, but i and j are located on different bases. Then the frequency of transition j is found as that frequency between the two peaks at which the CD is zero. When transition i and j do not coincide but are close, the offhand prediction is difficult and exact calculations have to be made.

From the discussion above it is clear that original and difference spectra contain the same frequency information. It should be kept in mind, however, that equation (1) is an approximation in which only base to base interactions are considered. Any contributions from base to backbone interactions[21] and intrinsic CD of the bases[12] should be added. The contribution of these factors to the CD is not well known, but it is evident that their contribution to a difference spectrum is smaller than to an original CD spectrum as they are either completely, or for the greater part, subtracted. Moreover, the number of base to base interactions which contribute to the difference spectrum is smaller. This may cause the difference spectra to be better resolved. The

difference spectrum of a denatured and a double stranded polynucleotide, for instance, is mainly determined by interstrand interactions since the contributions to the CD spectrum due to intrastrand interactions are largely subtracted. It is these facts which make the difference spectra obtained upon melting have a characteristic shape which is similar for poly[d(A)·d(T)] and poly[d(A-T)·d(A-T)].

Transition Frequencies

For the reasons mentioned above, we will try to determine the location of the rotational strength bands using mainly the difference spectra.

The (conservative) peaks at 254 nm and 273 nm in the polyd(T) difference spectrum must arise from the $\pi \rightarrow \pi^*$ transition at 263 nm[14,22] which also causes the absorption maximum to be at 264 nm. We do not find evidence for the presence of transitions at 256 nm and 278 nm as suggested in the literature.[23] The 216 nm peak in the polyd(T) difference spectrum may be one of a conservative pair due to a transition located near 206 nm.[14]

The polyd(A) difference spectrum is much more complicated. The 232 nm trough comes from a $\pi \rightarrow \pi^*$ transition as described by Bush and Scheraga.[20] The absorption maximum of the polynucleotide is at 258.5 nm so it is clear that a $\pi \rightarrow \pi^*$ transition must be located there. The 254 nm and 265 nm extrema and the crossover at 258 nm in the difference

spectrum arise from this transition. The 282 trough could then arise from an $n \rightarrow \pi^*$ transition as suggested by Bush and Scheraga.[20] A different interpretation will be discussed below, however.

It is clear that the change in conformation induced by denaturation of the double stranded polymers is quite drastic. Yet, above 220 nm the extrema and crossovers seen in the melting difference spectra of poly[d(A)·d(T)] and poly [d(A-T)·d(A-T)] occur at the same wavelengths. We will, therefore, focus our attention on this wavelength area. It is not evident *a priori* what the result of coupling the 258 nm A and 262 nm T transitions will be since they are very close. We therefore calculated the contribution to the CD of poly[d(A)·d(T)] and poly[d(A-T)·d(A-T)] due to interstrand interaction only. The calculations were performed using programs developed in this laboratory by C.M. Cech The transition wavelengths and the dipole strengths were the same as used by her ($\pi \rightarrow \pi^*$ transitions of A at 260 nm, 240 nm and 207 nm; $\pi \rightarrow \pi^*$ transitions of T at 262 and 206 nm). B-DNA geometry was assumed. The results are shown in figure 13. A very good agreement in sign and location of extrema and crossovers between the experimental results and the calculations is obtained between 215 nm and 260 nm. We conclude that the extrema at 246 nm and 258 nm in the experimental melting difference spectra arise from coupling of the 258 nm, 232 nm A transition with the 262 nm T transition. With the chosen input data it is impossible to

explain the experimental spectrum above 260 nm. We therefore propose that two transitions are present which were not incorporated in the calculations. Most likely the peak at 272 nm in the melting difference spectra is caused by a transition on A near this wavelength. This transition must be oriented in such a way that its contribution to the CD spectrum of polyd(A), poly[d(A)·d(T)] and poly[d(A-T)·d(A-T)] above 260 nm is opposite in sign to that due to the transitions close to 260 nm. This explains why the CD spectra of these polymers and of several A-T rich crab satellite DNAs[24,25] are non-conservative and do not look like a B-DNA spectrum. This transition near 272 nm may also be responsible for the crossover at 272 nm and (part) of the extrema at 265 nm and 282 nm in the polyd(A) difference spectrum.

The 287-289 nm peak in the melting difference spectra may be caused by a second transition not used in the calculations. From our experiments it is not clear whether this transition is an A or a T transition. Moreover, it is not possible to conclude whether this transition and the one near 272 nm are $\pi \rightarrow \pi^*$ or $n \rightarrow \pi^*$ transitions. In literature evidence was presented[26,27] for a $\pi \rightarrow \pi^*$ transition on A and an $n \rightarrow \pi^*$ transition on T both at long wavelengths.

Conformational Changes

From figures 9 and 10 it is clear that the premelt and the melting difference spectra measured for poly[d(A-T)·d(A-T)] are quite different. This raises the question: What kind of conformational change occurs before melting? It has been shown[2,28] that poly[d(A-T)·d(A-T)] fibers can assume several different structures. In solution all kinds of conformational intermediates occur. By analogy with film spectra of DNA in the C conformation[4] and films of d(A-T)·d(A-T) in the C geometry (M. Maestre, unpublished data), we propose that the poly[d(A-T)·d(A-T)]structure is much closer to a C-type structure than to a B-type geometry. Since the premelt difference spectrum bears much resemblance with an A-type DNA CD spectrum,[4,7] we believe that the premelt conformations is one in which the A-type (or A*-type[29]) nature of the conformation increases. Gennis and Cantor,[11] using different arguments, also suggest such a structural change for the premelting behavior.

In detail, the alteration of the low temperature geometry for d(A-T)·d(A-T) ("C" geometry), as the temperature is increased, involves a C to B transition whose geometrical variation is very similar in character to the one that is seen in the B to A transition. See figure 10. Thus it is those geometrical parameters which vary monotonically between A, B, and C forms which may be the controlling factor in the variation of the CD of DNA's as a function of secondary structure. One such paramater, proposed by

Ivanov, et al, is the rotation per residue angle which is 39° for the C form, 36° for the B form, and 32.7° for the A form geometries.

It is the alteration of this angle which can be correlated by the maximum in the 280-280 nm region. An inference favoring this interpretation can be drawn from the data of Maestre and Wang's[35] study of the CD of supercoiled DNA's as a function of number of superturns. In this work it is shown that the increase in rotational strengths in the 260-300 nm region is approximately proportional to the superhelical density. Thus, for small variations in the angle per residue a linear variation in the CD spectra can be expected. Similar conclusions were drawn by Ivanov, et al,[7] for transitions between B to C geometries.

At high relative humidities[29] poly[d(A)·d(T)] fibers are in a B type conformation called B' (Arnott and Selsing[3]) which is different from the B* structure of poly[d(A-T)·d(A-T)]. Instead the poly[d(A)·d(T)] premelt difference spectrum looks like a melting difference spectrum. In agreement with this a four percent increase in absorption was found before melting in buffer I. This may be due to breathing or chain slippage.[11,30] Just before melting, however, especially in buffer II, a discontinuity in the CD spectral changes was observed. The CD spectrum of poly [d(A)·d(T)] measured at 41.1° C (figure 4) resembles a low temperature poly[d(A-T)·d(A-T)] spectrum. This suggests that

just prior to melting the conformation changes, probably from a B' to a B* conformation.

V. Conclusion

In this study the determination of CD difference spectra was most useful. Although it is clear that difference spectra contain no more intrinsic information than present in the CD spectra from which they are derived, they are more easily interpreted. This may also hold true for other synthetic polynucltoeides. Gray, Tinoco and Chamberlin[31] calculated difference spectra for the melting of poly[(A)·(U)], poly [(A-U)·(A-U)], poly[(G)·(C), and poly[(G-C)·(G-C)]. They suggested that these difference spectra are base-pair specific.

Whether the use of difference spectra in native DNA studies will be useful is unknown. It must be expected that no specific information about optical transitions will be present since too many different interactions are occurring. Yet it may be that different conformational changes yield specific difference spectra.

A possible use of difference spectra may be to determine the nature of the DNA conformational changes which take place in nucleoproteins.[32,33]

From our experiments with poly[d(A-T)·d(A-T)] and poly[d(A)·d(T)] we conclude that an optical transition near 272 nm on A and a transition near 287 nm, probably T, are present. The premelting behavior of poly[d(A-T)·d(A-T)] is ascribed to a conformational change in which the A type

nature of the conformation increases. For poly[d(A)·d(T)] such a change is not found. Instead, a transition between two B type conformations takes place.

LEGENDS TO THE FIGURES

Figure 1: CD spectra of poly[d(A-T)·d(A-T)] in buffer II at different temperatures. At 71.5°C the poly [d(A-T)·d(A-T)] is melted. Figure 1a shows the premelting changes. Figure 1b shows the CD spectra at temperatures close to the melting temperature.

Figure 2: CD spectra of poly[d(A)·d(T)] in buffer I at different temperatures. At 48.2°C the poly[d(A)·d(T)] is melted.

Figure 3: CD spectra of poly[d(A)·d(T)] in buffer II at different temperatures. At 80.5°C the poly[d(A)·d(T)] is melted.

Figure 4: CD spectra of poly[d(A)·d(T)] in buffer II at 71.1°C and of poly[d(A-T)·d(A-T)] in buffer I at 1°C.

Figure 5: CD spectra of poly[d(A)] in buffer I at different temperatures.

Figure 6: CD spectra of poly[d(T)] in buffer I at different temperatures.

Figure 7: CD difference spectra for poly[d(A)·d(T)] in buffer I. The spectrum measured at 1°C has been subtracted from the spectra measured at higher temperatures.

Figure 8: CD difference spectra for poly[d(A)·d(T)] in buffer II. The spectrum measured at 2.5°C has been subtracted from the spectra measured at higher temperatures.

Figure 9: CD difference spectra for poly[d(A-T)·d(A-T)] in buffer II. The spectrum measured at 1°C has been subtracted from the spectra measured at higher temperatures.

Figure 10: CD difference spectra for poly[d(A-T)·d(A-T)] in buffer I. The spectrum measured at 1°C has been subtracted from the spectra measured at higher temperatures.

Figure 11: CD difference spectra for poly[d(A)] in buffer I. The spectrum measured at 1°C has been subtracted from the spectra measured at higher temperatures.

Figure 12: CD difference spectra for poly[d(T)] in buffer I. The spectrum measured at 1°C has been subtracted from the spectra measured at higher temperatures.

Figure 13: Measured and Calculated CD difference spectra of poly[d(A)·d(T)] and poly[d(A-T)·d(A-T)]. The measured difference spectra were obtained by subtracting the spectrum of the double stranded polymer from the spectrum of the melted polymer. The calculated spectra give the contribution to the CD spectra of the double stranded polymers due to interstrand interaction only. Before

plotting, the sign of the calculated CD was changed to make comparison with the measured spectra easier. The calculations were made using the classical all-order de Voe theory for the optical activity of polymers. Optical transitions were supposed to be located at: on A - 260, 240, 207, 187.5 and 119 nm; on T - 262, 206, 175 and 119 nm. The polymers were assumed to be in B-DNA geometry.

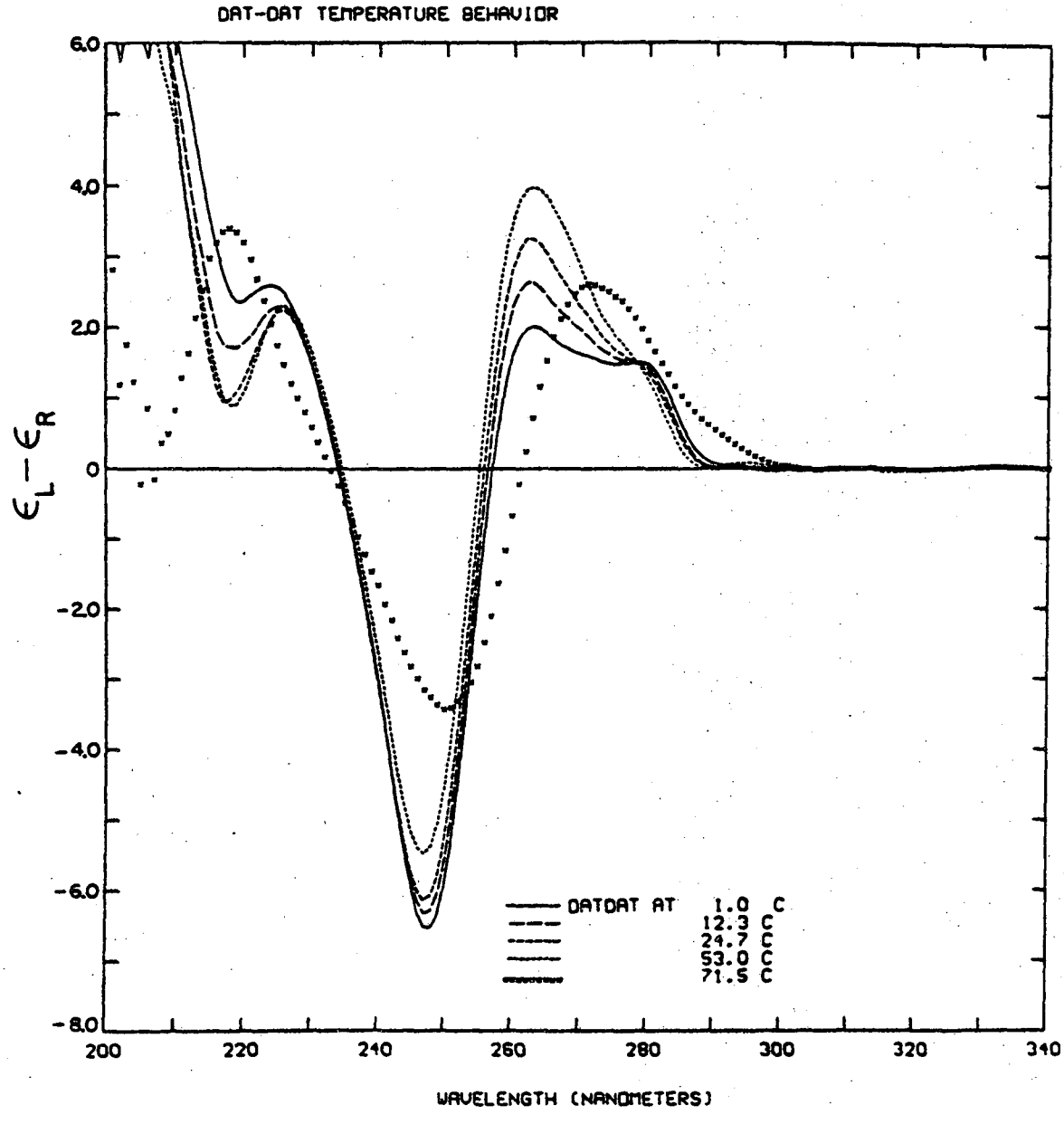
DAT-DAT TEMPERATURE BEHAVIOR
6.0
4.0
2.0
0
-2.0
-4.0
-6.0
-8.0
$\epsilon_L - \epsilon_R$
200
220
240
260
280
300
320
340
WAVELENGTH (NANOMETERS)
DATDAT AT 1.0 C
12.3 C
24.7 C
53.0 C
71.5 C

Figure 1a

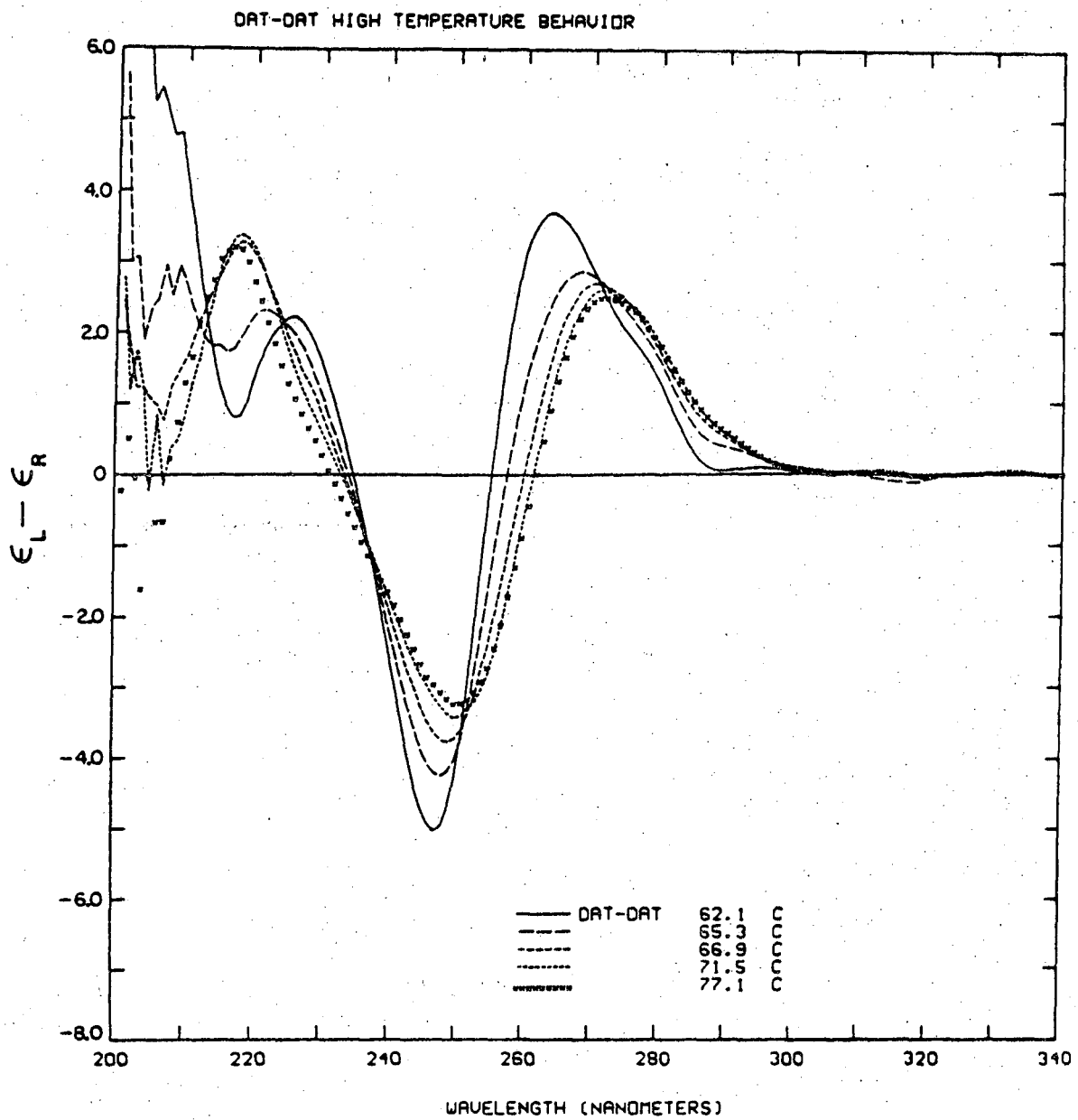
DAT-DAT HIGH TEMPERATURE BEHAVIOR
6.0
4.0
2.0
0
-2.0
-4.0
-6.0
-8.0
$\epsilon_L - \epsilon_R$
200
220
240
260
280
300
320
340
WAVELENGTH (NANOMETERS)
DAT-DAT
62.1 C
65.3 C
66.9 C
71.5 C
77.1 C

Figure 1b

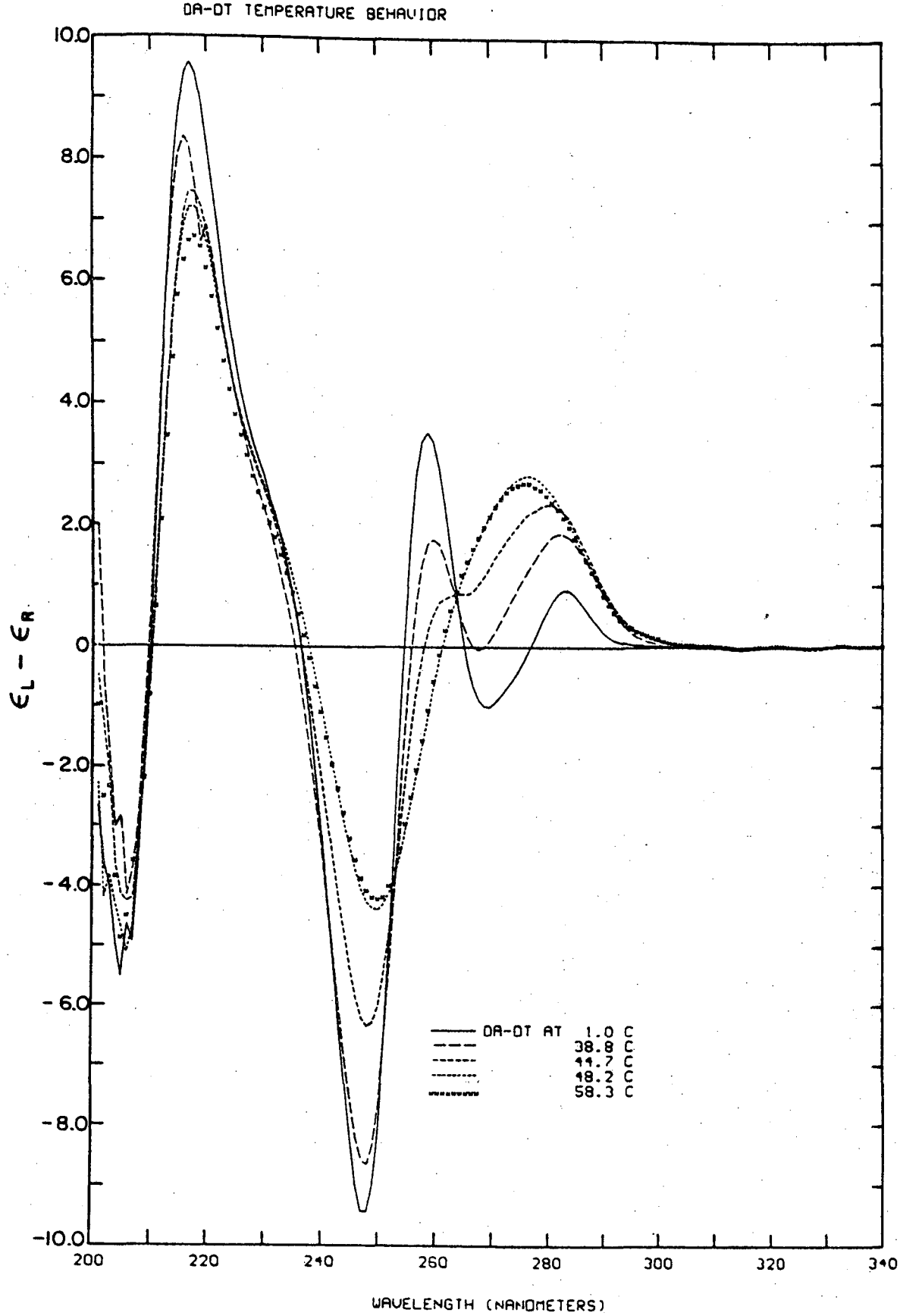
DA-DT TEMPERATURE BEHAVIOR
10.0
8.0
6.0
4.0
2.0
0
-2.0
-4.0
-6.0
-8.0
-10.0
$\epsilon_L - \epsilon_R$
200
220
240
260
280
300
320
340
WAVELENGTH (NANOMETERS)
DA-DT AT 1.0 C
38.8 C
41.7 C
48.2 C
58.3 C

Figure 2

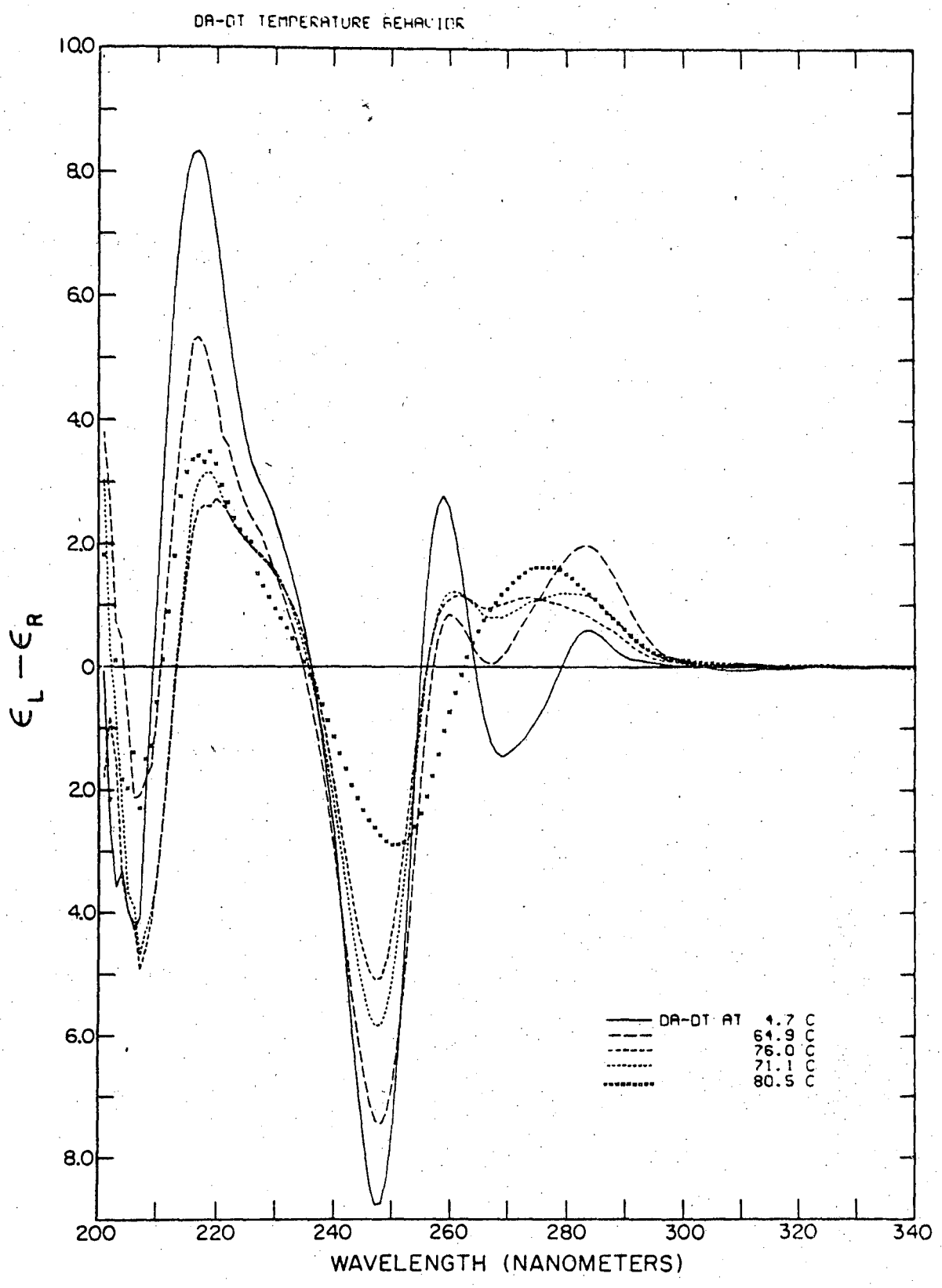

Figure 3

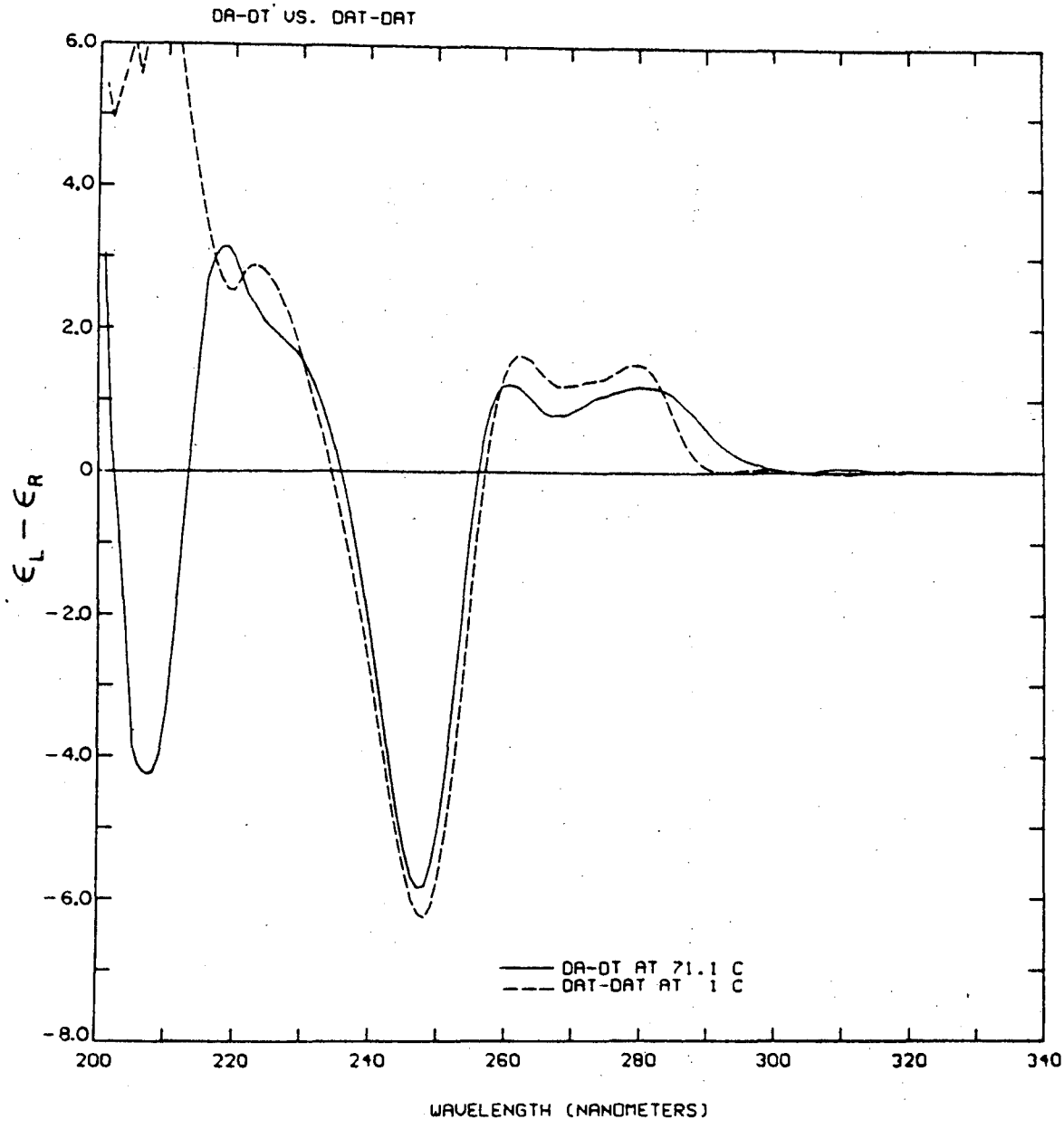
DA-DT VS. DAT-DAT
6.0
4.0
2.0
0
-2.0
-4.0
-6.0
-8.0
$\epsilon_L - \epsilon_R$
200
220
240
260
280
300
320
340
WAVELENGTH (NANOMETERS)
DA-DT AT 71.1 C
DAT-DAT AT 1 C

Figure 4

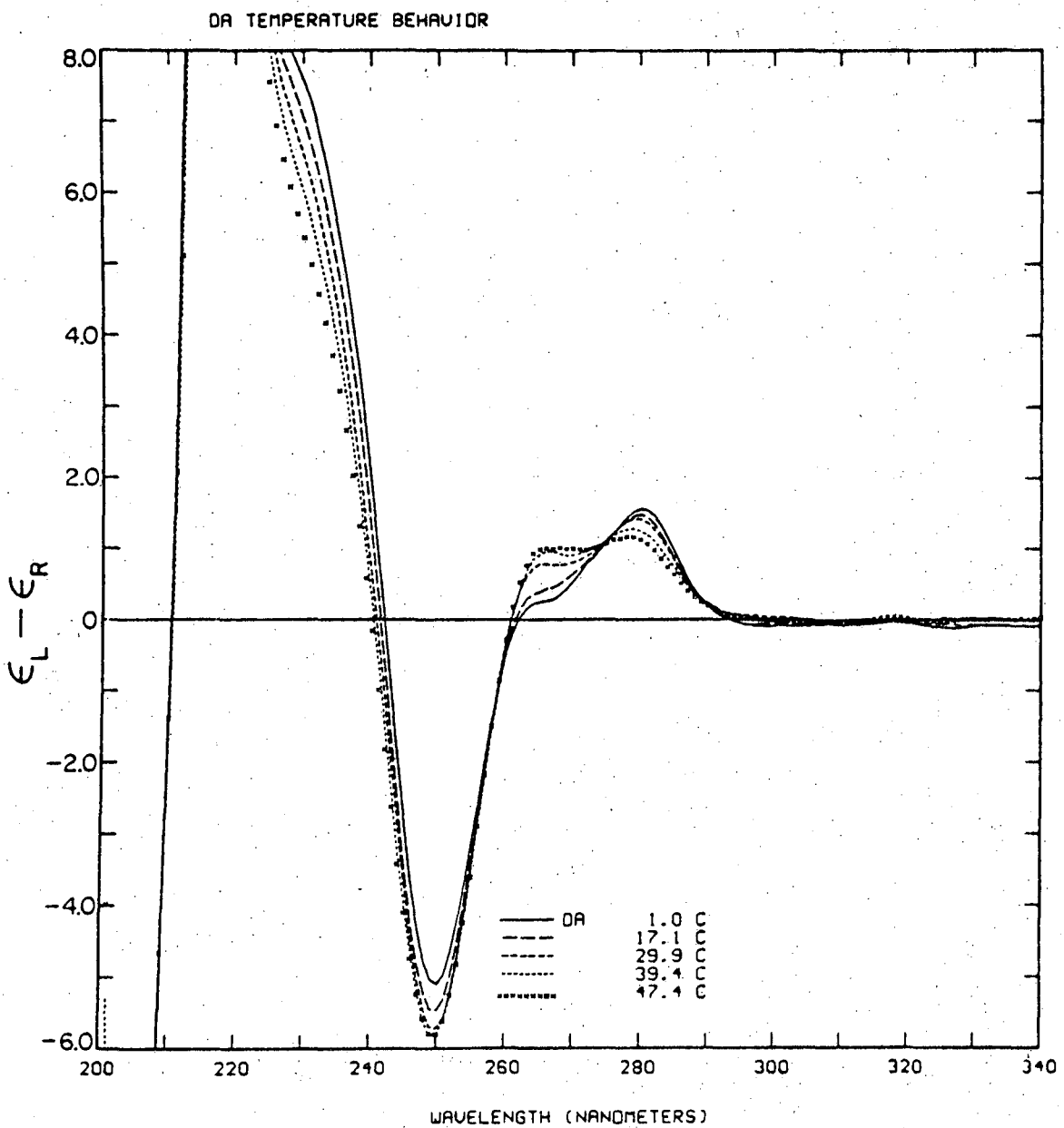

Figure 5

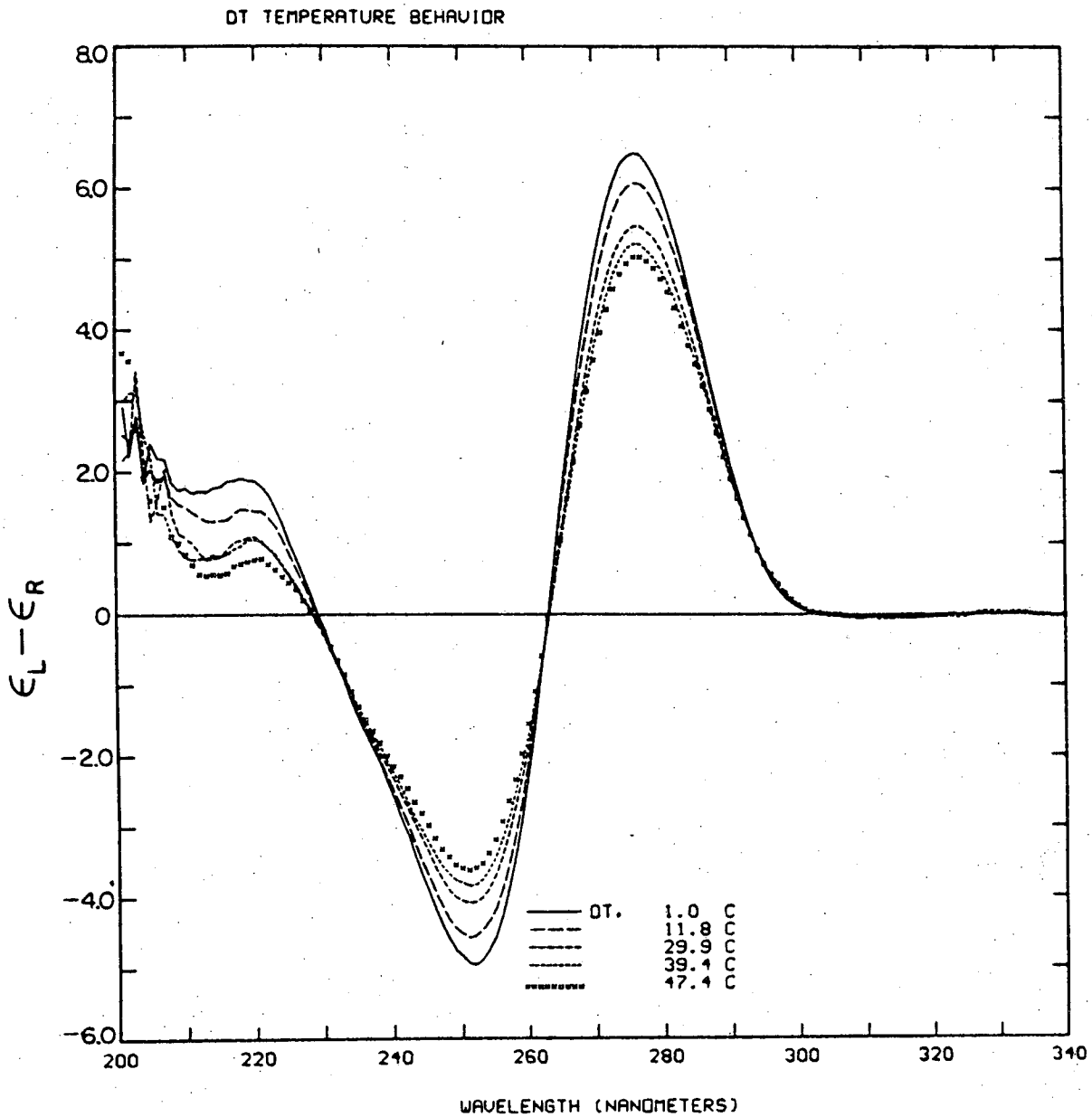
DT TEMPERATURE BEHAVIOR
8.0
6.0
4.0
2.0
0
-2.0
-4.0
-6.0
$\epsilon_L - \epsilon_R$
200
220
240
260
280
300
320
340
WAVELENGTH (NANOMETERS)
DT. 1.0 C
11.8 C
29.9 C
39.4 C
47.4 C

Figure 6

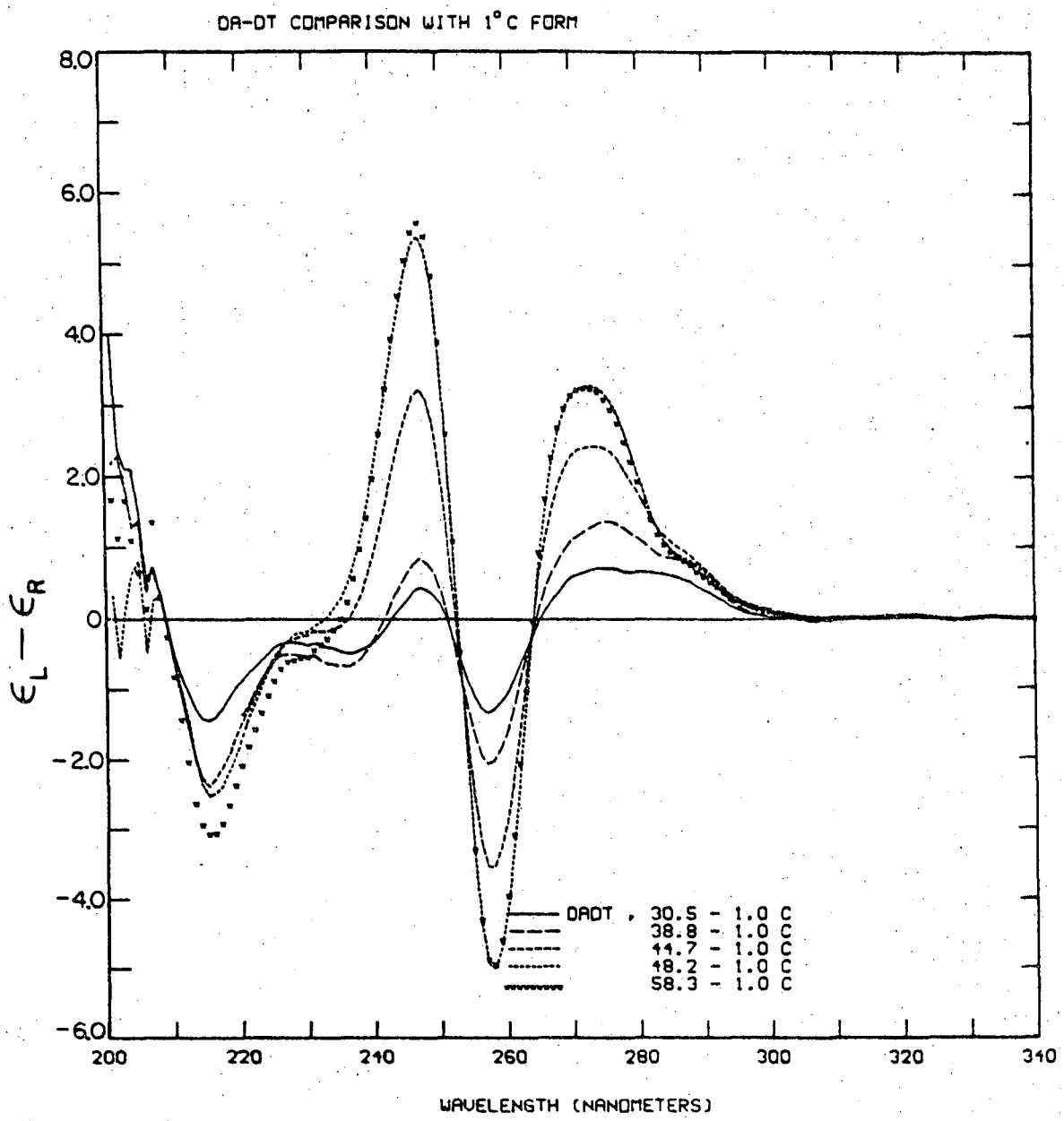

Figure 7

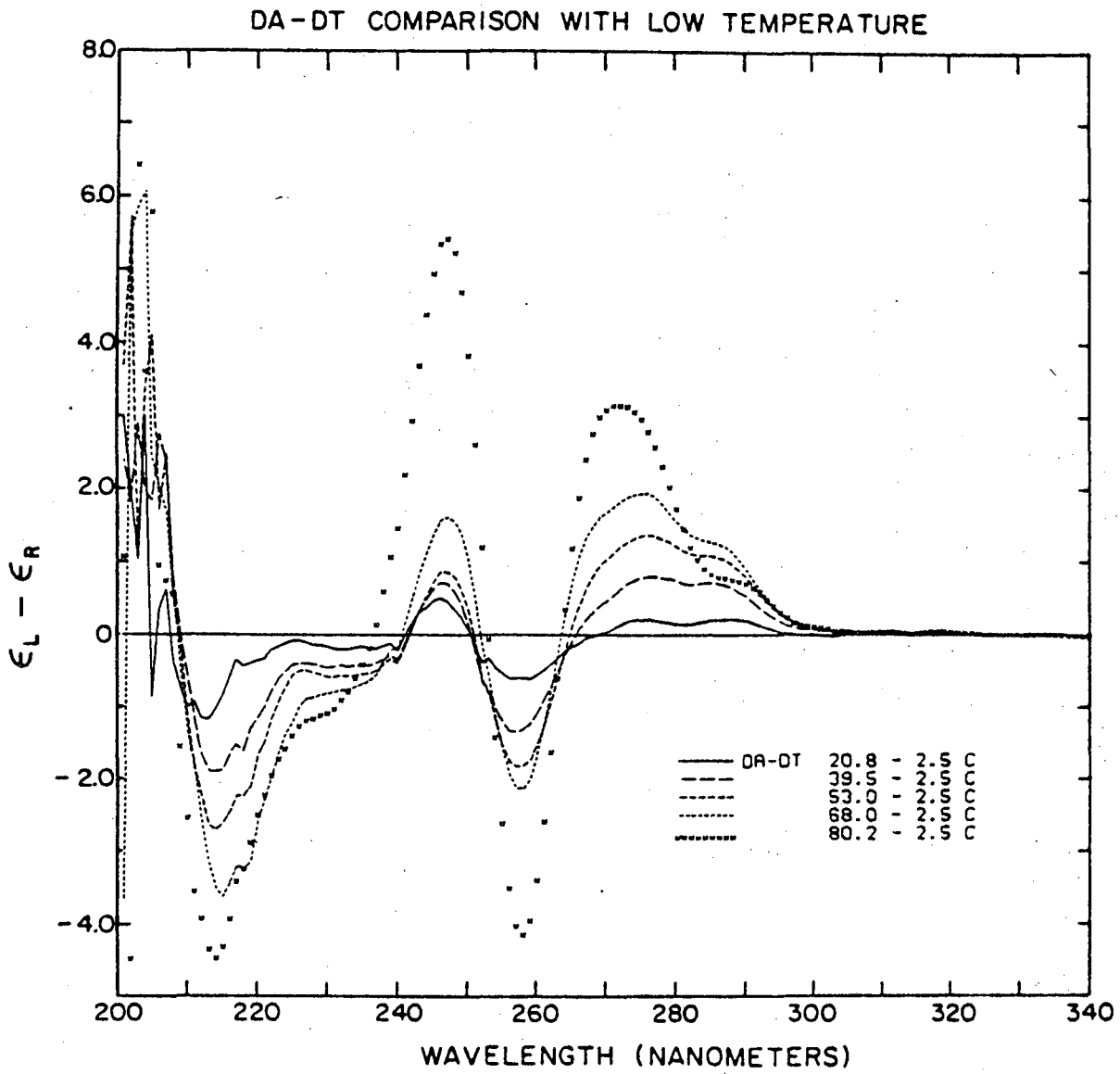
DA-DT COMPARISON WITH LOW TEMPERATURE
8.0
6.0
4.0
2.0
0
-2.0
-4.0
$\epsilon_L - \epsilon_R$
200
220
240
260
280
300
320
340
WAVELENGTH (NANOMETERS)
DA-DT 20.8 - 2.5 C
39.5 - 2.5 C
53.0 - 2.5 C
68.0 - 2.5 C
80.2 - 2.5 C

Figure 8

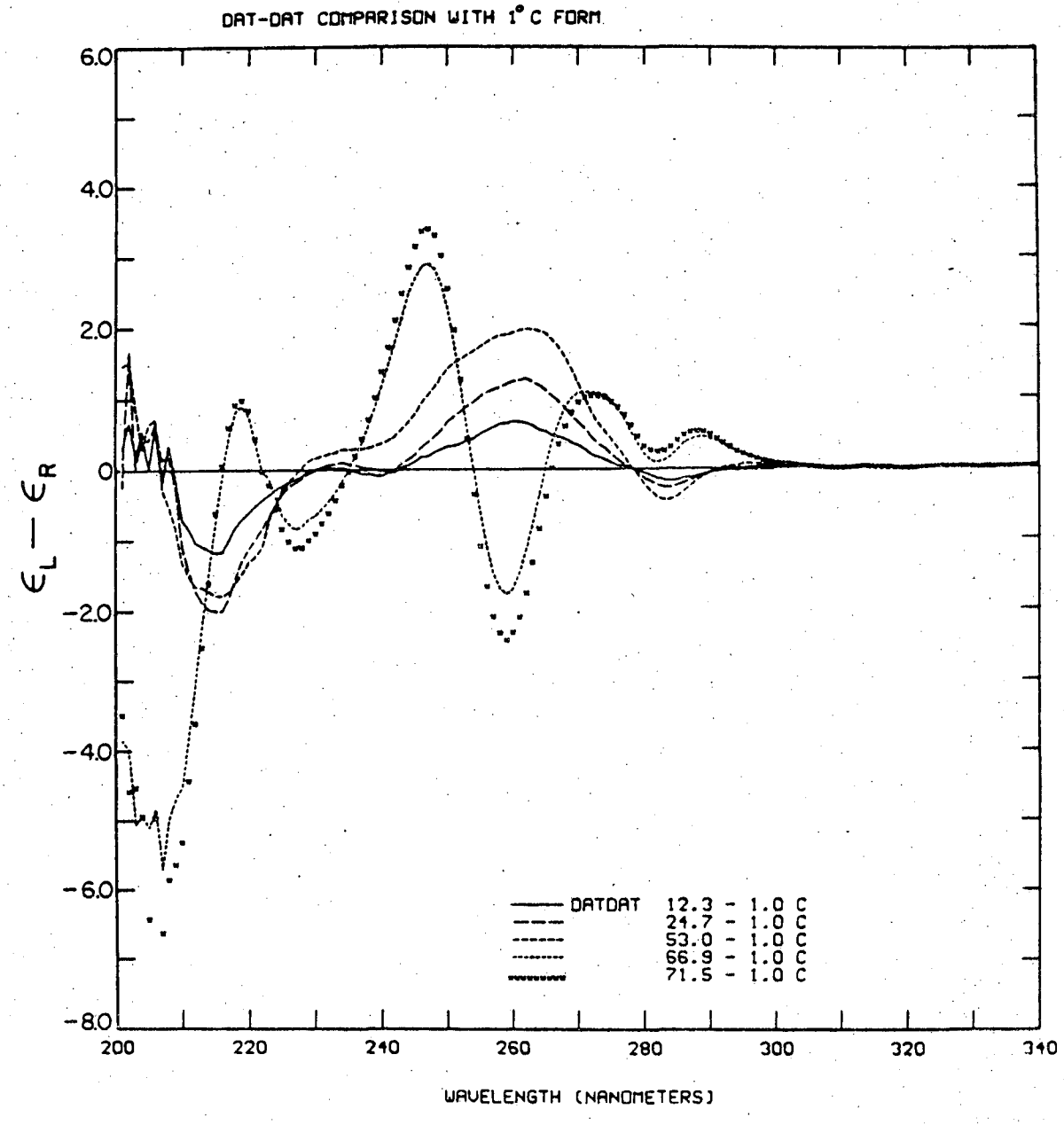

Figure 9

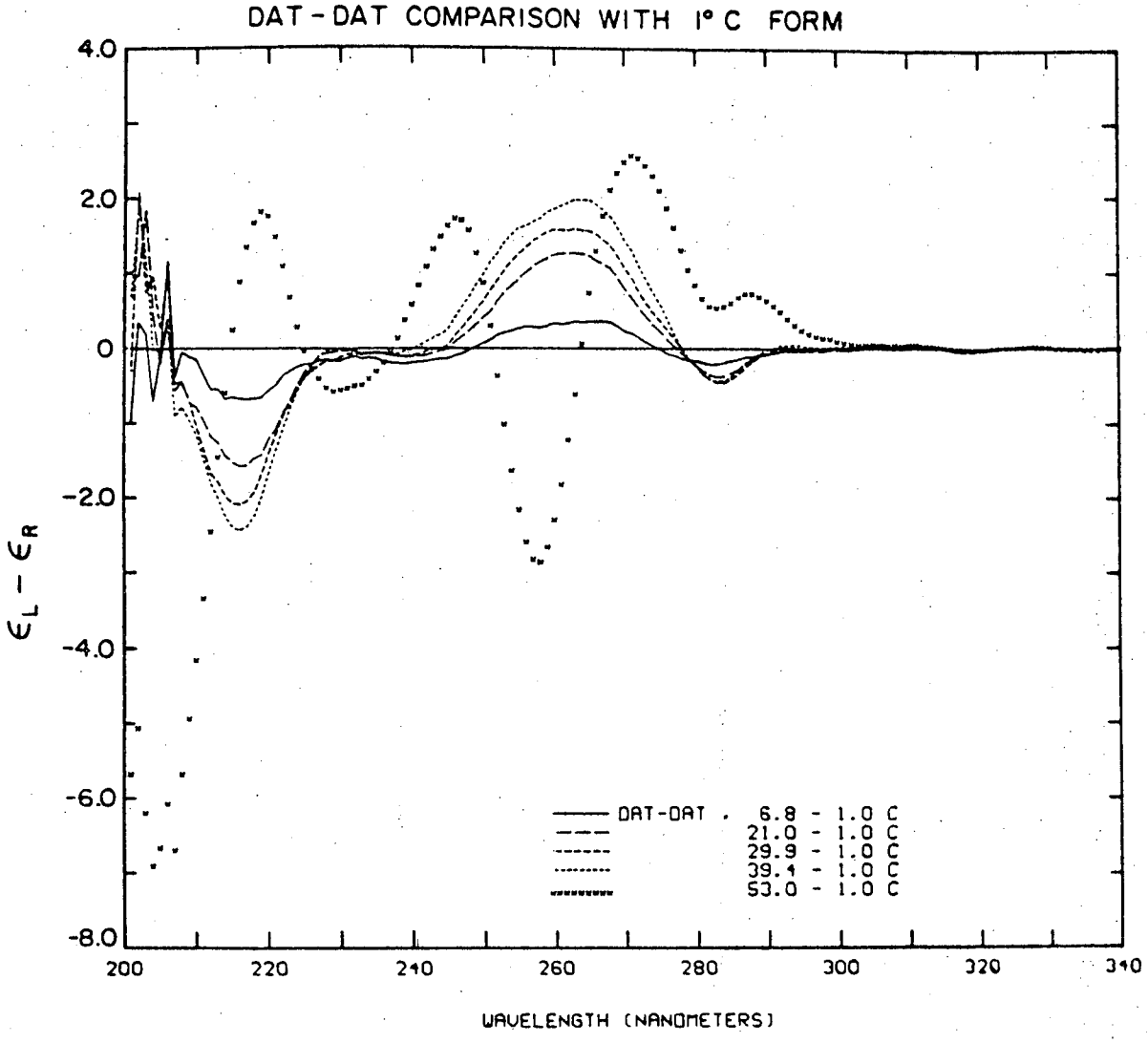
DAT - DAT COMPARISON WITH 1° C FORM
4.0
2.0
0
-2.0
-4.0
-6.0
-8.0
$\epsilon_L - \epsilon_R$
200
220
240
260
280
300
320
340
WAVELENGTH (NANOMETERS)
DAT-DAT . 6.8 - 1.0 C
21.0 - 1.0 C
29.9 - 1.0 C
39.1 - 1.0 C
53.0 - 1.0 C

Figure 10

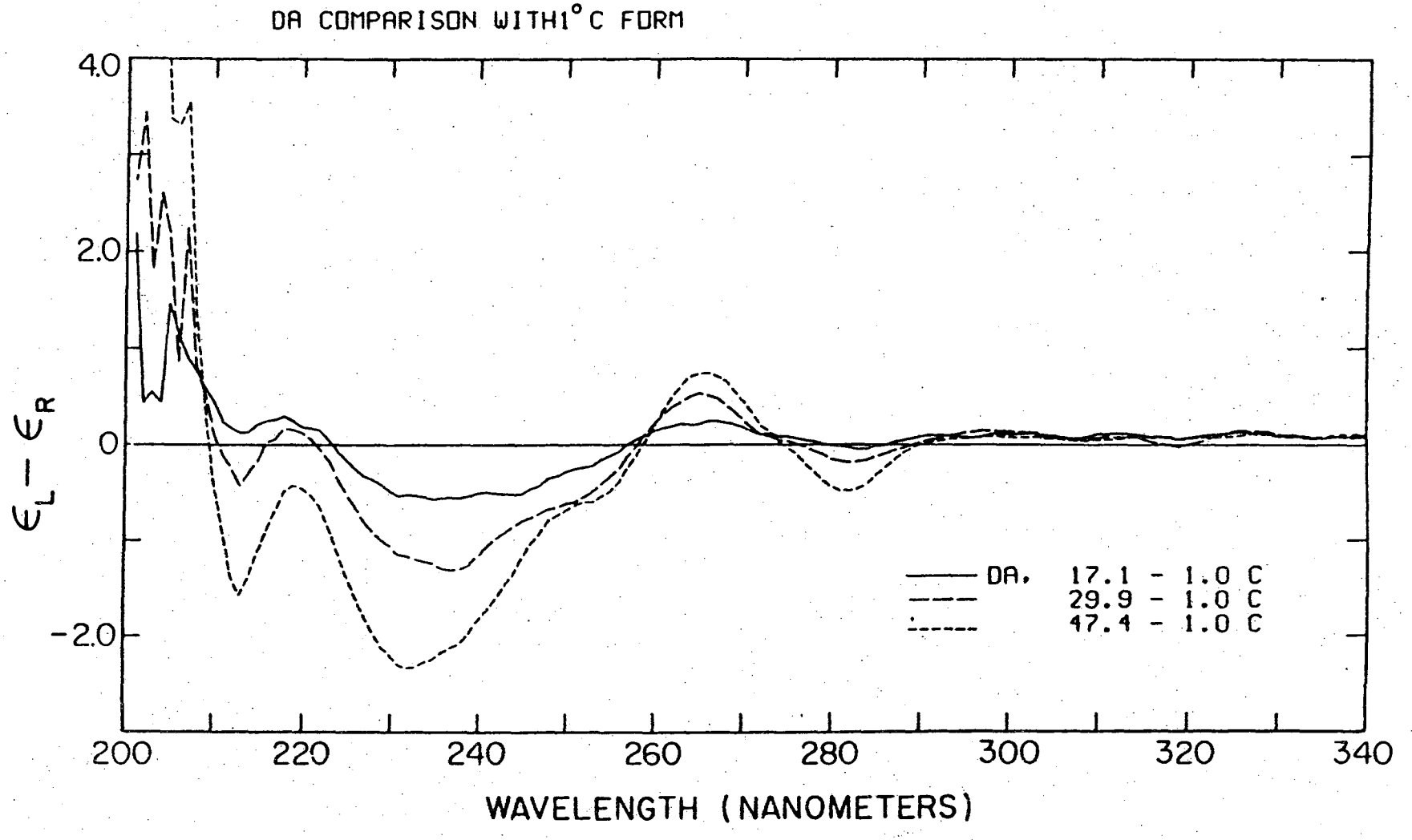

Figure 11

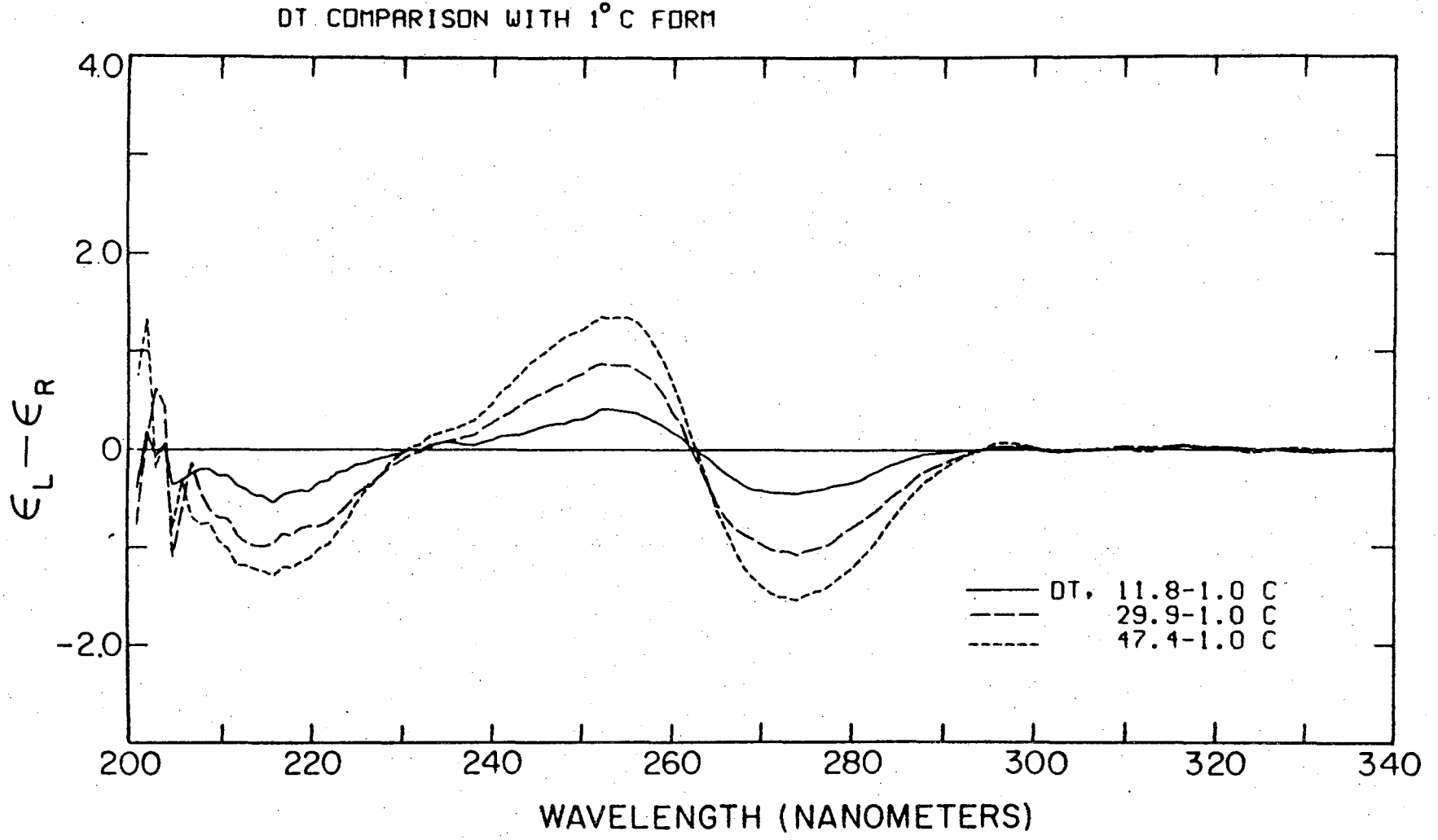
DT COMPARISON WITH 1° C FORM
4.0
2.0
0
-2.0
$\epsilon_L - \epsilon_R$
200
220
240
260
280
300
320
340
WAVELENGTH (NANOMETERS)
DT, 11.8-1.0 C
29.9-1.0 C
47.4-1.0 C

Figure 12

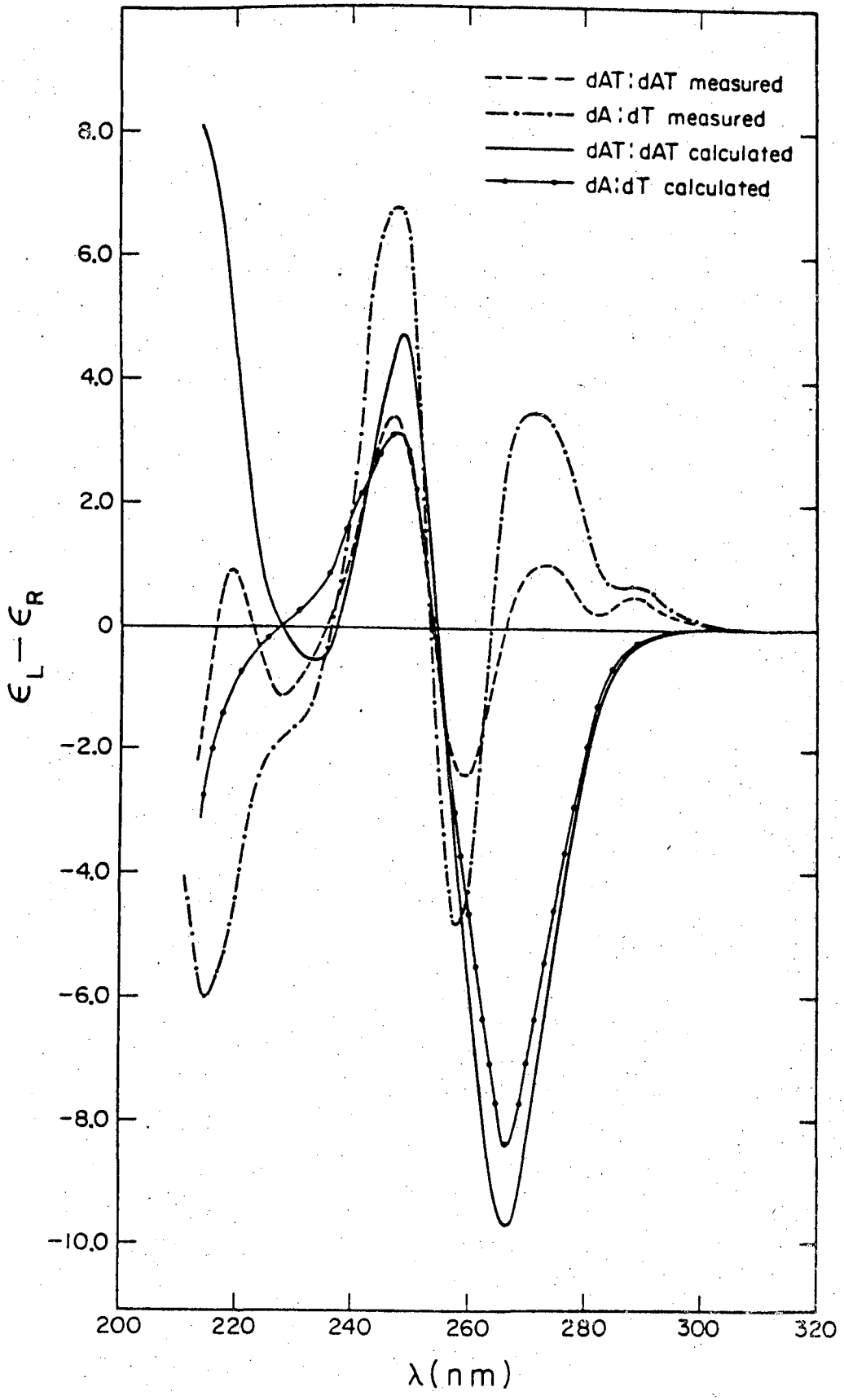

Figure 13

Chapter VI Bibliography

1. S. Arnott, Prog. Biophys. and Mol. Biol. 21, 265 (1970).
2. S. Arnott, R. Chandrasekaran, D.W.L. Hukins, P.J.C. Smith and L. Watts, J. Mol. Biol. 88, 523 (1974).
3. S. Arnott and E. Selsing, J. Mol. Biol. 88, 509 (1974).
4. M.J.B. Tunis-Schneider and M.F. Maestre, J. Mol. Biol. 25, 521 (1970).
5. C. Brunner and M.F. Maestre, Biopolymers 13, 345 (1974).
6. M.F. Maestre, J. Mol. Biol. 52, 543 (1970).
7. V.I. Ivanov, L.E. Minchenkova, A.K. Schyolkina and A.I. Poletayev, Biopolymers 12, 89 (1973).
8. D.S. Studdert, M. Patroni and R.C. Davis, Biopolymers 11, 761 (1972).
9. G. Green and H.R. Mahler, Biochemistry 10, 2200 (1971).
10. J. Brahms and W.F.H.M. Mommaerts, J. Mol. Biol. 10, 73 (1964).
11. R.B. Gennis and C.R. Cantor, J. Mol. Biol. 65, 381 (1972).
12. W.C. Johnson, Jr. and I. Tinoco, Jr., Biopolymers 7, 727 (1969).
13. H. De Voe, J. Chem. Phys. 43, 3199 (1965).
14. C.M. Cech, Thesis, University of California, Berkeley (1975) and Biopolymers 15, 131 (1976).
15. D.S. Studdert and R.C. Davis, Biopolymers 13, 1377 (1974).
16. D.S. Studdert and R.C. Davis, Biopolymers 13, 1391 (1974).
17. D.S. Studdert and R.C. Davis, Biopolymers 13, 1405 (1974).
18. W.C. Brunner and M.F. Maestre, Biopolymers 14, 555 (1975).

19. R.D. Wells, J.E. Larson, R.C. Grant, B.E. Shortle and C.R. Cantor, J. Mol. Biol. 54, 465 (1970).

20. C.S. Bush and H.A. Scheraga, Biopolymers 7, 395 (1969).

21. C.S. Moore and T.E. Wagner, Biopolymers 12, 201 (1973).

22. W. Hug and I. Tinoco, Jr., J. Am. Chem. Soc. 95, 2803 (1973).

23. J.N. Brown, L.M. Trefonas, A.F. Fucaloro and B.G. Anex, J. Am. Chem. Soc. 96, 1597 (1974).

24. D.M. Gray and J.C. Gall, J. Mol. Biol. 85, 665 (1974).

25. D.M. Gray and D.M. Skinner, Biopolymers 13, 843 (1974).

26. A.F. Fucaloro and L.S. Forster, J. Am. Chem. Soc. 93, 6443 (1971).

27. W.A. Eaton and T.P. Lewis, J. Chem. Phys. 53, 2164 (1970).

28. D.R. Davies and R.L. Baldwin, J. Mol. Biol. 6, 251 (1963).

29. J. Pilet, J. Blicharski and J. Brahms, Biochemistry 14, 1869 (1975).

30. P.H. von Hippel and G. Felsenfeld, Biochemistry 3, 27 (1964).

31. D.M. Gray, I. Tinoco, Jr. and M.J. Chamberlin, Biopolymers 11, 1235 (1972).

32. W. Xavier, G.M. deMarcia and M.P. Daune, Nucleic Acids Acids Research 1, 1043 (1974).

33. R. Clement and M.P. Daune, Nucleic Acids Research 2, 303 (1975).

34. D.M. Gray, R.L. Ratliff and D.L. Williams, Biopolymers 12, 1233 (1973).

APPENDIX A

Computer Programs

I. Program ROTOPI

Description:

This program calculates the absorption (ε) and circular dichroism (CD) spectra of poly nucleotides.

Input: (Cards)

geometry deck (see section a)

polarizability deck (see section b)

unit cell specification deck (see section c)

Output: (line printer)

reference base data

polarizability data (optional as per section b)

unit cell structure

optical data

Tapes:

TAPE 1 is used for scratch

TAPE 2 contains output suitable for teletype or 8 1/2 by 11 reports (similar to digitalized data in Appendix B)

Procedure:

1) read geometry deck

2) write reference base data

3) read polarizability deck

4) generate polarizabilities (as per section b)

5) write polarizability data (as per section b)

6) find largest common frequency range

7) read unit cell specification deck

8) generate unit cell structure

9) calculate interactions

10) at specified (in step 3) frequency intervals calculate CD and ε according to equations in Chapter IV.

11) write optical data

a. Geometry deck (all angles in °; all distances in Å)

1) geometry title card

(2F10.3, 5A10)

col.

1-10	helical rise per monomer
11-20	angle between monomers
21-70	tilting information

2) reference base card

(A1, 9x, I2, 8x, I2, 8x, I2, 47x, I1)

col.

1	base ID letter
11-12	# of atoms in base
21-22	total # of oscillators in base
31-32	# of in plane oscillators in base
80	control

3) base plane orientation card

(2F10.3)

col.

1-10	spherical polar angle of direction perpendicular to base plane

11-20 spherical azimuthal angle of direction perpendicular to base plane

4) cylindrical atomic coordinate cards (3 atoms per card)

(9F8.3)

col.

1-8, 25-32, 44-56	r
9-16, 33-40, 57-64	θ
17-24, 41-48, 65-72	z

5) oscillator card

(9F8.3, 6x, I2)

col.

1-8, 9-16, 17-24 cylindrical coordinates, coordinates of oscillator position, first r, then θ, then z.

25-32 polar angle of electric transition direction

33-40 azimuthal angle of electric transition direction

57-64 magnetic transition strength (b_i in equation III.3c)

65-72 dipole strength (in debye)

79-80 control

6) monopole cards

(8F10.6)

col.

1-10 One monopole for each atom of in plane
11-20 transitions; two monopoles for each atom
. of out of plane transitions. Order of
. monopoles must agree with order of atoms
. on cylindrical atomic coordinate cards.
. For out of plane transitions give first
. above plane and then below plane monopoles
71-80 for each atom.

Notes:

Cards 5) and 6) are repeated for each oscillator specified on the reference base card. The series of cards 2) through 6) may be repeated to input a maximum of 4 reference bases. If less than 4 bases are input the geometry deck should end with a card having a punch in col. 80. (a col. 80 punch card)

b. polarizability deck (all frequencies in kK)

1) polarizability specification card

(6E10.0, I2, 7x, I1)

col.

1-10 starting frequency
11-20 ending frequency
21-30 frequency intervals
31-40 dipole strength of transition (debye^2)

41-50 center of band. If this is specified a Lorentzian polarizability is generated according to equation I.14, if this is not specified or is 0, then polarizability is read from polarizability data cards.

51-60 half width of band

61-62 polarizability ID#. If not specified the polarizabilities are numbered sequentially as they are input

80 control

2) polarizability data cards (necessary if band center=0)

(2(E8.0,32x))

col.

1-8 First read in real polarizability over

41-48 the entire frequency range in interval specified in 1). Then read in imaginary polarizability.

Notes:

Card 1) and (if necessary) cards 2) may be repeated to input a maximum of 26 polarizabilities. If less than 26 are input the polarizability deck should end with a col. 80 punch card. If this card also has a 1 in col. 1, the polarizability data will be printed.

c. unit cell specification deck

1) polymer title card

(7A10, 2x, F4.0, 1x, I1, 1x, I1)

col.

1-70 tilting information

73-76 # of bases in unit cell

78 # of helical steps in unit cell

80 control

2) convergence card

(3I1, 7x, 6E10.0)

col. 11-20 # of unit cells used to calculate interaction. This corresponds to n_c in Chapter IV.
(no other fields in this card are used by ROTOPI)

3) base specification card

(A1, 3x, I2, 4x, 12(I2,3x), 9x, I1)

col.

1 base ID letter

5-6 Total # of transitions (≤ 7);specific

11-12 transitions to be included. Must be in

16-17 tegers between 1 and 7.

.

.

80 control

4) base position card

(10F5.0)

col.

1-5 Positions on the helix in the unit cell

6-10 on which to place base specified in 3).

. Positive number is Watson strand, negative

46-50 number is Crick strand.

Notes:

Cards 3) and 4) are repeated to construct the desired unit cell sequence. When the sequence is completely specified, the last base position card is followed by a col. 80 punch card. The series of cards 1) through 4) may be repeated to calculate as many polymers as desired. Two col. 80 punch cards signify the end of Input.

d. Sample output

Figures A1, A2, and A3 show the reference base data, the unit cell structure, and the optical data output of a typical calculation. In figure A3, "FREQ" is frequency, "CD" is circular dichroism, "A" is $a_{||}/\Delta z$, "B" is $b_{||}$ (see eqn. IV.6), "C" + "D" = $b_{\perp}$ (see eqn. IV.16), "Ex" is the extinction coefficient, "E" is $\varepsilon_{||}/c_1$, and "F" is $\varepsilon_{\perp}/c_1$ (see eqn IV.17).

Figure A1: Reference base data.

C. CECI EUTOPH (MONOPOLE INTERACTION) COUPLED OSCILLATOR MODEL TO INFINITE ORDER
C-DNA, WILKINS ET AL 1961, UP=.75 OUT OF PL ONLY OF H. DEVOE PROGRAM W. HUG

REFERENCE BASE DATA

A	ATOM	X	Y	Z	R	THETA	MP	XUP	YUP	ZUP	R	THETA	MP	XDN	YDN	ZDN	R	THETA
	1	-1.48	.61	.12	1.60	157.70	1	-1.54	.53	.86	1.63	161.04	2	-1.42	.68	-.62	1.57	154.23
	2	-.26	1.09	.28	1.12	103.30	3	-.32	1.01	1.02	1.06	107.63	4	-.19	1.17	-.46	1.18	99.41
	3	.06	2.35	.44	2.35	88.50	5	-.00	2.27	1.18	2.27	90.07	6	.13	2.43	-.30	2.43	87.03
	4	-.93	3.21	.44	3.34	106.10	7	-.99	3.13	1.18	3.29	107.55	8	-.86	3.29	-.30	3.40	104.70
	5	-2.23	2.80	.29	3.58	128.60	9	-2.30	2.72	1.03	3.56	130.18	10	-2.17	2.87	-.45	3.60	127.04
	6	-2.52	1.44	.12	2.90	150.20	11	-2.58	1.36	.86	2.92	152.13	12	-2.45	1.52	-.62	2.88	148.24
	7	-3.02	3.90	.33	4.93	127.60	13	-3.09	3.82	1.07	4.91	128.94	14	-2.96	3.97	-.41	4.95	126.67
	8	-2.24	4.89	.50	5.36	114.60	15	-2.30	4.82	1.24	5.34	115.57	16	-2.18	4.97	-.24	5.42	113.65
	9	-.96	4.57	.58	4.67	101.80	17	-1.02	4.49	1.32	4.61	102.78	18	-.89	4.65	-.16	4.73	100.85
	10	-3.72	1.02	-.03	3.86	164.70	19	-3.79	.94	.71	3.90	166.03	20	-3.66	1.10	-.77	3.82	163.34

OSC	DB	MONOPOLES IN ORDER FOR ATOMS 1 THRU 10 IN PL TRANS AND FOR POS 1 THRU 20 OUT OF PL TRANS									
1	3.78	-.068700	.117700	-.085900	-.028600	-.018700	.102500	.250700	-.402100	.069600	.077500
2	1.57	-.007400	-.118600	.086100	-.287300	.210400	.047200	-.101300	.087100	.065600	.018200
3	4.42	0.000000	0.000000	-.167191	-.013814	-.040460	-.176751	.190565	0.000000	.207651	0.000000
4	4.17	0.000000	0.000000	.129945	.225184	-.223532	-.106858	-.118326	0.000000	.093587	0.000000
5	10.79	0.000000	0.000000	-.408143	-.033721	-.098770	-.431480	.465202	0.000000	.506912	0.000000
6	9.26	0.000000	0.000000	-.286559	-.500048	.496381	.237291	.262757	0.000000	-.207822	0.000000
7	7.98	-.110800	.110800	-.110800	.110800	-.110800	.110800	-.110800	.110800	-.110800	.110800	-.110800
		.110800	-.110800	.110800	-.110800	.110800	-.110800	.110800	-.110800	.110800		

T	ATOM	X	Y	Z	R	THETA	MP	XUP	YUP	ZUP	R	THETA	MP	XDN	YDN	ZDN	R	THETA
	1	-.96	4.57	.58	4.67	101.80	1	-1.02	4.50	1.32	4.61	102.79	2	-.89	4.65	-.16	4.73	100.84
	2	-.74	3.22	.46	3.30	103.00	3	-.81	3.14	1.20	3.24	104.42	4	-.68	3.29	-.28	3.36	101.63
	3	-1.79	2.38	.28	2.96	126.90	5	-1.85	2.31	1.02	2.96	128.78	6	-1.72	2.46	-.46	3.00	125.05
	4	-3.03	2.87	.22	4.17	136.60	7	-3.10	2.79	.96	4.17	137.96	8	-2.96	2.94	-.52	4.18	135.24
	5	-3.26	4.23	.34	5.34	127.60	9	-3.32	4.16	1.08	5.32	128.65	10	-3.19	4.31	-.46	5.36	126.56
	6	-2.17	5.18	.52	5.54	113.10	11	-2.24	5.02	1.26	5.50	114.03	12	-2.11	5.17	-.22	5.58	112.18
	7	.41	2.76	.51	2.79	81.60	13	.34	2.69	1.25	2.71	82.74	14	.47	2.83	-.23	2.67	80.53
	8	-4.01	2.09	.05	4.91	152.90	15	-4.08	1.98	.79	4.54	154.12	16	-3.95	2.13	-.69	4.49	151.67

OSC	DB	MONOPOLES IN ORDER FOR ATOMS 1 THRU 8 IN PL TRANS AND FOR POS 1 THRU 16 OUT OF PL TRANS									
1	3.20	-.073100	.012000	-.012200	-.029400	.313200	-.266800	-.018100	.073800		
2	2.40	.036800	.074500	-.094700	-.125800	-.093000	.086800	-.133300	.253700		
3	4.37	.181727	.206128	.023167	-.182863	-.204915	-.023945	0.000000	0.000000		
4	6.92	.333608	.274908	-.001022	-.333272	-.272666	.058304	0.000000	0.000000		
5	6.70	.115886	-.222001	-.335916	-.166053	.219129	.330060	0.000000	0.000000		
6	6.66	-.115600	.115600	-.115600	.115600	-.115600	.115600	-.115600	.115600	-.115600	.115600	-.115600
		.115600	-.115600	.115600	-.115600	.115600					

C	ATOM	X	Y	Z	R	THETA	MP	XUP	YUP	ZUP	R	THETA	MP	XDN	YDN	ZDN	R	THETA
	1	-.36	4.57	.58	4.67	101.80	1	-1.02	4.50	1.32	4.61	102.79	2	-.89	4.65	-.16	4.73	100.84
	2	-.74	3.22	.46	3.30	103.60	3	-.81	3.14	1.20	3.24	104.42	4	-.68	3.29	-.28	3.36	101.63
	3	-1.79	2.38	.28	2.98	126.90	5	-1.85	2.31	1.02	2.36	128.78	6	-1.72	2.46	-.46	3.00	125.05
	4	-3.03	2.87	.22	4.17	136.60	7	-3.10	2.79	.96	4.17	137.96	8	-2.96	2.94	-.52	4.18	135.24
	5	-3.26	4.23	.34	5.34	127.60	9	-3.32	4.16	1.08	5.32	128.65	10	-3.19	4.31	-.40	5.36	126.56
	6	-2.17	5.10	.52	5.54	113.10	11	-2.24	5.02	1.26	5.50	114.03	12	-2.11	5.17	-.22	5.58	112.18
	7	.41	2.76	.51	2.79	81.60	13	.34	2.69	1.25	2.71	82.74	14	.47	2.83	-.23	2.87	80.53
	8	-4.01	2.05	.05	4.91	152.90	15	-4.08	1.98	.79	4.54	154.12	16	-3.95	2.13	-.69	4.49	151.67

OSC DU MONOPOLES IN ORDER FOR ATOMS 1 THRU 8 IN PL TRANS AND FOR POS 1 THRU 16 OUT OF PL TRANS

1	3.00	.161500	-.020000	-.163000	.061000	-.310000	.265000	-.001900	.012400
2	3.43	.161600	-.046300	.301000	-.120100	.000600	-.053200	-.023400	-.220200
3	4.82	.001152	.215582	.211940	-.006345	-.213092	-.209236	0.000000	0.000000
4	6.54	.335035	.170081	-.166039	-.332652	-.166996	.161971	0.000000	0.000000
5	6.34	-.001515	-.283566	-.278776	.008346	.280291	.275220	0.000000	0.000000
6	8.66	-.115600	.115600	-.115600	.115600	-.115600	.115600	-.115600	.115600	-.115600	.115600	-.115600	.115600	-.115600	.115600

G	ATOM	X	Y	Z	R	THETA	MP	XUP	YUP	ZUP	R	THETA	MP	XDN	YDN	ZDN	R	THETA
	1	-1.48	.61	.12	1.60	157.70	1	-1.54	.53	.86	1.63	161.05	2	-1.42	.68	-.62	1.57	154.23
	2	-.26	1.09	.28	1.12	103.30	3	-.32	1.01	1.02	1.05	107.61	4	-.19	1.17	-.46	1.18	93.42
	3	.06	2.35	.44	2.35	88.50	5	-.00	2.27	1.18	2.27	90.06	6	.13	2.43	-.30	2.43	87.04
	4	-.93	3.21	.44	3.34	106.10	7	-.99	3.13	1.18	3.23	107.54	8	-.86	3.29	-.30	3.40	104.70
	5	-2.23	2.80	.29	3.58	128.60	9	-2.30	2.72	1.03	3.56	130.18	10	-2.17	2.87	-.45	3.60	127.04
	6	-2.52	1.44	.12	2.90	150.20	11	-2.58	1.36	.86	2.92	152.13	12	-2.45	1.52	-.62	2.88	148.24
	7	-3.02	3.90	.33	4.93	127.80	13	-3.09	3.82	1.07	4.91	128.94	14	-2.96	3.97	-.41	4.95	126.67
	8	-2.24	4.89	.50	5.38	114.60	15	-2.30	4.81	1.24	5.34	115.57	16	-2.18	4.97	-.24	5.42	113.65
	9	-.96	4.57	.58	4.67	101.80	17	-1.02	4.49	1.32	4.61	102.77	18	-.89	4.65	-.16	4.73	100.85
	10	.79	.25	.28	.83	17.20	19	.73	.17	1.02	.75	13.03	20	.86	.32	-.46	.92	20.61
	11	-3.72	1.02	-.03	3.86	164.70	21	-3.79	.94	.71	3.90	166.03	22	-3.66	1.10	-.77	3.62	163.34

OSC DU MONOPOLES IN ORDER FOR ATOMS 1 THRU 11 IN PL TRANS AND FOR POS 1 THRU 22 OUT OF PL TRANS

1	2.22	-.025200	.012000	-.016100	-.048800	.056900	.015100	.163800	-.272100	.057300	.008500	.050600
2	4.19	.011200	.190100	-.150100	.388900	-.326600	-.032900	.140800	-.197000	-.051900	.075900	-.046400
3	4.22	0.000000	0.000000	.193741	.066668	-.037131	.124345	-.211012	0.000000	-.156611	0.000000	0.000000
4	4.64	0.000000	0.000000	.153264	.250990	-.246173	-.109034	-.141956	0.000000	.092596	0.000000	0.000000
5	10.31	0.000000	0.000000	-.384313	-.622597	-.163996	-.416815	.433325	0.000000	.488309	0.000000	0.000000
6	8.85	0.000000	0.000000	-.281583	-.478337	.472937	.220584	.257753	0.000000	-.191344	0.000000	0.000000
7	7.99	-.100700	.100700	-.100700	.100700	-.100700	.100700	-.100700	.100700	-.100700	.100700	-.100700	.100700

Figure A2: Unit cell structure.

POLY GT

BASE	POS ON HELIX	ELECTRIC OSCILLATOR POSITIONS							DIRECTION UNIT VECTORS					MAG OSC	
		X	Y	Z	R	THETA	OSC	POL	X	Y	Z	THETA	PHI	OSC	BI
G	W 1	-2.1834	3.6975	.3830	4.29	120.56	1	20	.9670	.2312	.1071	83.85	13.45		
		-1.4019	2.8487	.3620	3.17	116.20	2	21	-.3418	.8395	.0400	87.71	122.84		
		-1.5460	3.1555	.3820	3.51	116.10	3	22	-.5563	.8301	.0378	87.84	123.83		
		-1.5733	3.0050	.3640	3.39	117.64	4	23	-.9748	-.1973	-.1043	95.99	-168.56		
		-1.6561	3.1321	.3700	3.54	117.87	5	24	.2401	-.9675	-.0792	94.54	-76.06		
		-1.5762	3.0047	.3630	3.39	117.68	6	25	.9670	.2312	.1071	83.85	13.45		
		-1.4998	2.3739	.3050	2.81	122.28	7	26	-.0854	-.1023	.9911	7.66	-129.84		
T	W 2	-4.6671	1.6763	3.7170	4.96	160.24	8	8	.5405	.8335	.1145	83.43	57.04		
		-3.6990	.9171	3.6210	3.81	166.07	9	9	.9115	.4069	.0597	86.58	24.06		
		-3.8804	1.6638	3.7200	4.22	156.79	10	10	-.7514	-.6534	-.0917	95.26	-138.99		
		-3.8771	1.6639	3.7200	4.22	156.77	11	11	-.5405	-.8335	-.1145	96.57	-122.96		
		-3.8737	1.6791	3.7220	4.22	156.56	12	12	.8413	-.5364	-.0666	93.82	-32.52		
		-3.6388	1.4417	3.6920	3.91	158.39	13	13	-.0059	-.1323	.9912	7.61	-92.55		

Figure A3: Optical data.

CONVERGENCE= 20 UNIT CELLS

FREQ	CO	A	B	C	D	/ EX	E	F
33.800	8.5463E-02	7.4682E-01	-3.6783E+00	2.7110E+00	-4.3376E+00	7.8381E+02	-6.6660E+00	-7.2653E-02
34.800	-3.3648E-02	2.7400E+00	-1.2920E+01	9.3157E+00	-1.4460E+01	2.4451E+03	-2.0302E+01	-1.1535E-01
35.800	-2.6153E+00	9.4643E+00	-1.9899E+01	1.7666E+01	-2.4633E+01	4.5028E+03	-3.6324E+01	-2.2556E-01
36.800	-6.8123E+00	6.2626E+00	-1.2787E+01	2.3032E+01	-2.8564E+01	5.9823E+03	-4.6880E+01	-3.5816E-01
37.800	-6.7511E+00	4.7595E+00	-4.3268E+00	2.1934E+01	-2.7359E+01	7.1605E+03	-5.4601E+01	-4.4509E-01
38.800	-2.6600E+00	2.1526E+00	9.4293E-01	1.6801E+01	-2.3865E+01	8.2306E+03	-6.1158E+01	-4.8395E-01
39.800	1.9194E+00	-3.6307E-01	4.9682E+00	1.0468E+01	-1.8629E+01	8.3678E+03	-6.0628E+01	-4.6710E-01
40.800	3.3498E+00	-1.1973E+00	5.1896E+00	5.9913E+00	-1.3093E+01	7.0996E+03	-5.0163E+01	-4.0229E-01
41.800	3.0525E+00	-9.3811E-01	2.9332E+00	3.2320E+00	-8.0159E+00	5.1595E+03	-3.5544E+01	-3.2426E-01
42.800	2.0718E+00	-5.1857E-01	7.4282E-01	1.6465E+00	-4.1767E+00	3.3521E+03	-2.2507E+01	-2.5141E-01
43.800	2.1056E+00	-6.8764E-01	2.5859E-01	6.1152E-01	-1.3803E+00	2.4299E+03	-1.5924E+01	-1.9700E-01
44.800	3.6591E+00	-1.5381E+00	9.8506E-01	-2.2525E-01	1.0212E+00	2.4105E+03	-1.5473E+01	-1.6187E-01
45.800	6.7077E+00	-2.9171E+00	2.2130E+00	-7.6379E-01	3.1310E+00	3.2651E+03	-2.0561E+01	-1.5557E-01
46.800	1.0300E+01	-4.6327E+00	4.7396E+00	-1.1892E+00	5.4625E+00	4.6500E+03	-2.8634E+01	-1.7834E-01

e. Listing

```
      PROGRAM ROTOPI(INPUT,OUTPUT,PUNCH,TAPE5=INPUT,TAPE6=OUTPUT,
     1TAPE7=PUNCH,TAPE1,TAPE2)
      COMMON/MISC/GAM,DELT,NOS,UU,UL,DU,XMER,NMER
      COMMON/EMOS/XM(42),YM(42),ZM(42)
      COMMON/AIR/AI(26,101),AR(26,101),UA(26)
      COMMON/EEOS/XE(42),YE(42),ZE(42),RE(42)
      COMMON/IDET/IDA(42),BSUBI(42)
      COMMON/ROSC/XR(42),YR(42),ZR(42)
      COMMON/GMAT/G(42,42),G1(42,42),G2(42,42)
      COMMON/POL/AIT(26),ART(26),UP(6)
      COMMON/APOS/XA(22,42),YA(22,42),ZA(22,42)
      COMMON/MPOL/Q(22,7,4),DB(7,4),IDB(42),IDB(42),IDQ(42),IDN(42)
      COMPLEX G,G1,G2,ALPHA,G3(42,42)
      COMPLEX AA,BB,CC,DD,EE
      DIMENSION CO(101),EX(101),U(101)
  100 FORMAT(* *,*   FREQ*,5X,*CO*,11X,*A*,11X,*B*,11X,*C*,11X,*D*,
     15X,*/*,4X,*EX*,11X,*E*,11X,*F*)
  101 FORMAT(*1*,*CONVERGENCE= *,I2,* UNIT CELLS*)
  102 FORMAT(F7.3,8E12.4)
  110 FORMAT(F5.1,3F8.3,3F8.1)
  111 FORMAT(* *,* FREQ*,3X,*CO*,5X,*PARA*,4X,*PERP*,5X,*EX*,5X,
     1*PARA*,4X,*PERP*,5X,*N= *,I3)
C*****
C     THIS CALL TO INPUT READS IN THE GEOMETRY DECK; CALLS
C     ASHAPE TO READ IN THE POLARIZABILITY DECK; READS IN
C     THE FIRST POLYMER
C******
      CALL INPUT
 1000 N=UP(1)
      N IS THE CONVERGENCE (SET IT TO 20 IF NOT SPECIFIED)
      IF(N.EQ.0)N=20
      WRITE(6,101)N
      WRITE(2,111)N
      CALL INTRAC(N)
      WRITE(6,100)
C.....CALCULATE THE NUMBER OF FREQUNCY POINTS NI
      NI=1.01+(UU-UL)/DU
      DO 10 I=1,NI
C.....CACULATE FREQUENCY U(I) AND READ THE POLARIZABILITIES
C     INTO ART AND AIT ( NOTE CHANGE IN SIGN OF AIT )
      U(I)=UL+(I-1)*DU
      DO 1 N1=1,26
      IF(UA(N1).EQ.0.) GO TO 1
      K=1.01+(U(I)-UA(N1))/DU
      AIT(N1)=-AI(N1,K)
      ART(N1)=AR(N1,K)
    1 CONTINUE
C.....INTERACTION IS READ OFF TAPE1 RATHER THAN RECALCULATED
C     AT EACH FREQUENCY
      REWIND 1
      READ(1) ((G(J,L),G1(J,L),J=1,NOS),L=1,NOS)
C.....THE POLARIZABILITIES ARE ADDED TO THE INTERACTION PRIOR
C     TO INVERSION
      DO 2 N2=1,NOS
      M=IDA(N2)
      ALPHA=1.0/CMPLX(ART(M),AIT(M))
      G(N2,N2)=G(N2,N2)+ALPHA
      G1(N2,N2)=G1(N2,N2)+ALPHA
    2 CONTINUE
      CALL INVERT(G,NOS)
```

```
      CALL INVERT(G1,NOS)
      CALL MULT(G3)
      EX(I)=0.
      CO(I)=0.
      AA=(0.,0.)
      BB=(0.,0.)
      CC=(0.,0.)
      DD=(0.,0.)
      EE=(0.,0.)
      E=0.
      F=0.
      DO 4 N4=1,NOS
      DO 5 N5=1,NOS
C.....ALPHA IS THE IMAGINARY PART OF THE COMPLEX DOT PRODUCT:
C     THE REAL PART IS THE NORMAL DOT PRODUCT
      ALPHA=(0.,1.)*(XE(N4)*YE(N5)-XE(N5)*YE(N4))
      AIG=AIMAG(G(N4,N5))
      AA=AA-G3(N4,N5)*(XE(N5)*XE(N4)+YE(N4)*YE(N5)+ALPHA)
      BB=BB+(0.,1.)*G1(N4,N5)*(XE(N4)*XE(N5)+YE(N4)*YE(N5)+ALPHA)
     1*(ZR(N5)-ZR(N4))
      CC=CC-2.*G(N4,N5)*ZE(N4)*(XE(N5)*YR(N5)-XR(N5)*YE(N5))
      DD=DD+(0.,1.)*G1(N4,N5)*(
     1ZE(N4)*(XR(N4)*XE(N5)+YR(N4)*YE(N5)+(0.,1.)*(XR(N4)*YE(N5)
     2 -XE(N5)*YR(N4)))
     3-ZE(N5)*(XR(N5)*XE(N4)+YR(N5)*YE(N4)+(0.,1.)*(XE(N4)*YR(N5)
     4-XR(N5)*YE(N4)))
      EE=EE+((XE(N4)*XE(N5)+YE(N4)*YE(N5))+ALPHA)*G1(N4,N5)
      F=F+AIG*ZE(N4)*ZE(N5)
    5 CONTINUE
    4 CONTINUE
      A=AIMAG(AA)
      B=AIMAG(BB)
      C=AIMAG(CC)
      D=AIMAG(DD)
      E=AIMAG(EE)
      C1=-6.8826*U(I)/XMER
      C2=-4.3245E-4*U(I)**2/XMER
      EXPERP=C1*F
      EXPARA=C1*E
      COPERP=C2*(C+D)
      COPARA=C2*(DELT*A+B)
      EX(I)=EXPERP+EXPARA
      CO(I)=COPERP+COPARA
      WRITE(6,102)U(I),CO(I),A,B,C,D,EX(I),E,F
      WRITE(2,110)U(I),CO(I),COPARA,COPERP,EX(I),EXPARA,EXPERP
   10 CONTINUE
C.....THIS IS A CALL TO A SECONC ENTRY IN SUBROUTINE INPUT.
C     IT READS IN A NEW POLYMER WITHOUT READING IN NEW
C     GEOMETRY OR POLARIZABILITY DECKS
      CALL INPUT2
      GO TO 1000
      END
      SUBROUTINE INTRAC(NNN)
      COMMON/MISC/GAM,DELT,NOS,UU,UL,DU,XMER,NMER
      COMMON/APOS/XA(22,42),YA(22,42),ZA(22,42)
      COMMON/MPOL/Q(22,7,4),DB(7,4),IDB(42),IDDB(42),IDQ(42),IDN(42)
      COMMON/GMAT/G(42,42),G1(42,42),G2(42,42)
      COMMON/ROSC/XR(42),YR(42),ZR(42)
      COMMON/EECS/XE(42),YE(42),ZE(42),RE(42)
      DIMENSION R(3),RIJ(3),EI(3),EJ(3)
      COMPLEX G,G1,G2
      NL=2*NNN+1
```

```
      DO 10 I=1,NOS
      II=IDB(I)
      NI=IDQ(I)
      IDI=IDDB(I)
      DO 9 J=I,NOS
      JJ=IDB(J)
      NJ=IDQ(J)
      IDJ=IDDB(J)
      G(I,J)=(0.,0.)
      G1(I,J)=(0.,0.)
      G2(I,J)=(0.,0.)
C CALCULATE MONOPOLE-MONOPOLE INTERACTION FOR CLOSEST TEN UNIT CELLS
      DO 6 N6=1,NL
      N=N6-NNN-1
C     DO NOT INTERACT TRANSITIONS ON THE SAME BASE
      IF(N .EQ.0.AND.IDN(I).EQ.IDN(J)) GO TO 8
      FI=N*GAM
      SFI=SIN(FI)
      CFI=COS(FI)
      GG=0.
      IF(IABS(N).GT.10) GO TO 5
      DO 3 N3=1,NI
      DO 2 N2=1,NJ
      R(1)=XA(N3,I)-(XA(N2,J)*CFI-YA(N2,J)*SFI)
      R(2)=YA(N3,I)-(XA(N2,J)*SFI+YA(N2,J)*CFI)
      R(3)=ZA(N3,I)-ZA(N2,J)-N *DELT
      D=0.
      DO 1 N1=1,3
      D=D+R(N1)**2
    1 CONTINUE
      D=SQRT(D)
      GG=GG+Q(N3,IDI,II)*Q(N2,IDJ,JJ)/D
    2 CONTINUE
    3 CONTINUE
      GO TO 6
C     CALCULATE DIPOLE-DIPOLE FOR UNIT CELLS FURHTER THAN 10
    5 EIEJ=0.
      RIJEJ=0.
      RIJEI=0.
      RIJ(1)=XR(I)-(XR(J)*CFI-YR(J)*SFI)
      RIJ(2)=XR(I)-(XR(J)*SFI+YR(J)*CFI)
      RIJ(3)=ZR(I)-ZR(J)-N*DELT
      DIJ=RIJ(1)**2+RIJ(2)**2+RIJ(3)**2
      DIJ=SQRT(DIJ)
      EI(1)=XE(I)
      EI(2)=YE(I)
      EI(3)=ZE(I)
      EJ(1)=XE(J)*CFI-YE(J)*SFI
      EJ(2)=XE(J)*SFI+YE(J)*CFI
      EJ(3)=ZE(J)
      DO 4 N4=1,3
      EIEJ=EIEJ+EI(N4)*EJ(N4)
      RIJEI=RIJEI+RIJ(N4)*EI(N4)
      RIJEJ=RIJEJ+RIJ(N4)*EJ(N4)
    4 CONTINUE
      GG=EIEJ/DIJ**3-3.0*RIJEJ*RIJEI/DIJ**5
      GO TO 7
    6 GG=GG*4.80298**2/(DB(IDI,II)*DB(IDJ,JJ))
C     THIS IS THE EFFECTIVE DIELECTRIC CONSTANT
    7 GG=GG/2.
      G(I,J)=G(I,J)+GG
      G1(I,J)=G1(I,J)+GG*CMPLX(CFI,SFI)
```

```
      G2(I,J)=G2(I,J)+N*GG*CMPLX(-SFI,CFI)
    8 CONTINUE
      G(J,I)=G(I,J)
      G1(J,I)=CONJG(G1(I,J))
      G2(J,I)=CONJG(G2(I,J))
    9 CONTINUE
   10 CONTINUE
      REWIND 1
      WRITE(1)((G(K,L),G1(K,L),K=1,NOS),L=1,NOS)
      RETURN
      END
      SUBROUTINE MULT(C)
      COMMON/MISC/GAM,DELT,NOS,UU,UL,DU,XMER,NMER
      COMMON/GMAT/G(42,42),G1(42,42),G2(42,42)
      COMPLEX G,G1,G2,C(42,42),CKJ
      DO 10 I=1,NOS
      DO 10 J=1,NOS
      C(I,J)=(0.,0.)
      DO 10 K=1,NOS
      CKJ=(0.,0.)
      DO 8 L=1,NOS
      CKJ=CKJ+G2(K,L)*G1(L,J)
    8 CONTINUE
      C(I,J)=C(I,J)+G1(I,K)*CKJ
   10 CONTINUE
      RETURN
      END
      SUBROUTINE INPUT
      COMMON/MISC/GAM,DELT,NOS,UU,UL,DU,XMER,NMER
      COMMON/ROSC/XR(42),YR(42),ZR(42)
      COMMON/EEOS/XE(42),YE(42),ZE(42),RE(42)
      COMMON/EMOS/XM(42),YM(42),ZM(42)
      COMMON/POL/AIT(26),ART(26),UP(6)
      COMMON/IDET/IDA(42),BSUBI(42)
      COMMON/MPOL/Q(22,7,4),DB(7,4),IDB(42),IODB(42),IOQ(42),IDN(42)
      COMMON/APOS/XA(22,42),YA(22,42),ZA(22,42)
      DIMENSION A(7),B(5)
      DIMENSION NATOMS(4),IO(4),NIN(4),IOSC(12),POS(10)
      DIMENSION R(7,4),T(7,4),Z(7,4),TE(7,4),PE(7,4),IPOL(7,4)
      DIMENSION TM(7,4),PM(7,4),BI(7,4)
      DIMENSION TP(4),PP(4)
      DIMENSION AR(11,4),AT(11,4),AZ(11,4)
      DIMENSION AR1(22,4),AT1(22,4),AZ1(22,4)
      READ(5,300) THETA,D,B
  300 FORMAT (F10.3,F10.3,5A10)
      WRITE (6,99)
   99 FORMAT (1H1)
      WRITE (6,200)
  200 FORMAT (1X,*C. CECH     ROTOPM (MONOPOLE INTERACTION)*,45X,*COUPLE
     1D OSCILLATOR MODEL TO INFINITE ORDER*)
      WRITE (6,201) (B(I),I=1,5)
  201 FORMAT (1X,5A10,36X,*OF H. DEVOE     PROGRAM  W. HUG*)
      WRITE(6,220)
  220 FORMAT (/1X,*REFERENCE BASE DATA*)
      DO 380 I=1,4
      READ(5,301) IO(I),NATOMS(I),NOSC,NIN(I),ISEP
  301 FORMAT (A1,9X,I2,8X,I2,8X,I2,47X,I1)
      IF(ISEP.NE.0) GO TO 381
      READ(5,302) TP(I),PP(I)
  302 FORMAT (2(F10.3))
      JJJ=NATOMS(I)
      READ(5,303) ((AR(J,I),AT(J,I),AZ(J,I)),J=1,JJJ)
```

```
  303 FORMAT (9F8.3)
      RADT=TP(I)*.0174533
      RADP=PP(I)*.0174533
      XP=SIN(RADT)*COS(RADP)
      YP=SIN(RADT)*SIN(RADP)
      ZP=COS(RADT)
      WRITE (6,221) ID(I)
  221 FORMAT (/1X,1H*,A1,1H*,2X,*ATOM*,2X,*X*,5X,*Y*,5X,*Z*,5X,*R*,3X,
     1*THETA*,1X,*MP*,2X,*XUP*,3X,*YUP*,3X,*ZUP*,4X,*R*,3X,*THETA*,1X,
     1*MP*,2X,*XDN*,3X,*YDN*,3X,*ZDN*,4X,*R*,3X,*THETA*,/)
      DO 901 J=1,JJJ
C     DP SPECIFIES FRACTION ALONG UNIT VECTOR PERPENDICULAR TO PLANE
C     OF BASE THAT MONOPOLE POSITIONS ARE MOVED
      DP=.75
      K=2*J
      L=K-1
      RAD=AT(J,I)*.0174533
      X=AR(J,I)*COS(RAD)
      Y=AR(J,I)*SIN(RAD)
      XUP=X+(DP*XP)
      XDN=X-(DP*XP)
      YUP=Y+(DP*YP)
      YDN=Y-(DP*YP)
      RUP=XUP*XUP+YUP*YUP
      RDN=XDN*XDN+YDN*YDN
      AR1(K,I)=SQRT(RDN)
      AR1(L,I)=SQRT(RUP)
      AZ1(K,I)=AZ(J,I)-(DP*ZP)
      AZ1(L,I)=AZ(J,I)+(DP*ZP)
      ADN=ABS(XDN)
      AUP=ABS(XUP)
      IF(ADN.LT..0001) GO TO 910
      TDN=YDN/XDN
      AT1(K,I)=ATAN(TDN)*57.2958
      IF(XDN.LT.0) AT1(K,I)=AT1(K,I)+180.
      GO TO 911
  910 AT1(K,I)=90.
      IF(YDN.LT.0.) AT1(K,I)=-90.
      IF(YDN.EQ.0.) AT1(K,I)=0.
  911 CONTINUE
      IF(AUP.LT..0001) GO TO 912
      TUP=YUP/XUP
      AT1(L,I)=ATAN(TUP)*57.2958
      IF(XUP.LT.0) AT1(L,I)=AT1(L,I)+180.
      GO TO 913
  912 AT1(L,I)=90.
      IF(YUP.LT.0.) AT1(L,I)=-90.
      IF(YUP.EQ.0.) AT1(L,I)=0.
  913 CONTINUE
      WRITE(6,223) J,X,Y,AZ(J,I),AR(J,I),AT(J,I),L,XUP,YUP,AZ1(L,I),
     1AR1(L,I),AT1(L,I),K,XDN,YDN,AZ1(K,I),AR1(K,I),AT1(K,I)
  223 FORMAT (7X,I2,4(F5.2,1X),F6.2,1X,2(I2,F5.2,1X,F5.2,1X,F5.2,1X,
     1F5.2,1X,F6.2,1X))
  901 CONTINUE
      JJ=NIN(I)
      KJ=2*JJJ
      WRITE (6,222) JJJ,KJ
  222 FORMAT (/5X,*OSC*,2X,*DB*,3X,*MONOPOLES IN ORDER FOR ATOMS 1 THRU
     1*,I2,* IN PL TRANS AND FOR POS 1 THRU *,I2,* OUT OF PL TRANS*)
      IF(JJ.EQ.0) GO TO 240
      DO 382 J=1,JJ
      READ (5,304) R(J,I),T(J,I),Z(J,I),TE(J,I),PE(J,I),TM(J,I),PM(J,I),
```

```
   1BI(J,I),DB(J,I),IPOL(J,I)
304 FORMAT (9F8.3,6X,I2)
    READ(5,305) (Q(L,J,I),L=1,JJJ)
305 FORMAT (8F10.6)
    WRITE (6,224) J,DB(J,I),(Q(L,J,I),L=1,JJJ)
224 FORMAT (/5X,I2,1X,F5.2,2X,11(F8.6,1X))
382 CONTINUE
240 CONTINUE
    IF(JJ.EQ.NOSC) GO TO 241
    K=JJ+1
    DO 383 J=K,NOSC
    READ (5,304) R(J,I),T(J,I),Z(J,I),TE(J,I),PE(J,I),TM(J,I),PM(J,I),
   1BI(J,I),DB(J,I),IPOL(J,I)
    READ(5,305) (Q(L,J,I),L=1,KJ)
    WRITE (6,225) J,DB(J,I),(Q(L,J,I),L=1,KJ)
225 FORMAT (/5X,I2,1X,F5.2,2X,11(F8.6,1X),/,15X,11(F8.6,1X))
383 CONTINUE
241 CONTINUE
380 CONTINUE
381 CONTINUE
    CALL ASHAPE
    ENTRY INPUT2
390 CONTINUE
    READ(5,100) (A(I),I=1,7),XMER,NMER,ISEP
100 FORMAT(7A10,2X,F4.0,1X,I1,1X,I1)
    IF (XMER.EQ.0) XMER=1.
    IF(NMER.EQ.0) NMER=1
    IF (ISEP.NE.0) STOP
    GAM=.0174533*THETA*NMER
    DELT=D*NMER
    NIDN=0
    READ(5,102) IGMAT,IPNCH,IPLT,(UP(I),I=1,6)
102 FORMAT (3I1,7X,6E10.0)
    WRITE (6,99)
    WRITE (6,230) (A(I),I=1,7)
230 FORMAT (7A10)
    WRITE(2,231)(A(I),I=1,7)
231 FORMAT(///7A10//)
    WRITE (6,206)
206 FORMAT(//2X,*BASE*,2X,*POS ON*,7X,*ELECTRIC OSCILLATOR POSITIONS*,
   123X,*DIRECTION UNIT VECTORS*,15X,*MAG OSC*)
    WRITE (6,207)
207 FORMAT (8X,*HELIX*)
    WRITE (6,208)
208 FORMAT (20X,*X*,8X,*Y*,8X,*Z*,7X,*R*,6X,*THETA*,2X,*OSC*,1X,
   1*POL*,5X,*X*,8X,*Y*,8X,*Z*,5X,*THETA*,5X,*PHI*,4X,*OSC*,2X,*BI*)
    NOS=0
    DO 1 IJK=1,10
    READ(5,101) IBASE,NBR,(IOSC(I),I=1,12),ISEP
101 FORMAT (A1,3X,I2,4X,12(I2,3X),9X,I1)
    IF(ISEP.NE.0) GO TO 50
    READ(5,103) (POS(I),I=1,10)
103 FORMAT (10F5.0)
    LINE1=0
    WRITE (6,210)
    WRITE (6,209) IBASE
209 FORMAT (1H+,3X,A1)
    DO 3 I=1,4
    IF (IBASE.EQ.ID(I)) GO TO 4
  3 CONTINUE
    WRITE (6,204)
204 FORMAT (//1X,*BASE UNKNOWN*)
```

```
      STOP
    4 CONTINUE
      DO 2 J=1,10
      IF (POS(J).EQ.0) GO TO 1
      NION=NION+1
      STRAND=1.
      WC=1HW
      IF(POS(J).GT.0) GO TO 15
      STRAND=-1.
      WC=1HC
   15 POSJ=ABS(POS(J))
      IF(LINE1.EQ.1) WRITE(6,210)
      WRITE (6,211) WC,POSJ
  211 FORMAT (1H+,9X,A1,F2.0)
  210 FORMAT (1X)
      POSJ=POSJ-1.
      LINE2=0
      NNOS=NOS
      DO 5 M=1,NBR
      K=IOSC(M)
      NOS=NOS + 1
      TT=(T(K,I)*STRAND) + (POSJ*THETA)
      TRAD=TT*.0174533
      IDN(NOS)=NION
      RE(NOS)=R(K,I)
      XR(NOS)=R(K,I)*COS(TRAD)
      YR(NOS)=R(K,I)*SIN(TRAD)
      ZR(NOS)=(Z(K,I)*STRAND) + (POSJ*0)
      TTE=TE(K,I)
      IF(POS(J).LT.0) TTE=180.-TE(K,I)
      TERAD=TTE*.0174533
      PPE=(PE(K,I)*STRAND)+(POSJ*THETA)
      PERAD=PPE*.0174533
      XE(NOS)=SIN(TERAD)*COS(PERAD)
      YE(NOS)=SIN(TERAD)*SIN(PERAD)
      ZE(NOS)=COS(TERAD)
      IDA(NOS)=IPOL(K,I)
      IDB(NOS)=I
      IDDB(NOS)=K
      IF(LINE2.EQ.1) WRITE(6,210)
      WRITE(6,212) XR(NOS),YR(NOS),ZR(NOS),R(K,I),TT,NOS,IDA(NOS),
     1XE(NOS),YE(NOS),ZE(NOS),TTE,PPE
  212 FORMAT (1H+,15X,3(F7.4,2X),1X,F5.2,2X,F7.2,2X,I3,1X,I2,3(2X,F7.4)
     12X,F6.2,2X,F7.2)
      IF(BI(K,I).EQ.0) GO TO 6
      TTM=TM(K,I)
      IF(POS(J).LT.0) TTM=180.-TM(K,I)
      TMRAD=TTM*.0174533
      PPM=(PM(K,I)*STRAND)+(POSJ*THETA)
      PMRAD=PPM*.0174533
      XM(NOS)=SIN(TMRAD)*COS(PMRAD)
      YM(NOS)=SIN(TMRAD)*SIN(PMRAD)
      ZM(NOS)=COS(TMRAD)
      BSUBI(NOS)=BI(K,I)
      WRITE(6,213) NOS,BSUBI(NOS),XM(NOS),YM(NOS),ZM(NOS)
  213 FORMAT (1H+,91X,I5,F5.2,3F10.4)
      GO TO 9
    6 XM(NOS)=0.
      YM(NOS)=0.
      ZM(NOS)=0.
      BSUBI(NOS)=BI(K,I)
    9 CONTINUE
```

```
      MM=NIN(I)
      IF(K.GT.MM) GO TO 10
      NMPTS=NATOMS(I)
      IDQ(NOS)=NMPTS
      DO 8 L=1,NMPTS
      ANGLE=(AT(L,I)*STRAND)+(POSJ*THETA)
      RAD=ANGLE*.0174533
      XA(L,NOS)=AR(L,I)*COS(RAD)
      YA(L,NOS)=AR(L,I)*SIN(RAD)
      ZA(L,NOS)=(AZ(L,I)*STRAND)+(POSJ*D)
    8 CONTINUE
      GO TO 11
   10 CONTINUE
      NMPTS=2*NATOMS(I)
      IDQ(NOS)=NMPTS
      DO 7 L=1,NMPTS
      ANGLE=(AT1(L,I)*STRAND)+(POSJ*THETA)
      RAD=ANGLE*.0174533
      XA(L,NOS)=AR1(L,I)*COS(RAD)
      YA(L,NOS)=AR1(L,I)*SIN(RAD)
      ZA(L,NOS)=(AZ1(L,I)*STRAND)+(POSJ*D)
    7 CONTINUE
   11 CONTINUE
    5 LINE2=1
    2 LINE1=1
    1 CONTINUE
   50 CONTINUE
      RETURN
      END
      SUBROUTINE ASHAPE
      COMMON/MISC/GAM,DELT,NOS,DD,DL,DU,XMER,NMER
      COMMON/AIR/AI(26,101),AR(26,101),UA(26)
      COMMON/POL/AIT(26),ART(26),UP(6)
      EQUIVALENCE (TUA,UP(1)),(TUE,UP(2)),(TUD,UP(3)),(DS,UP(4)),
     1(UK,UP(5)),(GK,UP(6))
      DIMENSION UE(26),UD(26),IPTS(26)
      DO 25 I=1,26
      UA(I)=0.
      UE(I)=0.
      UD(I)=0.
   25 CONTINUE
      DO 1 I=1,27
      READ(5,100) TUA,TUE,TUD,DS,UK,GK,K,ISEP
  100 FORMAT (6E10.0,I2,17X,I1)
      IF (ISEP.NE.0)  GO TO 2
      IF (K.EQ.0)  K=I
      UA(K)=TUA
      UE(K)=TUE
      UD(K)=TUD
      RIZ=(TUE-TUA)/TUD
      RAB=ABS(RIZ) + 1.01
      IAB=RAB
      IPTS(K)=IAB
      IF(IAB.GT.101) GO TO 5
      IF (UK.NE.0)  GO TO 3
      READ (5,101) (AI(K,J),J=1,IAB)
      THIS IS INPUT FORMAT FOR 60 POINT DECK
  101 FORMAT (5(E8.0,8X))
C
C     THIS IS INPUT FORMAT FOR 14 POINT DECK
  101 FORMAT(2(E8.0,32X))
C
```

```
      READ (5,101) (AR(K,J),J=1,IAB)
      GO TO 7
    3 IF (GK.EQ.0)  GK=0.5*SQRT(UK)
      DO 6 J=1,IAB
      UDEL=(J-1)*TUD
      IF(RIZ.LT.0.) UDEL=-UDEL
      U=TUA+UDEL
      UKU=UK*UK
      UU=U*U
      UMU=UKU-UU
      UU=DS*UK*10.069/(UMU*UMU+UU*GK*GK)
      TBM=UMU*UU
      IF (ABS(TBM).GT.1000000.)  GO TO 5
      AR(K,J)=TBM
      TBM=U*GK*UU
      IF (TBM.GT.1000000.)  GO TO 5
      AI(K,J)=TBM
    6 CONTINUE
    7 CONTINUE
      IF(RIZ.GT.0.) GO TO 1
      IA=IAB/2
      DO 4 J=1,IA
      JT=IAB+1-J
      TBM=AI(K,J)
      AI(K,J)=AI(K,JT)
      AI(K,JT)=TBM
      TBM=AR(K,J)
      AR(K,J)=AR(K,JT)
      AR(K,JT)=TBM
    4 CONTINUE
      UA(K)=TUE
      UE(K)=TUA
    1 CONTINUE
    5 WRITE (6,220)
  220 FORMAT (1X,*POL OUT OF RANGE*)
      STOP
    2 UL=0.
      UU=10E5
      DO 22 I=1,26
      UL=AMAX1(UL,UA(I))
      UT=AMIN1(UU,UE(I))
      IF(UT.NE.0.)  UU=UT
      IF(UD(I).EQ.0.)  GO TO 22
      IF(I.LT.26) I1=I+1
      DU=UD(I)
      IF (UD(I1).EQ.0)  GO TO 22
      IF (UD(I).EQ.UD(I1))  GO TO 22
      WRITE (6,270)
  270 FORMAT (1X,*POL INCOMPATIBLE*)
      STOP
   22 CONTINUE
      IF(TUA.NE.0.) GO TO 33
      RETURN
   30 CONTINUE
      WRITE (6,200)
  200 FORMAT (///1X,*POLARIZABILITIES*)
      DO 31 I=1,26
      IF(UD(I).EQ.0.) GO TO 31
      WRITE (6,201) I,UA(I),UE(I),UD(I)
  201 FORMAT (//1X,*NBR=*,I3,10X,*START FREQ=*,F7.3,*   END FREQ=*,
     1F7.3,*   DELTA=*,F7.3)
      IAB=IPTS(I)
```

```
      WRITE (6,204)
  204 FORMAT (/1X,*IMAGINARY*)
      WRITE (6,205) (AI(I,J),J=1,IA8)
  205 FORMAT (1X,10F12.5)
      WRITE (6,206)
  206 FORMAT (/1X,*REAL*)
      WRITE (6,205) (AR(I,J),J=1,IA8)
   31 CONTINUE
      RETURN
      END
      SUBROUTINE INVERT(A,N)
      COMPLEX A(42,42),PIVOT(42,42),AMAX,SWAP,T
      DIMENSION IPIVOT(42),INDEX(42,2)
      EQUIVALENCE (IROW,JROW), (ICOLUM,JCOLUM), (AMAX, T, SWAP)
   15 DO 20 J=1,N
   20 IPIVOT(J)=0
   30 DO 550 I=1,N
   40 AMAX=0.0
   45 DO 105 J=1,N
   50 IF (IPIVOT(J)-1) 60, 105, 60
   60 DO 100 K=1,N
   70 IF (IPIVOT(K)-1) 80, 100, 740
   80 IF (CABS(AMAX)-CABS(A(J,K))) 85, 100, 100
   85 IROW=J
   90 ICOLUM=K
   95 AMAX=A(J,K)
  100 CONTINUE
  105 CONTINUE
      IF(CABS(AMAX)) 110,800,110
  110 IPIVOT(ICOLUM)=IPIVOT(ICOLUM)+1
  130 IF (IROW-ICOLUM) 140, 260, 140
  140 DETERM=-DETERM
  150 DO 200 L=1,N
  160 SWAP=A(IROW,L)
  170 A(IROW,L)=A(ICOLUM,L)
  200 A(ICOLUM,L)=SWAP
  260 INDEX(I,1)=IROW
  270 INDEX(I,2)=ICOLUM
  310 PIVOT(I)=A(ICOLUM,ICOLUM)
  330 A(ICOLUM,ICOLUM)=1.0
  340 DO 350 L=1,N
  350 A(ICOLUM,L)=A(ICOLUM,L)/PIVOT(I)
  380 DO 550 L1=1,N
  390 IF(L1-ICOLUM) 400,550,400
  400 T=A(L1,ICOLUM)
  420 A(L1,ICOLUM)=0.0
  430 DO 450 L=1,N
  450 A(L1,L)=A(L1,L)-A(ICOLUM,L)*T
  550 CONTINUE
  600 DO 710 I=1,N
  610 L=N+1-I
  620 IF (INDEX(L,1)-INDEX(L,2)) 630, 710, 630
  630 JROW=INDEX(L,1)
  640 JCOLUM=INDEX(L,2)
  650 DO 705 K=1,N
  660 SWAP=A(K,JROW)
  670 A(K,JROW)=A(K,JCOLUM)
  700 A(K,JCOLUM)=SWAP
  705 CONTINUE
  710 CONTINUE
  740 RETURN
  800 DETERM = 0.
```

II. Program ROTOPM (Author: C. Cech)

Description:

This program calculates the ε and CD spectra of oligonucleotides

Input: (cards)

geometry deck (see Ia)

polarizability (see Ib)

oligomer specification deck (see Chapter V ref. 17)

Output: (line printer)

reference base data

polarizability data (optional)

oligomer structure

optical data

Procedure is similar to ROTOPI except equations from chapter III are used in step 10. See Chapter V reference 17 for details.

Listing of ROTOPM is on microfiche labelled: "APPENDIX A PROGRAMS"

III. Program BASES (Author: I. Tinoco, Jr.)

Listing is given on microfiche labelled "APPENDIX A PROGRAMS"

APPENDIX B

This appendix contains the results of calculations on 16 polymers (see Chapter V, section III) in RNA, B-DNA and C-DNA geometries. These 14 pt calculations are given in digitalized form on the microfiche labelled: "APPENDIX B DIGITALIZED DATA" and as plots on the microfiche labelled: "APPENDIX B PLOTS".

Figure B1 shows a sample frame of digitalized data. The average extinction and CD are given as well as the perpendicular and parallel contributions to the average CD.

POLY GT C-DNA

LAMBDA	CD	PARA	PERP	EX	PARA	PERP
295.9	.085	-.316	.402	783.8	775.4	8.5
287.4	-.034	-1.381	1.347	2445.1	2431.3	13.8
279.3	-2.615	-4.540	1.925	4502.8	4475.0	27.8
271.7	-6.812	-8.432	1.620	5982.3	5936.9	45.3
264.6	-6.751	-8.427	1.676	7160.5	7102.6	57.9
257.7	-2.660	-4.960	2.300	8230.6	8166.0	64.6
251.3	1.919	-.876	2.795	8367.8	8303.8	64.0
245.1	3.550	.994	2.556	7099.6	7043.1	56.5
239.2	3.053	1.245	1.807	5159.5	5112.8	46.6
233.6	2.072	1.070	1.002	3352.1	3315.0	37.0
228.3	2.106	1.787	.319	2429.9	2400.2	29.7
223.2	3.659	4.005	-.345	2410.5	2385.5	25.0
218.3	6.708	7.781	-1.074	3265.1	3240.6	24.5
213.7	10.300	12.323	-2.024	4650.0	4621.3	28.7

Figure B2 shows a sample frame of the plotted data. The solid line is the average, the dots are the parallel contribution, and the ∇'s are the perpendicular contribution.

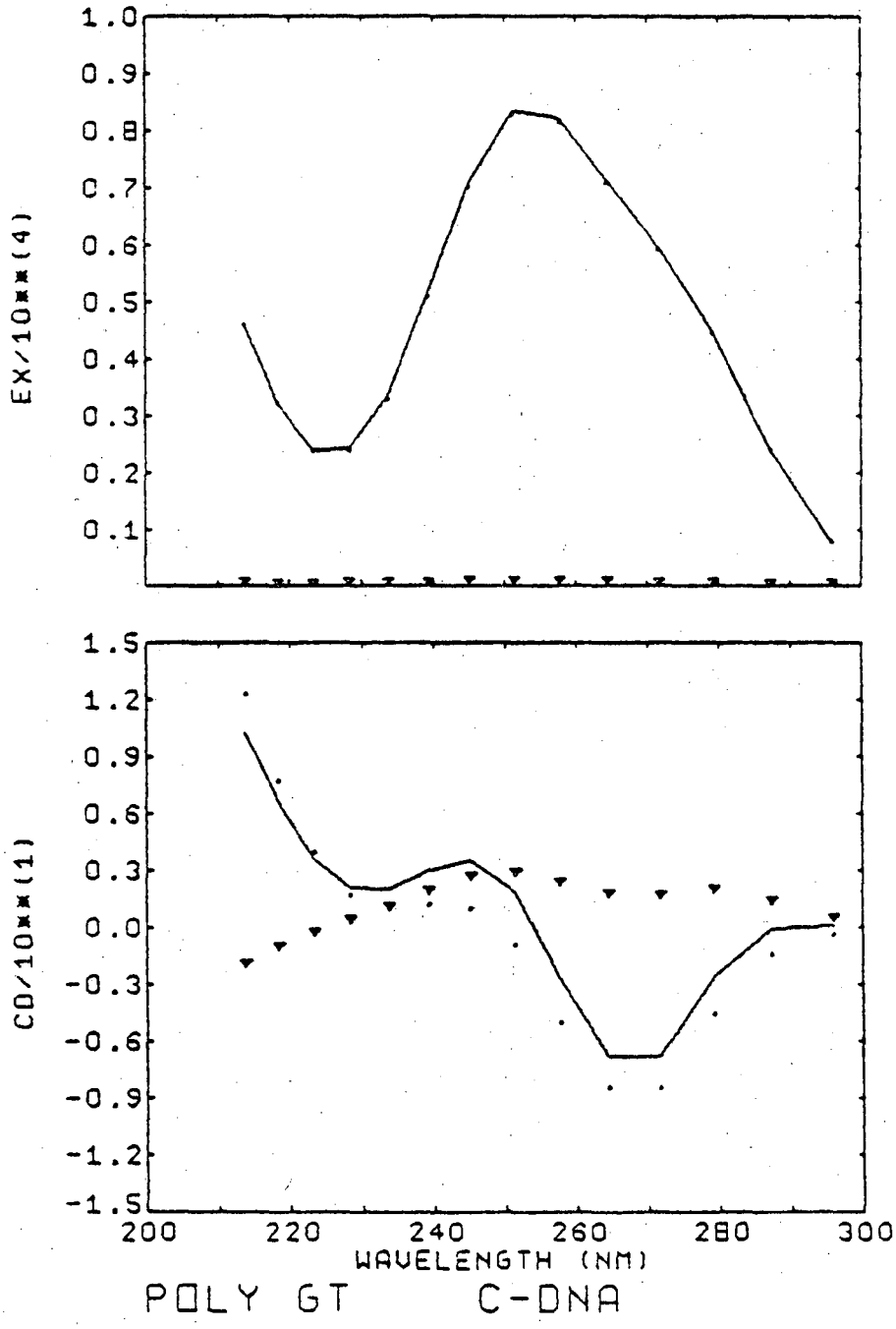
1.0
0.9
0.8
0.7
0.6
0.5
0.4
0.3
0.2
0.1
EX/10**(4)
1.5
1.2
0.9
0.6
0.3
0.0
-0.3
-0.6
-0.9
-1.2
-1.5
CD/10**(1)
200
220
240
260
280
300
WAVELENGTH (NM)
POLY GT C-DNA

MICROFICHE APPENDICES

This report was done with support from the United States Energy Research and Development Administration. Any conclusions or opinions expressed in this report represent solely those of the author(s) and not necessarily those of The Regents of the University of California, the Lawrence Berkeley Laboratory or the United States Energy Research and Development Administration.

TECHNICAL INFORMATION DIVISION
LAWRENCE BERKELEY LABORATORY
UNIVERSITY OF CALIFORNIA
BERKELEY, CALIFORNIA 94720